NEURAL AND BEHAVIORAL RESPONSES TO DEEP BRAIN STIMULATION OF THE SUBTHALAMIC NUCLEUS

by

Collin Anderson

A dissertation submitted to the faculty of
The University of Utah
in partial fulfillment of the requirements for the degree of

Doctor of Philosophy

Department of Bioengineering

The University of Utah

May 2016

The University of Utah Graduate School

STATEMENT OF DISSERTATION APPROVAL

The dissertation of **Collin Anderson**

has been approved by the following committee members:

Alan Dale Dorval II	, Chair	**1/07/2016** Date Approved
Richard D. Rabbitt	, Member	**1/07/2016** Date Approved
Christopher R. Butson	, Member	**1/07/2016** Date Approved
Alla R. Borisyuk	, Member	**1/07/2016** Date Approved
Lauren E. Schrock	, Member	**2/25/2016** Date Approved

and by **Patrick A. Tresco**,

Chair of the Department of **Bioengineering**

and by David B. Kieda, Dean of the Graduate School.

ABSTRACT

Parkinson's Disease (PD) motor symptoms, characterized most commonly by bradykinesia, akinesia, rigidity, and tremor, are brought about through the degeneration of dopaminergic neurons in the substantia nigra pars compacta, which leads to changes in electrophysiological activity throughout the basal ganglia. These symptoms are often effectively treated in the early stages of the disease by dopamine replacement therapies. However, as the disease progresses, the therapeutic window of pharmacological approaches reduces and patients develop significant side effects, even under minimally effective doses. When the disease reaches this stage, surgical therapies, such as high-frequency deep brain stimulation (DBS), are considered. DBS of the subthalamic nucleus partially treats the motor symptoms of PD and has been implemented to treat PD over 50,000 times worldwide, but its mechanisms are unclear.

In this work, we set out to advance the understanding of the mechanisms, function, and malfunction of DBS as a treatment for PD, keeping in mind the idea that DBS treats PD symptoms without restoring basal ganglia neural activity to that seen under healthy conditions. First, we demonstrated that neuronal information directed from the basal ganglia to the thalamus is pathologically increased in the parkinsonian condition and reduced by DBS in a standard 6-OHDA rat model of PD. Next, we developed a rodent model of DBS's role in the exacerbation of hypokinetic dysarthria, providing a framework for the study of this poorly understood side effect of DBS. Finally, we found

that DBS creates action suppression deficits independently from a parkinsonian state, and that PD creates apathy that is not rescued by DBS. Our specific results led to the interpretation that DBS, in its current form, might inherently create side effects that are largely unavoidable.

Our work fits into the following overarching idea. DBS successfully treats some motor symptoms of PD through the reduction of pathological information transmission. However, the fact that reducing pathological information does not restore neural activity to that present under healthy conditions underlies some of its failures to improve certain symptoms, as well as its exacerbations and side effects.

TABLE OF CONTENTS

LIST OF FIGURES

CHAPTER 1

INTRODUCTION

Parkinson's Disease (PD) is a progressive, neurological disorder that affects as many as ten million individuals worldwide. The disease progression typically begins with lesions in the glossopharyngeal and vagal nerves and anterior olfactory nucleus and ascends through the brain stem with little interindividual variation (Braak et al., 2003). The cortex is affected later, with mesocortex, neocortex, premotor areas, and primary sensory fields eventually affected. The basal ganglia, affected later in the progression, are thought to be primarily responsible for motor symptoms. Unsurprisingly, a prodromal stage lasting anywhere from months to decades (Hawkes, 2008) often precedes the onset of classical PD motor symptoms, with manifestations including gastrointestinal, urinary, and sexual dysfunction, REM sleep disorders, depression, anxiety (Truong and Wolters, 2009), and even ease of quitting smoking (Ritz et al., 2014).

Dopaminergic medication is usually prescribed following the onset of motor symptoms, at which point the disease has already reached an advanced stage (Koller, 1992). Dopaminergic medication is not typically thought to slow the progression of the disease, and the therapeutic window, the range of doses that treats symptoms without creating side effects, typically closes over time. Deep brain stimulation (DBS), consisting of high-frequency electrical pulses delivered to a specific target, typically the subthalamic

nucleus (STN) or internal globus pallidus (GPi), is often considered as an alternate therapy once dopaminergic medication loses efficacy, typically around 10 years after commencement of dopaminergic medication.

The exact mechanisms of DBS are not fully known. It is known that DBS can trigger action potentials via excitation of the axon hillock (McIntyre et al., 2004), even though it can have a net suppressive effect on cell bodies (Toleikis et al., 2012). Thus, the exact mechanism of therapeutic benefit is still debated, even at a cellular level. Unsurprisingly, the systems-level therapeutic mechanism is further obfuscated.

1.1 Neural Information Encoding

Prior to the use of DBS, it was commonly held that levodopa improved symptoms by restoring basal ganglia firing rates to those in healthy individuals. Likewise, early studies of DBS proposed the view that DBS alleviates hypokinetic PD symptoms by reducing gabaergic drive to thalamus, purportedly disinhibiting the thalamus (Benabid et al., 1998; Benazzouz et al., 2000; Beurrier et al., 2001; Boraud et al., 1996). However, other studies reported that DBS might not reduce gabaergic drive to thalamus, but instead possibly increase it, further reducing thalamic firing rates from those seen in PD (Anderson et al., 2003; Hashimoto et al., 2003; Hershey et al., 2003; Windels et al., 2000). Recent literature still disagrees on whether DBS increases (Dorval et al., 2008), decreases (Benazzouz et al., 2000; Burbaud et al., 1994), or does not drive a net change (Bosch et al., 2011; Moran et al., 2011; Shi et al., 2006) in basal ganglia firing rates. Additionally, despite the fact that certain symptoms of PD, such as tremor, often instantaneously respond to DBS (Krack et al., 2002), firing rates are not fully modulated until minutes

after DBS onset (Dorval and Grill, 2014). Thus, basal ganglia firing rates are not likely predictive of symptom severity.

Experiments dating back nearly a century have demonstrated that certain, mostly simple information can be encoded within neuronal firing rates, largely starting with Adrian's seminal work from the 1920s, when he experimentally demonstrated that the firing rate of muscle stretch receptors of frogs monotonically increases with increases in strength of physical stimulation until saturation at the maximal firing rate of the neuron (Adrian, 1928). However, as evidenced by language, more complex messages are often more efficiently encoded by patterning than by rate. If one were to imagine a human language system in which all possible messages were encoded rate or volume, it would be difficult to imagine how various messages, such as conveyances of various emotions, often complicated and overlapping, over one-hundred-thousand nouns, tens of thousands of verbs, etc., could be encoded in a rate-based language that could allow for reasonably expeditious communication. Such a hypothetical situation makes it abundantly clear that, when all possible system messages are not easily able to exist simply as scaled versions of one another, patterning within signals becomes important. Therefore, it seems unlikely that certain neuronal messages considerably more complex than simple scaled somatosensation — such as those responsible for governing fine motor control, behavioral and emotional regulation, and cognition — would be most efficiently encoded via simple firing rate-based measures. While the number of messages any single subset of neurons needs to communicate is likely considerably smaller than the number of different messages within an entire human language, it is still unreasonable to expect that neurons with even a moderately large set of non-scalable messages communicate via firing rates.

1.2 Differential Responses to Different Treatments of Parkinson's Disease

Deep brain stimulation and levodopa modulate many aspects of basal ganglia signaling in different ways (Asanuma et al., 2006; Bäumer et al., 2009; Giannicola et al., 2010, 2013; Hilker et al., 2002; Zsigmond and Göransson, 2014). While levodopa reduces firing rates in basal ganglia outputs, such as SNr (Gilmour et al., 2011) from rates increased by PD (Wang et al., 2010), DBS regularizes firing pattern activity (Dorval et al., 2010). Additionally, it is known that DBS does not restore neuron patterning to that in healthy conditions (Agnesi et al., 2013; Dorval and Grill, 2014; Wichmann and Delong, 2011).

Levodopa and DBS do lead to similar lateral motor improvements (Groiss et al., 2009; Herzog et al., 2009), but, given that levodopa and DBS modulate neuronal activity in quite different ways, it is unsurprising that the two therapies result in differences in a number of motor measurements (Herzog et al., 2009; Rocchi et al., 2002; Skodda, 2012; Yamada et al., 2004).

DBS has been reported as improving Unified Parkinson's Disease Rating Scores (UPDRS) in dyskinesias on average by 70%, motor fluctuations by 50%, freezing by 50%, as well as reducing levodopa dosage by 39 and 30% at 12 and 30 months (Krack et al., 2003). However, it frequently does not restore speed of movements (Vaillancourt et al., 2004). Additionally, a large number of PD patients report side effects as a result of DBS (Okun MS et al., 2005). While 46% of patients reporting side effects in the above study were found to have misplaced leads and 12% of patients were found to be misdiagnosed, the remainder suffered side effects despite diagnosis confirmation and stimulation within the intended target. After follow ups, 15% of patients saw only

moderate improvement and 34% of patients failed to improve.

More specifically, DBS has been tied to each of the following side effects: hallucinations, psychosis, depression, apathy, mania, hypomania, euphoria, mirth, hypersexuality, anxiety, cognitive deficits (Burn and Tröster, 2004), and impulsive behavior (Hälbig et al., 2009) Additionally, DBS has been reported as worsening the following PD symptoms: hypokinetic dysarthria and other motor speech problems (Skodda, 2012), apraxia of eyelid (Tommasi et al., 2012), pseudobulbar affect (Chattha et al., 2015), and cognitive deficits and dementia (Fleury et al., 2015).

It is generally thought that some of these side effects are tied to stimulation falling outside the target region. For example, apraxia of the eyelid may be related to lateral current spread into the corticobulbar tract in the internal capsule (Tommasi et al., 2012). However, it is currently unknown how many of these side effects are specifically related to mis-stimulation and how many are inherent side effects of proper stimulation in properly-diagnosed cases with the current stimulation technology and paradigms. Given that DBS does not restore basal ganglia neuronal activity to that observed in healthy individuals, it is unsurprising that some of these side effects are thought to be inherent to stimulation.

1.3 Specific Motivation for and Brief Description of Our Work

Based on all of the above, it was important that we explore the therapeutic mechanisms of deep brain stimulation, as well as the mechanisms of its failures. Given an improved understanding of exactly how DBS works and fails, it would be easier to improve it in the future, enabling better treatment of more patients. The goal of such

improvements in our understanding of DBS underlies the motivation behind the reported work: we set out to advance the understanding of the mechanisms, function, and malfunction of DBS as a treatment for PD. We set out to achieve these goals while focused on the following idea: DBS modulates the messages created and transmitted within and from the basal ganglia, taking signals that correspond with pathological motor activity and adding to them or overriding them in such a way that improves lateral motor pathology while, sometimes, worsening medial motor symptoms and behavioral symptoms.

First, we felt it necessary to expand the systems-level answer to the very important question of how exactly DBS manages to treat lateral motor symptoms of PD as effectively as it does. With this in mind, we determined to test whether directed information between the rodent substantia nigra pars reticulata (SNr) and ventral anterior thalamus (VA) covaried with symptom severity. This connection was chosen given the long-time clinical focus on the basal ganglia's inhibition of the thalamus. The main outputs from the basal ganglia, the internal globus pallidus (GPi) — with a homologue of the entopenduncular nucleus (EN) in rodents — and SNr, act in coordination and apply gabaergic inhibition to their targets in thalamus, the ventrolateral thalamic nucleus (VL), and the VA, respectively. While the GPi–VL pathway is dominant in primates, as evidenced by the larger size of the GPi in comparison to the SNr, the SNr–VA pathway is dominant in rodents, as evidenced by the much larger SNr. Figure 1-1 shows the relevant elements of the basal ganglia pathway in rodents.

We were interested in quantifying informational changes between SNr and VA to understand how pathology arises in a quantitative sense. If information were to covary

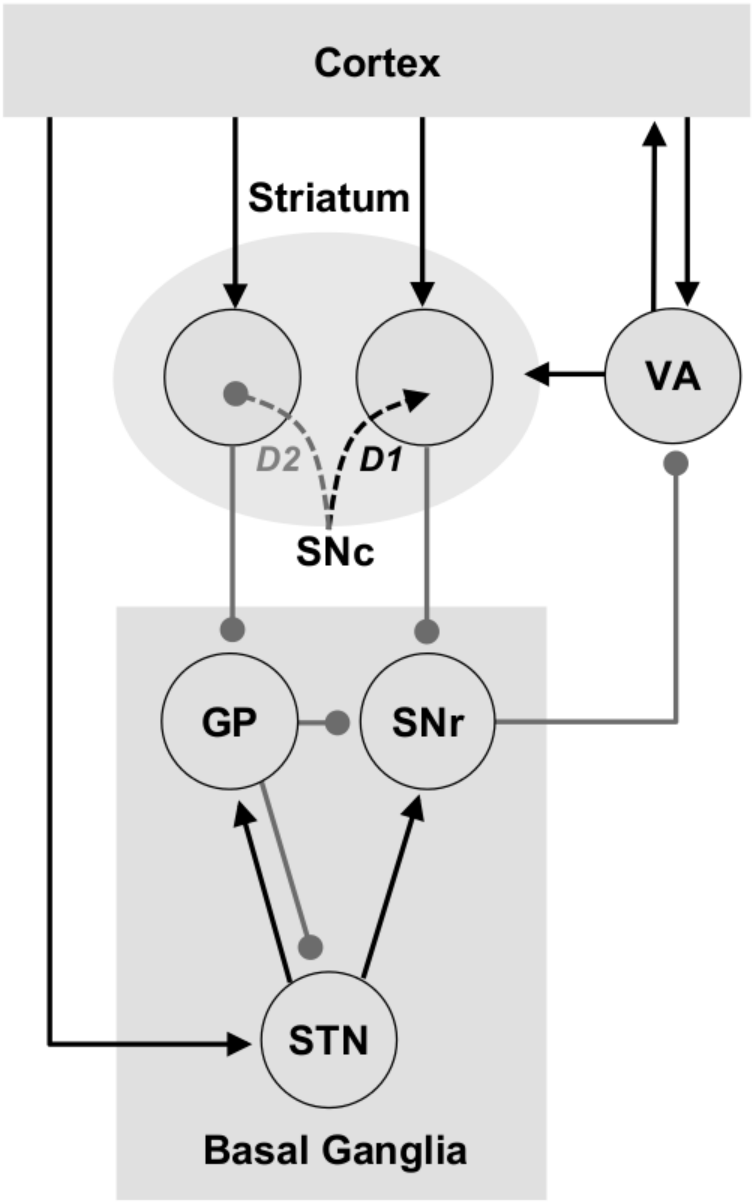

Figure 1-1. Diagram of connections in rodent basal ganglia. Solid black arrows represent excitatory glutamatergic projections; solid grey circles represent inhibitory gabaergic projections; dashed lines from SNc depict dopaminergic projections, with excitatory effects onto D1 neurons in black, and inhibitory effects onto D2 neurons in grey.

with symptom severity, two competing outcomes seemed likely. First, directed information could be increased by Parkinsonism and reduced by DBS from that in the parkinsonian condition. Second, directed information could be reduced by Parkinsonism and increased by DBS from that in the parkinsonian condition. While interspike interval (ISI) entropy bounded the directed information and SNr entropy had previously been reported as increased in the parkinsonian condition and decreased from those levels by DBS, information measures need not increase with increased entropy. While the increased information with PD hypothesis is more intuitive, it is entirely possible for two connected neuron groups to become disordered in a disjointed fashion, thereby increasing their entropies while reducing their directed information.

Either hypothesis would have led to a potentially reasonable interpretation. Had Parkinsonism reduced the directed information between SNr and VA, we would have interpreted this to mean that the transmission of signals responsible for healthy motor function in lateral muscles is reduced by Parkinsonism and DBS functions by reducing the entropic noise floor, enabling information propagation. Instead, we found that Parkinsonism increased the directed information between SNr and VA. We took this to mean that Parkinsonism results in a loss of information channel independence – matching previous work demonstrating that basal ganglia receptive fields widen under PD conditions (Leblois et al., 2006; Vitek et al., 1998) – thus reducing the number of independent information channels, reducing the scope of possible motor activities, driving hallmark parkinsonian motor symptoms. In this model, DBS eliminates or masks pathological information transmission, enlarging the scope of possible motor activities.

Our results and interpretations bring about an interesting explanation for the

parkinsonian symptoms of rigidity, bradykinesia, akinesia, increased muscle tone, and difficulty in movement initiation. If many informational channels that should be independent are no longer independent in the parkinsonian brain, signals containing movement instructions for, say, a bicep, may be transmitted to other muscle groups. When the parkinsonian patient attempts to contract his or her bicep, other muscle groups contract simultaneously. Due to the simultaneously contracting counteracting muscle groups, limbs become rigid, resulting in increased muscle tone. A large barrier to movement develops and a higher effort is required for movements, resulting in bradykinesia. As the disease develops and information channels become less and less independent, bradykinesia eventually develops into akinesia.

Having developed a novel, quantitative explanation of the generation of a number of hallmark parkinsonian symptoms, as well as how DBS treats these symptoms without restoring basal ganglia neural activity to that under healthy conditions, we next sought to develop a better understanding as to how DBS results in certain side effects. Since DBS is implicated in both motor and behavioral side effects, we found it important to study both.

Classic studies have reported that as many as 90% of PD patients have at least some degree of speech dysfunction (Logemann et al., 1978). Most PD speech disturbances are caused by reduced or disrupted motor activity of the vocal system and classified as hypokinetic dysarthria (HD), which is defined as “a multidimensional impairment leading to abnormalities in speech breathing, phonation, articulation, and prosody” (Skodda, 2011). PD patients often experience improvements in speech dysfunction with dopaminergic medication (De Letter et al., 2007a, 2007b), but late-stage

surgical interventions such as pallidotomy, thalamotomy, and DBS have all been reported as worsening HD (de Bie et al., 2002; Burghaus et al., 2006; Intemann et al., 2001; Kim et al., 1997; Romito et al., 2002; Tröster et al., 2003; Umemura et al., 2011).

Despite the fact that PD-associated vocal disturbances have been reported for the better part of a century (Kaplan et al., 1954), these symptoms are still poorly understood, largely due to the ethics of studies of human patients. Prior to our work, high-throughput rodent models had only been used minimally to study parkinsonian vocalization (Ciucci et al., 2008, 2009) and these studies only examined rats under control and 6-OHDA conditions, with analysis performed on the "best" calls.

While previous work demonstrated the capability of a rodent model to match some vocal characteristics of human parkinsonian HD, it had fairly serious limitations in the context of comparison with human HD. First, vocal analysis was not automated and only the "best" 10% of vocalizations were analyzed, potentially introducing selection bias. Additionally, only a subset of rodent vocalizations from one bandwidth category was studied. Finally, the group limited their studies to control and parkinsonian animals and did not confirm whether DBS exacerbated vocal symptoms of Parkinsonism.

With the goal of enabling future electrophysiological work directed at elucidating the underpinnings of the exacerbation of parkinsonian HD by DBS, we improved upon each of these limitations. First, we studied a set of rats under each of control, hemiparkinsonian, and hemiparkinsonian+DBS conditions to demonstrate that DBS does exacerbate vocal symptoms. Second, we designed a methodology for vocal analysis that fully automated the process of vocalization selection using a novel algorithm featuring time-frequency pixelation and de-noising, removing the possibility of selection bias.

Finally, we split our analyses into not only individual utterances (sounds) and multi-syllable vocalizations (words), but we separated frequencies into the common frequency categories of rodent mating call vocalizations (Brudzynski, 2013; Willadsen et al., 2014; Wöhr and Schwarting, 2013). Sounds were split into high frequency (35 kHz and up) and low frequency (20 to 35 kHz) categories, while words were split into high, low, and complex (sounds in both high and low) categories to demonstrate consistency across categories.

Our results, due to automation of vocalization selection, are more robust than those previously presented from other groups and additionally match a number of descriptions of human parkinsonian HD, suggesting the utility of our model for electrophysiological study into parkinsonian HD's underpinnings. We interpret our results as matching human parkinsonian reductions in speech rate, complexity, and word duration.

Despite more than half a century of reports about parkinsonian HD, our work represents the first model from which electrophysiological studies can be performed with regards to the exacerbation of PD vocalization symptoms by DBS. Based on our results, we have proposed a neural-activity-based explanation of HD exacerbation by DBS taking into account the basal ganglia somatotopy, to be discussed in Chapters 3 and 5.

Having studied a DBS side effect that we believe to be dependent on location of stimulation within the somatotopically organized basal ganglia, we next studied a DBS side effect that we hypothesized to be inherent to stimulation that treats side effects, independent of stimulation outside target boundaries. Both dopamine agonist drug therapies and DBS have been associated with impulsive behavior in PD patients, with

some reporting that as many as 39% of patients taking dopamine agonists and 56% of patients receiving DBS experience new-onset impulse control disorders (ICD) of varying severity (Bastiaens et al., 2013; Demetriades et al., 2011; Frank et al., 2007; Jahanshahi et al., 2015; Weintraub and Nirenberg, 2013; Witt et al., 2004).

As with hypokinetic dysarthria, it is difficult to study the mechanisms of ICDs in human patients. Some work has been performed examining DBS-induced ICDs in animal models, which have been used to show that DBS leads to some impulsive behaviors, such as premature responding (Aleksandrova et al., 2013; Desbonnet et al., 2004; Sesia et al., 2010; Summerson et al., 2014), increased perseverative responses (Baunez et al., 2007), and changes in intertrial response (Sesia et al., 2010). Additionally, it has been found that STN lesion leads to many similar behaviors, such as premature response (Baunez et al., 1995; Phillips and Brown, 2000; Uslaner and Robinson, 2006), increased perseverative responses (Baunez and Robbins, 1997, 1999), increased stop response error (Eagle et al., 2008a), and impaired no-go responses (Eagle et al., 2008b).

The studies mentioned above have resulted in improvements in our understanding of ICDs seen in a large percentage of PD patients using both drug therapies and DBS, but certain aspects of new-onset ICDs during DBS use are poorly understood. While results from humans regarding new-onset ICDs following the start of dopamine agonist administration are fairly straightforward, similar human studies regarding new-onset ICDs following DBS are more abstruse. Most measures of impulsivity exhibit worsening under DBS, such as Stroop interference tasks (Jahanshahi et al., 2000; Schroeder et al., 2002; Witt et al., 2004), high-conflict decision making (Cavanagh et al., 2011; Frank et al., 2007), response thresholds (Pote et al., 2016), and a reduction of an influence of task

difficulty on decision making (Green et al., 2013). However, some measures of impulsivity have been reported as both worsening and unchanged, such as go/no-go response time (Campbell et al., 2008; Hershey et al., 2010). While PD patients with slow stop signal reaction times (SSRTs) generally improve with DBS, some patients with relatively normal SSRTs actually become slower with DBS (Ray et al., 2009).

Thus, we chose to study impulsive behavior in a rodent STN-DBS model. We studied task response success and response timing, as well as other measures of impulsive behavior, such as impulsive reward seeking and non-instructed task attempts, in the context of both a go/stop task and a go/no-go task. Our results demonstrate that DBS of a healthy rodent leads to more impulsive behavior in the form of stop and no-go task failure, impulsive reward seeking, and non-instructed task attempts. However, when analyzing the timing of stop and no-go failures, it appears that DBS may induce more serious failures in the context of a go/stop task, lending support to the role of the basal ganglia in action suppression, with necessary information from the STN for action cancellation being interrupted by DBS.

Additionally, our results demonstrate that Parkinsonism fundamentally alters reward circuitry in a way that is not restored by DBS, as evidenced by a reduced response to cues after the onset of parkinsonian symptoms. Additionally, while DBS generally treats motor symptoms, it does not restore response rates. Thus, it may be that PD degrades certain aspects of action selection, and this change is not restored by DBS.

1.4 Summary

These three successfully executed projects fit into the main idea of this dissertation: while DBS is ultimately successful at treating lateral motor symptoms of PD due to modulation of the basal ganglia and, thus, the downstream thalamus, it fails to treat all symptoms and even induces side effects based on its failure to restore basal ganglia neural activity to that seen in healthy individuals. While functional, therapeutic DBS does not revert firing unit or field activity from that seen under hemiparkinsonian conditions to that seen under control conditions, it restores information transmission rates, which covary with — and possibly underlie, at least indirectly — many motor symptoms. When pathological information transmission is reduced, lateral motor symptoms are reduced. While our results demonstrate that DBS exacerbated all vocal symptoms of hemiparkinsonism that we studied, we expect that this could be reversed with multisite stimulation or electrode technologies with current steering capability, such as the μDBS (Willsie and Dorval, 2015b). While we expect that some DBS side effects, such as medial motor symptom exacerbation, could be eliminated or reduced with better electrode technologies, we expect that, because therapeutic DBS does not restore neural activity to that under control conditions, certain side effects, such as impulsive behavior, may be unavoidable with current electrical stimulation techniques.

We have developed a plausible explanation for how PD symptoms emerge and how DBS treats them, a new model of DBS's exacerbation of vocal symptoms experienced by a large percentage of PD patients, new methodology for automatically measuring vocal features and disturbances without selection bias, and a new model of DBS leading to multifaceted impulsive behavior independently from PD symptom

severity. Our work could enable a great deal of future studies and biomedical development, discussed in detail in Chapter 5.

CHAPTER 2

DBS REDUCES PATHOLOGICAL INFORMATION TRANSMISSION

Deep brain stimulators (DBS) have been implanted tens of thousands of times in an effort to treat the motor symptoms of Parkinson's Disease (PD), but the mechanisms of action are unclear. Since linear measures, such as excitation- and inhibition-based changes in firing rate and correlation, have failed to provide insight into the electrophysiological underpinnings of both PD and DBS, we proposed to study these through the lens of information theoretic metrics. We performed these studies in a rodent model of Parkinsonism, examining information transmission between the output of the basal ganglia and its relay center back to cortex in the thalamus. Thus, this chapter presents the study into the relevance of directed information between the rodent substantia nigra pars reticulata and ventral anterior thalamus in the study of deep brain stimulation for Parkinson's Disease.

2.1 Abstract

Subthalamic deep brain stimulation reduces pathological information transmission to the thalamus in a rat model of Parkinsonism. The degeneration of dopaminergic neurons in the substantia nigra pars compacta leads to parkinsonian motor symptoms via changes in electrophysiological activity throughout the basal ganglia.

High-frequency deep brain stimulation (DBS) partially treats these symptoms, but the mechanisms are unclear. We hypothesize that motor symptoms of Parkinson's disease are associated with increased information transmission from basal ganglia output neurons to motor thalamus input neurons, and that therapeutic DBS of the subthalamic nucleus (STN) treats these symptoms by reducing this extraneous information transmission. We tested these hypotheses in a unilateral, 6-hydroxydopamine-lesioned rodent model of hemiparkinsonism. Information transfer between basal ganglia output neurons and motor thalamus input neurons increased in both the orthodromic and antidromic directions with hemiparkinsonian onset, and these changes were reversed by behaviorally therapeutic STN-DBS. Omnidirectional information increases in the parkinsonian state underscore the detrimental nature of that pathological information, and suggest a loss of information channel independence. Therapeutic STN-DBS reduced that pathological information, suggesting an effective increase in the number of independent information channels. We interpret these data with a model in which pathological information and fewer information channels diminishes the scope of possible motor activities, driving parkinsonian symptoms. In this model, STN-DBS restores information-channel independence by eliminating or masking the Parkinsonism-associated information, and thus enlarges the scope of possible motor activities, alleviating parkinsonian symptoms.

2.2 Introduction

Deep brain stimulation (DBS) is an accepted therapy for several neurological conditions (Benabid et al., 1998; Hariz et al., 2013). In particular, DBS of the subthalamic nucleus (STN) or globus pallidus internus (GPi) can alleviate motor

symptoms of Parkinson's disease (PD), including bradykinesia, rigidity, and tremor (Limousin-Dowsey et al., 1999; Lyons and Pahwa, 2004). These motor symptoms are associated with pathological neural activity in basal ganglia that propagates into the thalamocortical motor loop (Chesselet and Delfs, 1996; Galvan et al., 2015). Effective DBS modulates the neural activity in basal ganglia (Benazzouz et al., 2000; Boraud et al., 1996; Da Cunha et al., 2015) and consequently motor thalamus (Anderson et al., 2003; Hashimoto et al., 2003; Hershey et al., 2003), but the therapeutic mechanisms of this modulation are poorly understood.

Over the past two decades, the accepted model of pathological neural activity in PD has shifted, from one based merely on excitation- and inhibition-driven changes in firing rate, to one based on changes in firing patterns. Throughout the basal ganglia-thalamic circuit, neurons burst (Bergman et al., 1994; Magnin et al., 2000; Tang et al., 2005) and oscillate (Brown et al., 2004; Raz et al., 2000) more in the parkinsonian brain. Supporting this change in firing pattern model, therapeutic DBS reduces those bursts (Anderson et al., 2003; Grill et al., 2004; Tai et al., 2012) and oscillations (McConnell et al., 2012; Meissner et al., 2005). With others, we have argued that this PD-associated pathological activity constitutes substantial neurological disorder, and that DBS alleviates PD-symptoms by regularizing neural activity in computational (Dorval et al., 2009; Guo et al., 2008; Rubin and Terman, 2004; So et al., 2012a), rodent (Degos et al., 2005; Dorval and Grill, 2014), non-human primate (Bar-Gad et al., 2004; Dorval et al., 2008; Hashimoto et al., 2003), and human studies (Dorval et al., 2010).

Neuronal disorder is readily quantified as firing pattern entropy, which bounds and contributes to information directed between neurons. This directed information

measures the influence that one cell has on another cell. If disordered firing patterns contribute to parkinsonian symptoms, we hypothesize that they do so by transmitting pathological information from basal ganglia to downstream structures in the thalamo-cortical motor loop (Grill et al., 2004). To test this hypothesis experimentally, we used a rodent model of PD to examine neuronal information directed from basal ganglia efferents in substantia nigra pars reticulata (SNr), to the ventral anterior (VA) thalamus under healthy and hemiparkinsonian (hPD) conditions, and in the presence of behaviorally therapeutic STN-DBS. In hPD relative to control, we found large increases in information directed orthodromically (i.e., in the anterograde direction) from SNr to VA, and antidromically (i.e., in the retrograde direction) from VA to SNr. These hPD-associated informational increases were reversed entirely by therapeutic STN-DBS.

2.3 Materials and Methods

All surgical and experimental procedures were performed at the University of Utah, approved by the Institutional Animal Care and Use Committee of the University of Utah, and complied with U.S. Public Health Service policy on care and use of laboratory animals.

2.3.1 Experimental Procedures

The timeline of the protocol for 5 Long-Evans rats of both sexes weighing 225 to 325 g, comprised the following: surgical implantation followed by a 2-week recovery period; 2-5 control recording sessions at least one day apart; 6-OHDA injection followed by a two week recovery period; and 4-8 experimental recording sessions at least one day

apart; and for three rats, terminal perfusion, fixing, and brain removal.

2.3.1.1 Surgical procedure. Rats were administered orally 10 mg of rimadyl (Bio-Serv, Flemington, NJ), and after consumption, anesthetized with 2% isoflurane. The surgical site was shaved and disinfected with isopropyl alcohol and povidone-iodine. Rats were placed on a heating pad in a stereotactic frame (Kopf Instruments, Tujunga CA), and an incision was made and opened to the skull. Craniotomy sites were measured and marked with respect to bregma (Paxinos and Watson, 2008). Seven titanium bone screws were inserted through burr holes in the skull to anchor the eventual acrylic cap to the skull. Stainless steel ground wires were attached to two of the anchor screws.

Neural implants included a cannula, four-channel stimulating array, and two 16-channel recording arrays. To enable the eventual insertion of a needle to the medial forebrain bundle (MFB), a 23-gauge stainless steel cannula was implanted through a burr hole 1.0 mm anterior and 2.0 mm lateral, in the sagittal plane and angled 26.5° posteriorly from the coronal plane. A four-channel micro-stimulating array – 2×2 grid of 75 μm platinum-iridium electrodes (~100 kΩ @ 1 kHz) with 400 μm spacing (Microprobes for Life Science, Inc., Gaithersburg, MD) – was implanted vertically into the STN (3.6 mm posterior, 2.6 mm lateral, and 7.8 mm ventral). Medial electrodes were 500 μm longer than their lateral counterparts to match STN anatomy. Sixteen-channel micro-recording arrays – 4×4 grid of 20 μm stainless steel electrodes (~1.0 MΩ @ 1 kHz) with 400 μm spacing (ibid) were implanted into VA and SNr. The VA array reached its target (2.1 mm posterior, 1.9 mm lateral, and 6.2 mm ventral) by advancing 6.3 mm through a burr hole 1.1 mm posterior and 1.9 mm lateral, in the sagittal plane and angled 9.0° posteriorly from the coronal plane. The SNr array reached its target (5.5 mm

posterior, 2.3 mm lateral, and 7.7 mm ventral) by advancing 7.8 mm through a burr hole 6.5 mm posterior and 2.3 mm lateral, in the sagittal plane and angled 7.4° anteriorly from the coronal plane.

After each hardware element was implanted, a layer of dental acrylic was applied to attach it firmly to at least one of the anchor screws. Following all implantations, ground contacts of the recording arrays were tied to wires on the ground screws. The screws, cannula, and arrays were encased in a thick dental acrylic cap, built smoothly to include no sharp edges or points. The incision was sutured around the acrylic head-cap, with triple antibiotic ointment applied inside and outside of the wound to prevent infection. Rats were administered the analgesic ketoprofen (5 mg/kg) via intraperitoneal injection, monitored for 2 hours, and allowed to recover for 14 days prior to recordings.

2.3.1.2 Unilateral dopamine lesion. After completion of both behavioral and electrophysiological recordings (see below), rats were anesthetized with 2% isoflurane and given intraperitoneal injections of desipramine hydrochloride (25 mg/kg) and pargyline hydrochloride (50 mg/kg) before being placed in the same stereotactic frame. A 32-gauge needle (Hamilton Co., Reno, NV) was inserted through the angled cannula 6.7 mm beyond the cranial surface, to the MFB target (2.0 mm posterior, 2.0 mm lateral, 6.0 mm ventral). The needle was inserted an additional 0.5 mm, left for 5 minutes to create a pocket, and then retracted by 0.5 mm. Thirty minutes after the intraperitoneal injections, 8.0 µg of 6-OHDA dissolved in 8.0 µl of saline were injected at a rate of 1.0 µl/min. Ten minutes after injection, the needle was withdrawn at a speed not exceeding 1.0 mm/min. Rats were returned to their home cages for 14 days before recording under hPD and STN-DBS conditions.

2.3.1.3 Deep brain stimulation. To provide DBS to the STN, rats were briefly anesthetized with 2% isoflurane and a four-channel tether was attached to the connector of the micro-stimulating array on the head. Rats were quickly moved to the recording chamber before awaking, and the other end of the tether was connected to an analog stimulator (Grass Technologies, Warwick, RI). Bipolar stimulation was delivered through the micro-stimulating array, with both medial contacts set as anode and both lateral contacts set as cathode. The stimulation waveform consisted of symmetric, 100 μs biphasic current pulses repeating at 100 Hz. Two weeks following 6-OHDA injection, stimulation thresholds were determined by gradually increasing stimulation amplitude until threshold, denoted by the appearance of physical side effects (~200 μA). The DBS-associated side effects included atypical whisker twitching, other dystonic facial contractions, or repetitive rotations contralateral to stimulation. This process was repeated 3 times for each animal to determine a truly minimal threshold. Therapeutic DBS amplitude was then set to 90% of the minimum side-effect threshold. While stimulation was applied only during DBS trials, the tether was connected during some healthy-control and hPD trials to ensure that the tether did not induce significant changes in either behavior or electrophysiological activity.

2.3.1.4 Behavioral recording protocol. In four of five rats, left-side versus right-side body asymmetry was quantified using a custom rat tracking system. Rats were placed in a darkened 30×45 cm box and recorded from above with an infrared camera for 60 minutes. In real time, custom software differentiated the dark coat of the rat from the white bedding, and calculated rat position and orientation within the box. Rats were typically untethered during healthy and hPD trials, but were necessarily tethered during

DBS trials. Subsequent to the behavioral sessions, data files containing rat location and orientation were analyzed to quantify the leftward and rightward turns the rat made in each trial.

A fifth rat completed the study before completion of the rat tracking system. In this rat, a standard dextroamphetamine-induced rotation protocol was used to verify an increase or decrease of left-side versus right-side body asymmetry under each condition (Maesawa et al., 2004). Briefly, under each condition, 5 mg/kg of dextroamphetamine was injected intraperitoneally. The rat was placed in its home cage, and complete rotations in both directions were counted manually for 30 minutes. An hPD condition was identified when the rat performed at least 10 more ipsilateral rotations than contralateral rotations per minute; an hPD-alleviated condition, produced by STN-DBS, was identified when the rat performed at most 6 more ipsilateral rotations than contralateral rotations per minute.

2.3.1.5 Electrophysiological recording protocol. Rats were briefly anesthetized with 2% isoflurane and the connectors of their micro-recording arrays were attached to a pair of sixteen-channel head stages and associated tethers to a multichannel stimulation and recording system (SnR, Alpha Omega, Alpharetta, GA). For STN-DBS trials, rats were additionally connected to an analog stimulator with a four-channel tether, as described above. Ten minutes after waking in their home cages with lids removed, electrophysiological recordings began and lasted 15 min. Local field potentials (LFPs) and threshold-crossing segmented data were referenced to transcranial ground screws and recorded simultaneously from both SNr and VA. Segmented data thresholds were chosen to include action potential traces, while minimizing noise and low-amplitude multiunit

activity.

2.3.1.6 Histological analysis. Of five rats in the study, the head-caps of two dislodged before the target number of hPD and DBS trials (5 each) had been completed, and those rats were euthanized without perfusion. The remaining three rats were perfused with phosphate buffer solution and fixed with 4% paraformaldehyde. Brains were immediately removed and soaked in the same formalin. After 24 hours, brains were transferred to phosphate buffer solution, sectioned into 200 μm slices, and set onto slides. After 24 hours of drying, slides including STN, SNr, or VA were stained with cresyl violet by standard methods. Gross anatomical analysis verified all electrode locations as being within SNr, VA, and STN.

2.3.2 Data Analyses

Analyses were performed on standard computers. Unit spike sorting was done in Plexon Offline Sorter (Plexon, Inc., Dallas, TX) and all other analyses were done in MATLAB (The MathWorks, Natick, MA).

2.3.2.1 Behavioral analysis. Rat position and orientation during behavioral trials were recorded by custom tracking software at 5-10 samples/s. We integrated the total degrees rotated to the right (θ_R) and to the left (θ_L) during each 60-min trial. Given an injection of 6-OHDA to the right MFB, symptoms of hPD should present on the left side of the body, and the rats should rotate to the right, ipsilateral to injection. Ipsilateral rotation preference was calculated as: $100\% \times \theta_R / (\theta_L + \theta_R)$.

2.3.2.2 Spike train analysis. Voltage-threshold crossing segments were extracted from 500 μs before threshold crossing to 1500 μs after threshold crossing. Unit

waveforms were isolated in Plexon Offline Sorter using standard techniques. Large cross-channel events and stimulation artifacts, which were consistently much larger than neuronal unit activity, were invalidated. Principle components of the remaining waveforms were calculated and used to sort the waveforms into clusters via expectation maximization. When that algorithm failed to identify an obvious unit cluster, the waveforms were resorted via the valley seek algorithm. Unit clusters with an average waveform that differed qualitatively from a stereotypical extracellular action potential were manually removed. Units separated from an unsorted noise cluster and all other unit clusters at an alpha-level of 0.05 were included in subsequent analysis.

Because stimulation artifacts prevented waveform detection over ~1 ms windows every 10 ms, we analyzed data both with and without blanking 1.0 ms of activity, repeated every 10 ms. Comparing data collected under control or hPD conditions to data collected under STN-DBS conditions, qualitative differences in information metrics between analyses that did or did not include the blanking procedure were uncommon and are described in results. In general, we present information results from data analyzed without the blanking procedure. However, to correct for the simple spike frequency bias from detecting threshold crossings for only 9 ms out of every 10 ms, firing rates from STN-DBS trials were multiplied by ten-ninths.

Firing rate was found for each unit with at least 500 spike waveforms. Firing pattern entropy was estimated for the same units, from relative duration distributions of inter-spike intervals (ISIs) segmented logarithmically into 5 bins per decade (Dorval, 2008). From each distribution of ISIs y, firing pattern entropy was calculated according to the following:

$$H(y) = -\sum_i p(y_i) \log_2 p(y_i) \quad (1)$$

where $p(y_i)$ is the probability of an ISI being in bin i, and the entropy $H(y)$ has units of bits/spike (Rieke et al., 1993; Strong et al., 1998).

Cross-correlations were calculated between all simultaneously recorded neurons. Unit impulse spike trains were convolved by a gaussian kernel with a 25 ms standard deviation and unit area. The waveforms were mean subtracted, and correlated with those from other units recorded simultaneously. Those cross correlation functions were compared for maximum values and periodicity.

2.3.2.3 Neuronal information. Directed information was estimated for each pair of neurons recorded simultaneously, from distributions of the cross-spike intervals (CSIs) binned identically to the ISIs (Dorval, 2011; Dorval and Grill, 2014). From each distribution of CSIs x, information directed from cell x to y was found as:

$$I(y:x) = H(y) - H(y \mid x) \quad (2)$$

from conditional entropy

$$H(y \mid x) - H(y,x) - H(y) \quad (3)$$

and joint entropy,

$$H(y,x) = -\sum_{ij} p(y_i, x_i) \log_2 p(y_i, x_i) \quad (4)$$

where $p(y_i, x_j)$ is the probability that an ISI is in bin i and the simultaneous CSI is in bin j. Entropy and information estimates from two-dimensional, consecutive ISI and CSI distributions yielded qualitatively similar results for high firing rate pairs, but variable results for low rate pairs due to under-sampling problems associated with too few ISIs and CSIs. Thus, we present only one-dimensional entropy and information estimates.

We label the information defined above as the conditional information.

$$I_{cond} = H_{naive} - H_{cond} \quad (5)$$

Conditional information I_{cond} is necessarily non-negative, as the conditional entropy H_{cond} must be less than or equal to the naive entropy H_{naive}. Problematically, for two completely unrelated spike trains given finite data sets, conditional entropy H_{cond} will be less than naive entropy H_{naive}, ensuring that conditional information I_{cond} will be positive, despite signal independence. To correct for this positive bias, we estimated directed information as:

$$I_{dir} = I_{cond} - I_{shuf} \quad (6)$$

from the shuffled information.

$$I_{shuf} = H_{naive} - \langle H_{shuf} \rangle \quad (7)$$

The mean shuffled entropy $<H_{shuf}>$ was found as the average of the conditional entropy calculated from each of 100 simulations in which the ISIs *y* were kept in the same order, but the CSIs *x* were reordered randomly (Gaudry and Reinagel, 2008).

The shuffled information quantifies the mean information that would be estimated from the ISI and CSI distributions given true independence of cells *x* and *y*. Subtracting this shuffled information from the conditional information yields a bias-corrected, directed information I_{dir}. For a set of truly independent neurons, the distribution of bias-corrected information would be gaussian with zero mean. When this process was applied to our data, the resulting distribution was nearly gaussian, with a prominent mode near 0 bits/spike but a long tail in the positive direction. This long positive tail comprises pairs with substantial directed information, while the negative side represents the left half of the zero-mean distribution of truly independent pairs. Thus, the left half of a gaussian curve was fit to the negative side of the bias-corrected distribution, yielding the expected standard deviation if all pairs were truly independent. Directed information between pairs at least 1.645 standard deviations above zero, and thus highly unlikely to be independent, were considered significantly informative ($\alpha = 0.05$).

2.3.2.4 Local field potentials. In 4 animals, field activity was recorded simultaneously with unit activity and low pass filtered below 675 Hz. Power spectral densities were calculated for all LFPs via standard methods. To co-analyze LFPs with single unit activity, spike times were converted to unit impulse trains. Spectral cross bicoherence was computed for simultaneously recorded LFPs and spike trains on the

same channels, according to standard methods. This cross bicoherence reports the strength of phase coupling between all frequencies in the LFPs with all frequencies in the spike trains, normalized from 0 to 1. Qualitative effects regarding beta-beta bicoherence were similar in all animals, but one animal was excluded from the population average due to a substantially lower bicoherence across all frequencies.

2.3.2.5 Statistical comparisons. Where statistical significances are associated with results, as noted in several of the figures, the relevant statistical test is abbreviated in the text. Summary values of approximately gaussian-distributed results are presented as mean plus or minus standard error, mean±s.e. Summary values of non-gaussian results were found from 100,000 bootstrapped populations resampled with replacement, presented as means spanning the 25^{th} to 75^{th} percent confidence intervals, mean±c.i. Statistical test abbreviations: anova = analysis of variance; Ttest = student T test; bca = bootstrapped confidence assessment.

2.4 Results

The following includes results from 5 rats that developed hPD symptoms alleviated by STN-DBS.

2.4.1 Model Validation

Motor symptoms of hPD were assessed from video analysis of unrestrained movements in 1-hour behavioral trials (Fig. 2-1a). Rats turned more ipsilaterally than contralaterally in the hPD condition ($p_{Ttest}<.05$), and exhibited no directional preference in either control or STN-DBS conditions (Fig. 2-1b). Further, there was a behavioral

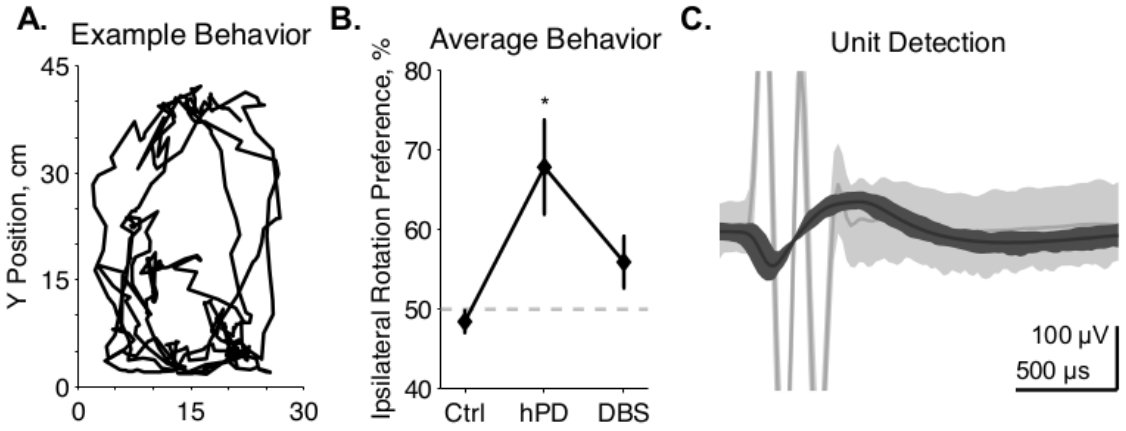

Figure 2-1. Experimental methods. (A) Example movements from 2 min of unrestrained rat behavior, collected 2 weeks after 6-OHDA injection to the right MFB. Rat completed multiple clockwise circles, ipsilateral to injection. (B) Behavioral effects of 6-OHDA injections and STN-DBS, quantified as rotation to the right divided by the integrated rotation in both directions, expressed as a percentage, mean ± SE. Asterisk denotes statistically significant difference from 50% ($p_{\text{t-test}} < 0.05$). Lesioned rats rotate preferentially ipsilateral to injection, and are thus classified as hemiparkinsonian (hPD). (C) Representative example of a neuronal spike unit (*dark gray*) sorted separately from a DBS artifact (*light gray*), with center lines showing the average waveforms of both clusters.

effect of condition ($p_{anova}<.05$), with rats rotating more ipsilaterally than contralaterally in the hPD condition ($p_{Ttest}<.05$). These data summarize the responses of 4 of the 5 rats; a fifth rat had symptoms quantified via free rotation counting under dextroamphetamine injection and had similar results to those evaluated with the video-tracking system.

2.4.2 Single-Unit Activity

We recorded extracellularly from SNr and VA during unrestrained behavior in all conditions – healthy, hPD, and with STN-DBS – and isolated individual unit action potentials offline (Table 2-1). Firing rates of individual neurons varied greatly and standard deviations were large in both anatomical locations under all conditions (Fig. 2-2a,b). No significant changes were noted between conditions in the SNr. However, the mean firing rate in VA did depend on condition ($p_{anova}<.05$), significantly reduced in the STN-DBS condition ($p_{bca}<.001$), relative to both healthy and hPD conditions. Distributions of ISIs for each unit were compared between the hPD and DBS conditions (Fig. 2-2c). With a fine temporal resolution (25 bins per decade), neurons in the DBS condition exhibited strongly multimodal distributions in both SNr and VA (Fig. 2-2C, *thin lines*), with peaks at 10 ms and the subharmonics thereof (i.e., 20 ms, 30 ms, etc). This regularity follows from entrainment of the neuronal activity to the 100 Hz DBS. However, for units with lower firing rates, 15-min trials did not yield enough data to use this high of a temporal resolution. To include all neurons under identical analytical conditions, we constructed all distributions with a lower resolution of 5 bins per decade (Fig. 2-2C, *thick lines*). In the example, note that the 10 ms intervals are no longer visible, but the STN-DBS distribution is substantially narrower than the hPD distribution.

Table 2-1. Number of neuronal units and pairs

	Ctrl	hPD	DBS
Single Units			
SNr	53	26	30
VA	50	27	25
Unit Pairs			
SNr → VA *(Orthodromic)*	95	95	73
VA → SNr *(Antidromic)*	95	95	73

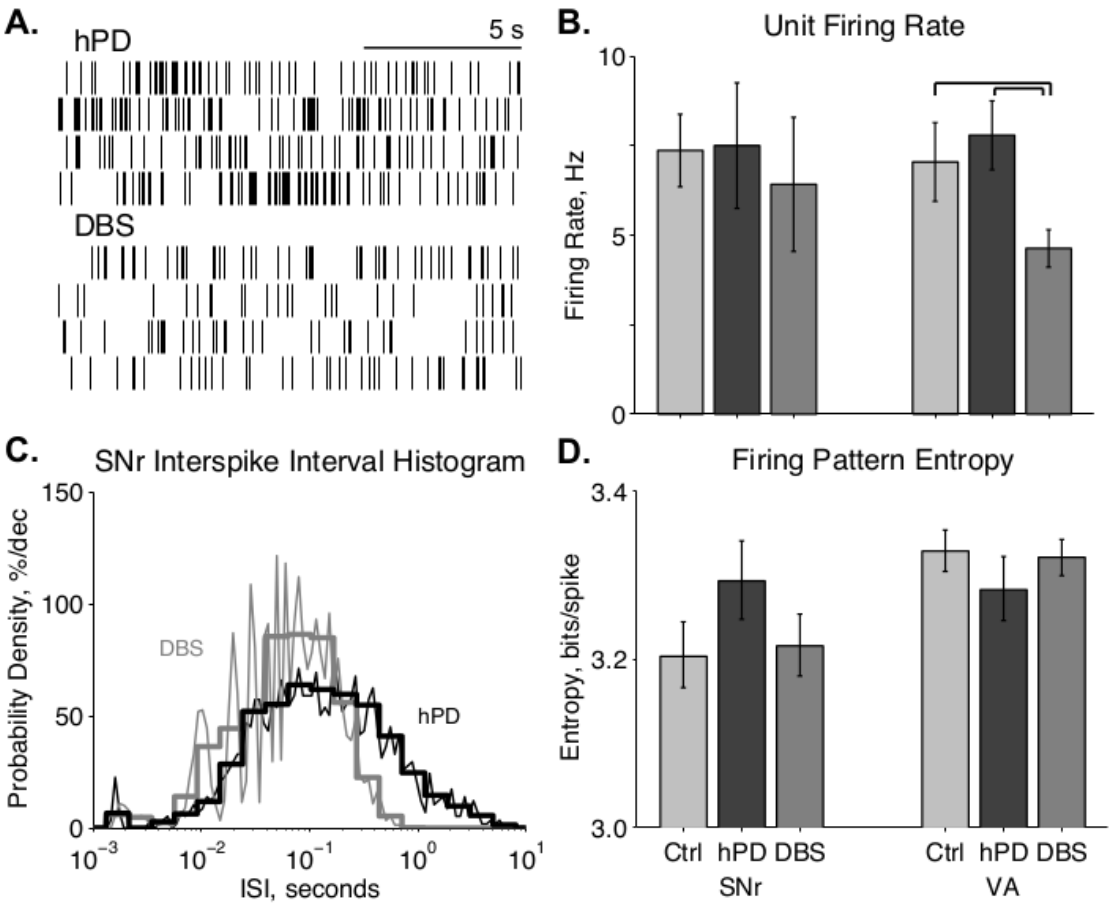

Figure 2-2. Single unit firing pattern activity. (A) Representative rastergrams of four consecutive 15 s intervals recorded from the same VA neuron in hPD and STN-DBS conditions, firing at ~8 Hz and ~3 Hz, respectively. (B) Population firing rates of single units in SNr and VA in all conditions, mean ± 50% c.i. Unit rates ranged from ~1 Hz to over 50 Hz, and this extreme variability nullified statistical differences between most conditions. In VA, however, STN-DBS did reduce firing rates significantly from healthy and hPD levels ($p_{bca} < 0.001$). (C) Representative fine (*thin lines*, 25 bins/decade) and coarse (*thick lines*, five bins/decade) ISI histograms of an SNr neuron in the hPD and STN-DBS conditions. The wide distribution in the hPD case is regularized via entrainment to 100 Hz DBS, as shown by ISI peaks at 10 ms and subharmonics thereof, and a narrowing of the full distribution. (D) Population firing pattern entropy estimated from coarse (five bins/decade) ISI histograms, mean ± 50% c.i. A trend toward SNr entropy increase in the hPD condition did not reach significance with respect to either healthy ($p_{bca} = 0.06$) or STN-DBS ($p_{bca} = 0.07$) conditions.

From those distributions, firing pattern entropy was estimated for all neurons in both SNr and VA in all conditions. In VA, there were no significant changes in firing pattern entropy between conditions. In SNr, there was a trend toward increased entropy in the hPD condition relative to both the healthy (p_{bca}=.06) and DBS conditions (p_{bca}=.07); while not significant, the amplitude of these changes closely matched previously published results (Dorval and Grill, 2014). These same distributions and entropy estimates were then used to calculate directed information, as described below.

2.4.3 Paired-Unit Activity

Cross correlations of neuron pairs across SNr and VA yielded no statistically significant changes in correlation between conditions. To test whether pairs of neurons were truly independent, and not merely uncorrelated, we calculated the information directed from each neuron to all other simultaneously recorded neurons.

Distributions of inter-spike intervals (ISIs) and cross-spike intervals (CSIs) were calculated from the spike times of simultaneously recorded neurons, and the directed information (bits/spike) was estimated for all simultaneously recorded pairs. The information that one cell directs toward another can be quantified as the amount by which the firing activity of the first cell modifies the activity of the second cell (Fig. 2-3a). In this example, when an SNr cell (not shown) has not fired in the past second, the ISI distribution of a VA cell has a mode of ~40 ms (dark grey), indicating rapid firing. In contrast, when that SNr cell has fired in the past second, the ISI distribution of the VA cell has a mode of ~250 ms (light grey), indicating slow firing. Thus, by observing only

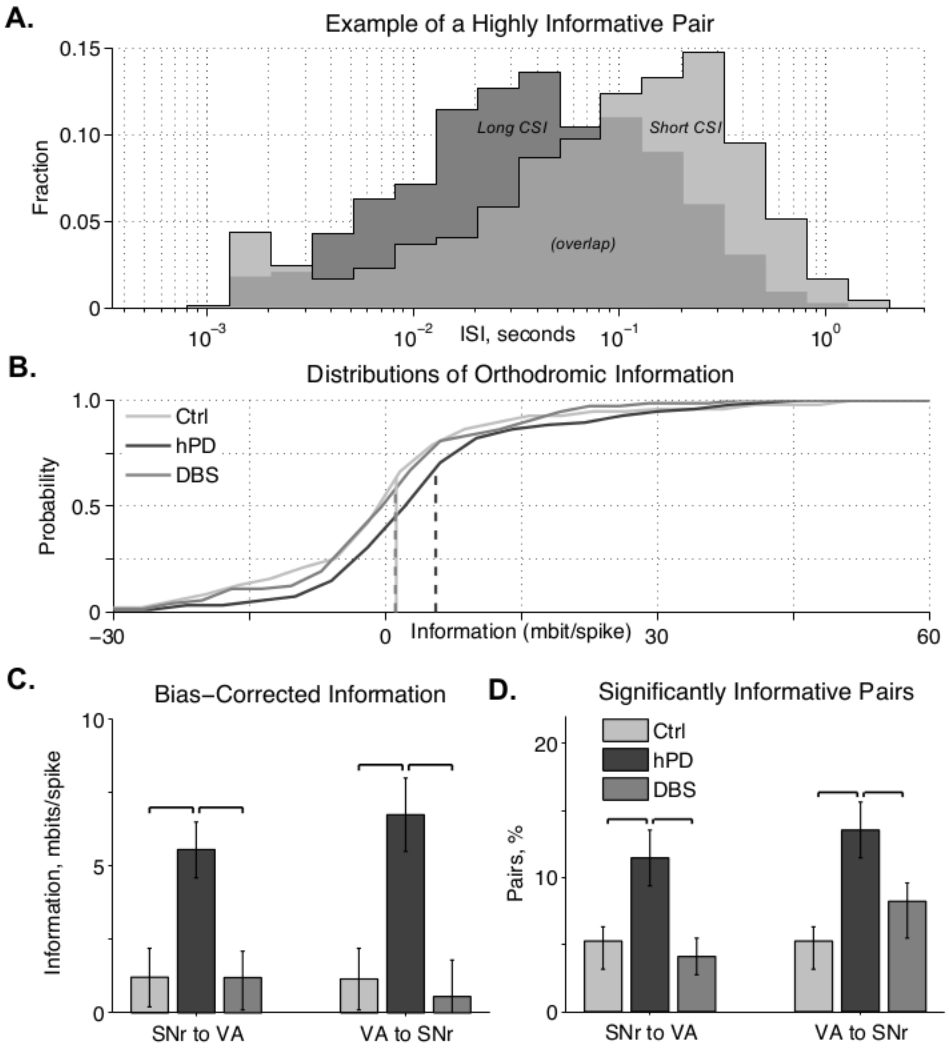

Figure 2-3. Paired unit directed information. (A) Example ISI histograms of one VA neuron, when a particular SNr neuron has (*light gray*) or has not (*dark gray*) spiked in the past second. A spike in the SNr cell alters the ISI histogram of the VA cell, meaning that the VA spike train carries information about the SNr spiketrain. (B) Cumulative information distributions of all SNr to VA pairs directed orthodromically. Control and STN-DBS distributions have negligible medians (i.e., at zero information probability ≈0.5) and means (*dashed lines*), which happen to overlap at ~1 mbit/spike, indicating that randomly selected cell pairs do not transmit significant information; in the hPD condition, however, the distribution has a substantially greater median and mean, indicating that many pairs do transmit information. (C) Bias-corrected information between all pairs in both directions, mean ± 50% c.i. Directed information was increased by hPD induction, and decreased by therapeutic STN-DBS; significance noted with black overscores ($p_{bca} < 0.05$). (D) Percentage of pairs in each condition transmitting significant information quantified as at least 1.645 standard deviations (i.e., $p < 0.05$) above 0, percentage ± 50% c.i. More pairs transmitted significant information in the hPD compared to the other conditions; significance noted with black overscores ($p_{bca} < 0.05$).

the output of the VA cell, one can predict the recent activity of the SNr cell; in other words, the VA cell conveys information about the SNr cell.

After correcting for undersampling bias, the negligible information pairs are expected to constitute a zero mean, approximately gaussian distribution. Thus, highly positive information pairs that do not fit under the gaussian curve (Fig. 2-3b, *right-hand tail*) do not come from the zero-mean distribution, and thus convey directed information. Directed information between regions varied with condition ($p_{anova}<.05$) in both directions (Fig. 2-3c). Directed information increased between the healthy and hPD conditions, orthodromically from SNr to VA ($p_{bca}=.005$) and antidromically from VA to SNr ($p_{bca}=.004$). Further, application of STN-DBS reduced directed information in both the orthodromic ($p_{bca}=.003$) and antidromic ($p_{bca}=.003$) directions. There were no significant differences in directed information between healthy and DBS conditions.

To isolate only the pairs conveying statistically significant levels of information at the $\alpha = 0.05$ level, we computed the standard deviation of the zero-mean gaussian distributions, and counted the fraction of pairs conveying at least 1.645 standard deviations worth of information (Fig. 2-3d). In the hPD condition relative to healthy, more pairs were significantly informative in both orthodromic ($p_{bca}=.017$) and antidromic ($p_{bca}=.008$) directions. In the DBS condition, relative to hPD, fewer pairs were significantly informative in the orthodromic ($p_{bca}=.006$) and antidromic direction ($p_{bca}=.05$). There were no significant differences between healthy and STN-DBS conditions, in either direction.

The above comparisons were repeated with an imposed 1.0 ms blanking period to simulate the artifact in healthy and hPD trials, and qualitative results were mostly

unchanged with or without blanking. The one exception was that the reduction in the number of informative antidromic pairs from hPD to STN-DBS lost significance with blanking (p_{bca}=.16). However, the result that STN-DBS reduces antidromic information is still supported with blanking, through the reduction in the mean VA-to-SNr information from hPD to STN-DBS (p_{bca} = .03).

2.4.4 Unit-Field Coherence

The power-spectral densities of LFPs revealed very little of interest in either SNr or VA. In particular, changes in 20-30 Hz beta activity were not significant between conditions. However, the expected field activity at 100 Hz and its harmonics were observed in the STN-DBS condition in both locations, consistent with stimulation of the STN (Fig. 2-4, *left*). Similarly, the cross correlations of LFPs recorded from different electrodes in SNr and VA did not change significantly between conditions.

To test whether local field activity was independent of unit activity, we found the cross bicoherence of each unit with the local field recorded from the same electrode (Fig. 2-4, *right*). Unit-field cross bicoherence revealed a prominent interaction between high beta frequencies in SNr in the hPD condition in all four rats with recorded LFPs, but not the healthy or STN-DBS conditions in any of the rats. While beta power was not strong enough or enduring enough to manifest in the power spectra, the strong coherence between neuronal and LFP beta activity underscores the relevance of the 25-35 Hz frequency range to the hPD condition.

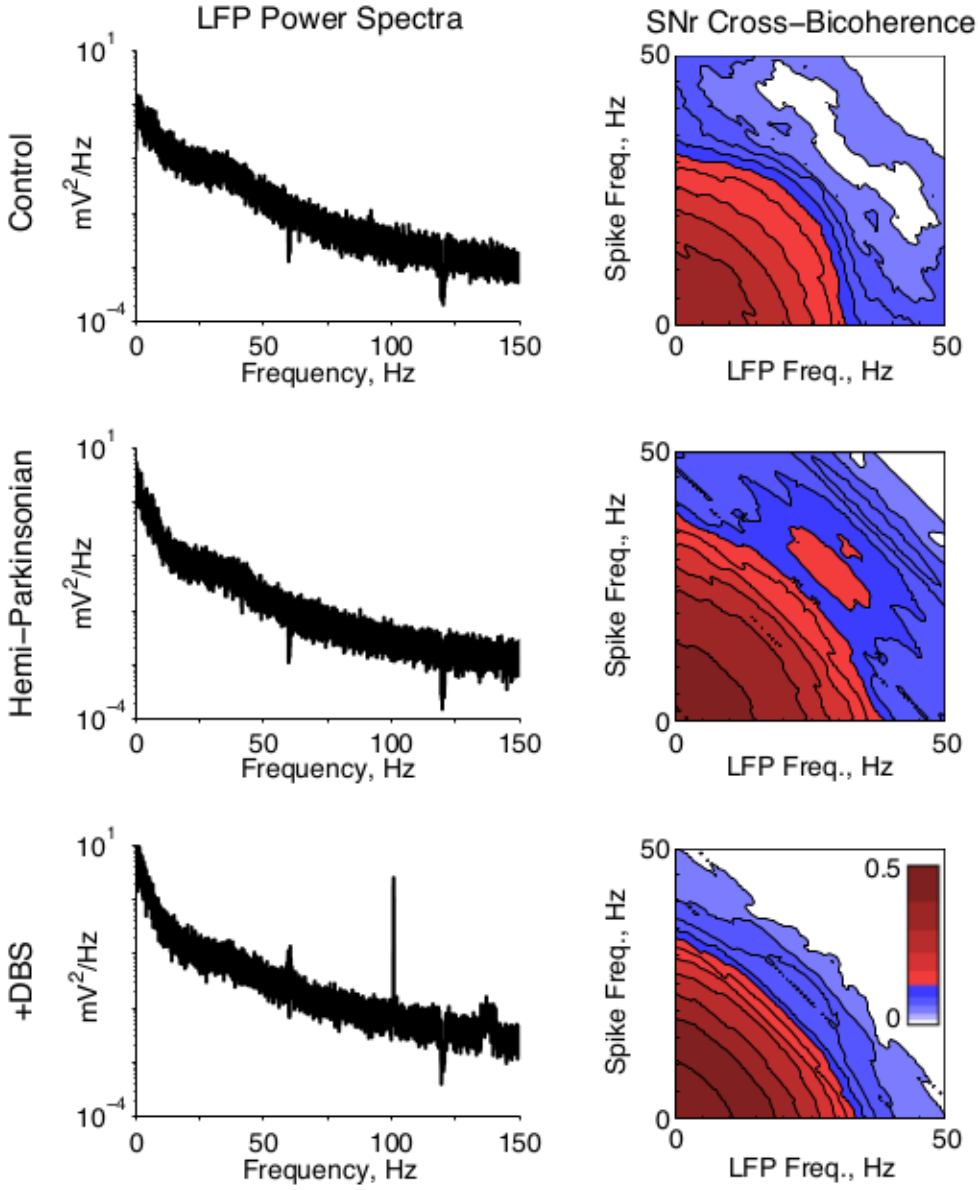

Figure 2-4. Local field potential activity. (Left) Representative LFP power spectra from SNr in all conditions. A strong 100 Hz peak in the STN-DBS condition reflects the stimulation frequency. (Right) Population average of the cross bicoherence between the unit activity and LFPs recorded on the same electrode in SNr, for all conditions. A prominent peak indicates strong beta-beta bicoherence centered at ~28 Hz in both unit and LFP frequency. Cross bicoherence at higher frequencies was generally elevated in hPD condition relative to control, suggesting stronger spike entrainment to higher frequency synaptic activity; and generally suppressed in the STN-DBS condition relative to hPD and control, suggesting relative independence of spiking from higher frequency synaptic activity.

2.5 Discussion

The hallmark motor symptoms of PD are driven by changes in basal ganglia neural activity. Early models of PD focused on neural firing rates, predicting that symptoms resulted from over-inhibition of the thalamus by the outputs from the basal ganglia (Bergman et al., 1994; Mink, 1996; Molnar et al., 2005). However, firing rate models of basal ganglia neural activity are not adequate to explain parkinsonian motor symptom severity, as DBS can actually increase the firing rates of neurons that inhibit the thalamus (Anderson et al., 2003; Bar-Gad et al., 2003; Hashimoto et al., 2003). Several therapies – specifically medication with levodopa, stereotactic ablation of the STN, and high-frequency DBS of the STN or internal globus pallidus – alleviate motor symptoms, but these therapies each modify neuronal activity in distinct ways.

Given the variety of neuronal responses to disparate therapeutic interventions, it is unsurprising that the motor symptoms of PD manifest from changes in firing patterns, rather than merely changes in firing rate (Wichmann and DeLong, 2003). In this work, we began with the hypothesis that these changes in firing pattern constitute changes in neural information directed between neurons and nuclei. We demonstrated that lesioning the rat SNc increased information transmission between the SNr and VA, in both the orthodromic (i.e., anterograde) and antidromic (i.e., retrograde) directions, and that STN-DBS decreased information transmission back to levels similar to those seen prior to 6-OHDA administration.

Our results support the hypothesis that parkinsonian motor symptoms result from the passage of extraneous information from the ventral basal ganglia to thalamic relay neurons (Grill et al., 2004). Neuronal information transmission is bounded by neuronal

firing pattern entropy, and computational studies have suggested that increased entropy in the globus pallidus, upstream from the SNr, induces errors in information transmission through the thalamus (Dorval et al., 2010; Guo et al., 2008; Rubin and Terman, 2004). While some previous work has focused on the covariance of entropy with PD symptoms (Alam et al., 2012; Lindemann et al., 2013), the reported entropy changes between conditions have been small, especially in the SNr or GPi (Dorval and Grill, 2014; Dorval et al., 2008). In the present study, entropy changes were not significant, although the general trends in SNr entropy were consistent with the reports cited above.

Despite small and insignificant changes in entropy however, changes in information transmission were large and robust. Directed information between SNr and VA was elevated in hPD, relative to both the healthy and hPD with STN-DBS conditions. Conceptually, increases in orthodromic information transmission might be presumed as behaviorally beneficial, but recent work in non-human primates supports that basal ganglia information transmission is actually reduced by effective DBS (Agnesi et al., 2013). Furthermore, the motor symptoms of Parkinsonism are not beneficial, so information increases associated with them are likely detrimental to well being. Thus, this additional information should be classified as pathological.

The pathological information in the parkinsonian condition may dictate symptoms by deleteriously modulating thalamic activity. However, the nature of this pathological modulation remains poorly understood. Signals from basal ganglia could constitute either of the following: active information that commands symptoms, or passive information that generates symptoms merely by interfering with downstream neural processing in thalamus or motor cortex. Computational studies report that prototypically parkinsonian

activity from basal ganglia drives thalamic neurons to make relay errors (Guo et al., 2008; Rubin and Terman, 2004), and that the error rate increases with basal ganglia firing pattern entropy (Dorval et al., 2009). Recent studies in human DBS patients support the hypothesis that these thalamic errors passively interfere with healthy activity, rather than actively dictating symptoms. In particular, presenting increasingly entropic DBS to basal ganglia or thalamus exacerbated symptoms of PD (Dorval et al., 2010) or essential tremor (Birdno et al., 2008), respectively. The DBS signals in those studies were pseudo-random pulse trains, and thus could not have been generating meaningful commands to actively drive symptoms.

The presented analyses are subject to limitations. Our estimates of information use only the most recent ISI and CSI in their calculations. While this approach accounts for simple statistical variations like changes in firing rate, it may ignore complex dependencies that integrating over the last several CSIs could reveal. However, each additional ISI or CSI adds another dimension to the information space, dramatically increasing the data needed to estimate it (Dorval, 2008). Further, while supporting the idea that information metrics can be used to distinguish symptomatic from asymptomatic conditions, neuronal information would be difficult to measure from clinical populations. To improve DBS therapy, researchers are seeking biomarkers of PD symptom severity that can be measured in real time (Thompson et al., 2014). Thus, we extended this work to examine LFP activity relevant to information processing.

While beta activity is prominent in dorsal STN and motor cortex of parkinsonian animals, the strength of beta power is highly dependent upon behavioral state (Lehmkuhle et al., 2009). Recordings in human patients have found beta power

progressively attenuated from dorsal STN, through ventral STN, and into SNr (Alavi et al., 2013). Recordings in the present study were collected from unrestrained rats that alternated between bouts of movement and bouts of rest. We did not find statistically significant beta power in field potentials collected from either SNr or VA. Further, single-unit action potentials were not particularly beta-rhythmic, even in the hPD condition.

However, the cross bicoherence between LFPs and simultaneously recorded unit activity in SNr revealed the appearance of a robust beta-beta peak in the hPD condition. This finding supports previous work that some beta coherence – which is the diagonal of our cross bicoherence – in SNr LFPs may be generated locally (Alavi et al., 2013). Further, beta-beta coherence was suppressed by therapeutic STN-DBS (Fig. 2-4). This work supports the idea that beta synchronization throughout the basal ganglia gates parkinsonian symptoms (Brittain et al., 2014). Since LFPs likely report an integration of spatial synaptic activity, we observe that unit spike times were coherent to local synaptic activity at beta frequencies, even though beta power was not significantly larger than power in lower (e.g., alpha) or higher (e.g., gamma) frequency ranges. These findings support that a PD-associated predilection for beta entrainment is involved with the PD-associated increases in directed information. These ideas will be thoroughly explored in future work.

We do not expect that we recorded from any of the same neuronal pairs in both the healthy and hPD conditions. Given the robust increases in directed information, however, we hypothesize that neuronal pairs not functionally connected in the healthy condition received and transmitted signals with similar information content in the hPD

condition. This could occur if neurons in different regions became highly coherent to a particularly widespread input, as we report for beta activity (Fig. 2-4). A recent paper showed increases in phase-amplitude coupling between beta and 250-350 Hz activity with increasing PD severity in a non-human primate model (Connolly et al., 2015). Together these studies suggest a PD-associated loss of channel independence, meaning that parallel projections from basal ganglia to motor thalamus carry redundant information in the PD condition. Even if the information between any two neurons increases with PD, if that information is redundant with information between other pairs, the net information could be reduced (Schneidman et al., 2003, 2011).

Supporting the hypothesis that PD is associated with large increases in neural signal redundancy, directed information was similar in orthodromic and antidromic directions. Antidromic information could reflect connectivity from VA through putamen back to SNr, but more likely reflects global levels of redundant information. Recent computational work supports this interpretation, suggesting that irregular firing patterns in PD is a network phenomenon of the cortico-basal ganglia-thalamo-cortical loop, and that DBS suppresses these irregular firing patterns through orthodromic and antidromic activation (Santaniello et al., 2015). Future efforts recording from many neurons simultaneously could be used to test this hypothesis concretely. Regardless of redundancy, the hPD-associated increase and DBS-associated restoration of directed information support the notion that fewer independent channels exists in the parkinsonian condition.

A loss of channel independence through motor pathways of the basal ganglia might constrain the behaviors that a parkinsonian individual could express. Somatotopic mappings, for example – as present throughout motor basal ganglia (Nambu, 2011) – are

organized by musculoskeletal, anatomical relations. Thus, two independent neural pathways through basal ganglia associated with antagonistic muscles are anatomical neighbors. Increased information between neighboring neurons in antagonistic pathways would reduce the independence of the antagonistic muscles, as seen in the hallmark parkinsonian symptoms of tremor and rigidity. Similarly, loss of channel independence would reduce the ability of the basal ganglia to fulfill its action selection role (Frank, 2006; Helmich et al., 2009), particularly if the appropriate action was contaminated by alternative actions that the basal ganglia is trying to select against. This indecision may contribute to the hypokinetic symptoms of PD.

In a rodent model of PD, information transmission from SNr to VA increased in the parkinsonian condition, and was restored to near healthy levels by functionally restorative STN-DBS. This study supports the growing body of work that identifies informational metrics as useful biomarkers of neurological disorders (Trevelyan et al., 2013). The pathological information generated in the parkinsonian basal ganglia likely interferes with downstream signal processing in thalamus and motor cortex, driving parkinsonian symptoms. We hypothesize that the increased information at the neuronal pair level reflects the loss of channel independence between neighboring motor command networks, and widespread informational redundancy within the parkinsonian brain.

CHAPTER 3

DBS EXACERBATES PARKINSONIAN HYPOKINETIC DYSARTHRIA IN A RODENT MODEL

Parkinson's disease is associated with the speech disturbances, which have been reported in as many as 90% of patients (Logemann et al., 1978). Most of these are caused by reduced or disrupted motor activity of the vocal system and categorized as hypokinetic dysarthria, the mechanisms of which are poorly understood. DBS is associated with an exacerbation of these symptoms, despite improving many other motor symptoms. Because human studies are complex, both logistically and ethically, we developed a model of DBS-exacerbated dysarthria in a rodent. We used mating calls from male rats to demonstrate that the 6-OHDA model of hemiparkinsonism led to fewer calls, with shorter and less complex vocalizations, all exacerbated by DBS. We additionally developed an automated methodology for analyzing all calls recorded, preventing selection bias. This model will be useful in helping researchers study how DBS treats most motor symptoms while exacerbating speech deficits.

3.1 Abstract

Motor symptoms of Parkinson's disease (PD) follow the degeneration of dopaminergic neurons in the substantia nigra pars compacta. Deep brain stimulation

(DBS) treats some parkinsonian symptoms, such as tremor, rigidity, and bradykinesia, but may worsen certain medial motor symptoms, including hypokinetic dysarthria. The mechanisms by which DBS exacerbates dysarthria while improving other symptoms are unclear and difficult to study in human patients. This study proposes an animal model of DBS-exacerbated dysarthria. We use the unilateral, 6-hydroxydopamine (6-OHDA) rat model of PD to test the hypothesis that DBS exacerbates quantifiable aspects of vocalization. Mating calls were recorded from sexually experienced male rats under healthy and parkinsonian conditions and during DBS of the subthalamic nucleus. Relative to healthy rats, parkinsonian animals made fewer calls with shorter and less complex vocalizations. In the parkinsonian rats, putatively therapeutic DBS further reduced call frequency, duration, and complexity. The individual utterances of parkinsonian rats spanned a greater bandwidth than those of healthy rats, potentially reducing the effectiveness of the vocal signal. This utterance bandwidth was further increased by DBS. We propose that the Parkinsonism-associated changes in call frequency, duration, complexity, and dynamic range combine to constitute a rat analog of parkinsonian dysarthria. Because DBS exacerbates the Parkinsonism-associated changes in each of these metrics, the subthalamic stimulated 6-OHDA rat is a good model of DBS-induced hypokinetic dysarthria in PD. This model will help researchers examine how DBS alleviates many motor symptoms of PD while exacerbating parkinsonian speech deficits that can greatly diminish patient quality of life.

3.2 Introduction

Parkinson's disease (PD) is a neurological disorder associated with motor and non-motor symptoms. Motor signs of PD can include tremor, rigidity, reduced movements manifesting as bradykinesia or akinesia, and speech disturbances. Nonmotor symptoms of PD can include depression, apathy, anxiety, and executive dysfunction that may include bradyphrenia and slowness of thought (Caballol et al., 2007; Jankovic, 2008). Speech described as “slurred, thick, indistinct” has been reported for PD patients for many decades (Kaplan et al., 1954), and classic studies have found speech dysfunctions in as many as 90% of PD patients (Logemann et al., 1978). Most speech disturbances in PD patients are caused by reduced or disrupted motor activity of the vocal system and categorized as hypokinetic dysarthria, a “multidimensional impairment leading to abnormalities in speech breathing, phonation, articulation, and prosody” (Skodda, 2011).

Although treatments for PD motor signs exist, dysarthric symptoms do not always respond to these treatments as favorably as do motor symptoms. With the administration of dopaminergic medications, persons with PD typically experience improvements in speech intelligibility, comprehensibility, and variability of pitch and loudness (De Letter et al., 2007a, 2007b). However, late-stage surgical interventions such as pallidotomy, thalamotomy, and deep brain stimulation (DBS) have been reported to worsen hypokinetic dysarthria (de Bie et al., 2002; Burghaus et al., 2006; Intemann et al., 2001; Kim et al., 1997; Romito et al., 2002; Tröster et al., 2003; Umemura et al., 2011). With the increasing prevalence of DBS to alleviate motor symptoms of PD, the worsening of dysarthria will reduce quality of life for more and more patients (Wertheimer et al., 2014). Understanding how DBS therapy can exacerbate hypokinetic dysarthria may help us to

devise alternative strategies to treat motor and speech signs simultaneously.

Because of obvious ethical and experimental boundaries in human studies, progress with respect to the mechanisms of parkinsonian dysarthria has been limited, despite more than 60 years of work. Recent observations that hypokinetic dysarthria may be worsened by otherwise therapeutic DBS are largely unexplored. We propose using the existing 6-hydroxydopamine (6-OHDA) rodent model of Parkinsonism to study hypokinetic dysarthria and its exacerbation by DBS. Previous studies have demonstrated reductions in vocalizations and vocalization complexity in the 6-OHDA rat (Ciucci et al., 2008; Johnson et al., 2011), but, to our knowledge, none has reported the effects of DBS in this model.

We advanced a vocalization protocol (Ciucci et al., 2009) to record and to quantify the effects of PD and DBS in the 6-OHDA rat model. Under normal (NAL), parkinsonian (PD), and parkinsonian with subthalamic stimulation (DBS) conditions, ultrasonic mating calls from sexually frustrated males were recorded in the presence of an estrous female. Individual sounds were isolated in time and frequency from their neighbors, and sounds in rapid succession were grouped together as vocalization strings that we called *phonological words*. Sounds and words were separated into two frequency bands (Brudzynski, 2005, 2013). Rats use the low-frequency 20–35-kHz band for aversive situations, including social defeat (Litvin et al., 2007; Wöhr and Schwarting, 2013), and the high-frequency 35–100-kHz band for appetitive situations, including social excitement (Sales, 1972; Willadsen et al., 2014). Male rats make calls in both bands during successful and/or frustrated female solicitation (Barfield et al., 1979; Seffer et al., 2014).

We found that the rich vocalization structure of male rats was substantially diminished by parkinsonian onset for both short vocalizations and long vocalization strings in both frequency bands. Under the PD condition, rats generated fewer and shorter vocalizations that were less acoustically complex than under the normal condition. Supporting a model of DBS-exacerbated hypokinetic dysarthria, stimulation of the subthalamic nucleus worsened these parkinsonian vocalization symptoms. Under the DBS condition, rats generated even fewer and shorter vocalizations that were less acoustically complex than those under the PD condition. The frequency bandwidth of individual sounds increased slightly with parkinsonian onset and increased substantially with DBS. These findings support the hypothesis that DBS in the 6-OHDA rat model of PD provides a viable platform for the study of hypokinetic dysarthria, allowing future work to explore the mechanisms of aggravated dysarthric symptoms caused by DBS.

3.3 Materials and Methods

All surgical and experimental procedures were performed in the Department of Bioengineering at the University of Utah, were approved by the institutional animal care and use committee of the University of Utah, and complied with U.S. Public Health Service policy on the care and use of laboratory animals.

3.3.1 Experimental Protocols

Vocalization data were collected from male rats in the presence of estrous female rats. The timeline of the protocol for eight adult Long-Evans male rats weighing 400–600 g was as follows. Each rat underwent stereotactic surgery to receive two chronic

brain implants (Chang et al., 2003; Dorval and Grill, 2014): a cannula accessing the medial forebrain bundle (MFB), and an electrode array to stimulate the subthalamic nucleus. Beginning at least 1 week after surgery, ultrasonic recordings of each male calling to an estrous female were collected during 5-min trials. After 2 weeks of these healthy-normal recordings, animals were injected intracranially with 6-OHDA through the implanted cannula to degenerate dopaminergic neurons in the substantia nigra pars compacta. Two weeks later, the rats were injected with 5 mg/kg intraperitoneal amphetamine, and Parkinsonism was diagnosed by the rapid rotations ipsilateral to 6-OHDA injection. Five rats developed a severe, unilateral Parkinsonism; 2 of these were placed in the control group, and 3 were placed in the experimental group. The ultrasonic recording protocol in the presence of an estrous female was resumed for rats in both groups. For alternate recording sessions, rats in the experimental group received DBS through the subthalamic electrode array. Rats in the control group never received DBS, although they did have an electrode array in the subthalamic nucleus to control for the effects of surgery and neuronal damage. After 1–2 months of recordings, rats were euthanized.

3.3.1.1 Surgical procedures. Male rats were provided 20 mg of carprofen (Bio-Serv, Flemington, NJ) and after consumption were anesthetized with 2–3% isoflurane. The surgical site was shaved and disinfected, and the rats were placed on a body-temperature heating pad in a stereotactic frame (Kopf Instruments, Tujunga, CA). The scalp was opened and cleaned to the skull, and craniotomy sites were measured and marked with respect to bregma (Paxinos and Watson, 2008). Seven titanium bone screws were driven through burr holes into the skull to anchor the eventual acrylic cap. To allow

the eventual injection of 6-OHDA into the MFB, a 23-gauge stainless-steel cannula was implanted through a burr hole 2.0 mm posterior and 2.0 mm lateral to bregma. For DBS of the subthalamic nucleus, a four-channel microstimulating array—2 × 2 grid of 75-μm platinum–iridium electrodes (~100 kΩ at 1 kHz) with 400-μm spacing (Microprobes for Life Science, Gaithersburg, MD)—was implanted through a burr hole 3.6 mm posterior and 2.6 mm lateral to bregma at a ventral depth of 7.8 mm. Medial electrodes were 500 μm longer than their lateral counterparts to match the anatomy of the subthalamic nucleus. After each of the hardware elements was lowered to its target depth, a layer of dental acrylic was applied to attach it firmly to the anchor screws. After these implantations, the screws, cannula, and array were encased in a thick dental acrylic cap, built smoothly over multiple layers. The incision was sutured around the acrylic cap and covered with topical antibiotics. Rats were returned to their home cages and given 7 days of recovery prior to experimental recordings.

After healthy-normal recordings, each rat was injected with 6-OHDA to induce Parkinsonism (Dorval and Grill, 2014; Fibiger et al., 1972). Rats were anesthetized with 2–3% isoflurane and returned to the stereotactic frame. A needle was inserted to 0.5 mm beyond target depth, left for 5 min to create a pocket, and then retracted by 0.5 mm. A bolus of 8.0 μg 6-OHDA dissolved in 8.0 μl saline was injected at a rate of 1.0 μl/min. Ten minutes after the completion of the injection, the needle was withdrawn at a speed not exceeding 1.0 mm/min. Rats were returned to their home cages to develop Parkinsonism over the next 2 weeks. To verify symptoms after 14 days of rest, rats were injected with 5 mg/kg amphetamine intraperitoneally and placed in a cylindrical chamber (Castall et al., 1977; Pieri et al., 1975). Parkinsonism was confirmed in the 5 rats that

turned ipsilateral to the 6-OHDA injection at a rate exceeding six complete rotations per minute. Data from those 5 rats are included in the following analyses.

3.3.1.2 DBS. For trials that included DBS, rats were briefly anesthetized with 2–3% isoflurane, and a four-channel tether was attached to the connector of the microstimulating array on the head. Rats were quickly moved to their cages before awaking, and the other end of the tether was connected to an analog current stimulator (Grass Technologies, Warwick, RI). Current amplitudes ranged from 100 to 500 μA, varying by animal; bipolar stimulation was delivered through the microstimulating array, with both medial contacts set as anodes and both lateral contacts set as cathodes. The stimulation waveform consisted of symmetric 100-μsec biphasic current pulses repeating at 100 Hz. Stimulation was applied for 5 min prior to recordings and during 5-min recordings for a total duration of 10 min per trial. Two weeks after 6-OHDA injection, stimulation thresholds were determined by gradually increasing the current amplitude until the appearance of physical side effects, including atypical whisker twitching, other dystonic facial contractions, and repetitive rotations contralateral to stimulation. Therapeutic DBS amplitude was then set to 90% of the minimum current that yielded side effects. Although stimulation was applied during only DBS trials, a tether was connected during some healthy-control and PD trials to ensure that it did not induce significant changes in behavior. Unilateral behavioral deficits after 6-OHDA injection and improvements with the application of DBS were observed and qualitatively determined as matching those observed in previous work from our group (Anderson et al., 2015; Dorval and Grill, 2014). Specifically, 6-OHDA induced a rotational movement ipsilateral to the lesion that was partially reversed by DBS.

3.3.1.3 Behavioral task. Ultrasonic male rat mating calls were recorded in the presence of an estrous female under each of three conditions, NAL, PD, and DBS. Other than connecting the DBS tether as described above, the experimental configuration was identical for all conditions and lasted for 5 min per male rat. Multiple males were recorded in succession on each day to take full advantage of the female being in heat. Prior to experimental recording sessions, estrus was induced in one of the four females used in this study. Beginning 48 hours before the session, a female rat was injected intraperitoneally with 10 mg/kg β-estradiol diacetate in 0.2 ml corn oil. Four hours prior to the session, the female was injected intraperitoneally with 10 mg/kg progesterone in 0.2 ml corn oil. Posture and movement were observed to determine whether the female displayed ear wiggling and lordosis, characteristics of being in heat. After the female displayed these signs, experimental recording could begin.

The male rat was placed in the lower chamber of the behavioral configuration (Fig. 3-1a) to acclimate to the environment. After 5 min, the estrous female was placed in the same chamber. Whenever the male attempted to mount the female, the experimenter physically removed him from her back. After three separations, the female was moved to the upper chamber (Fig. 3-1a). A fan in the upper chamber blew the female scent down through 10 1.0-mm-diameter holes between the chambers. The male reared and vocalized in apparent attempts to attract the attention of the female. Mating calls were recorded with an ultrasonic microphone (CM16; Avisoft Bioacoustics, Glienicke, Germany). The microphone output (Fig. 3-1b) was recorded at 200 kHz on a standard Windows personal computer (LabView; National Instruments, Austin, TX).

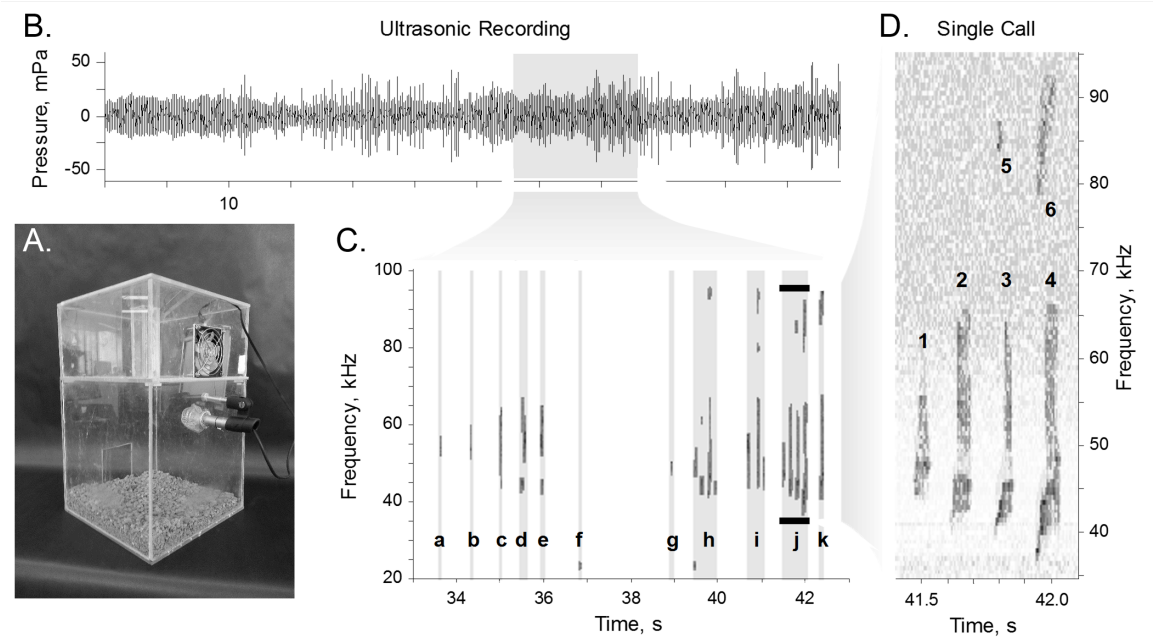

Figure 3-1. Experimental design. A: Behavioral configuration in which an estrous female rat was placed in the top chamber, and a male rat was placed in the bottom chamber. A fan in the top chamber blew the scent of the female through holes down into the bottom chamber. An ultrasonic microphone in the bottom chamber collected calls made by the male rat. B: One-minute example of sound recording converted into pressure. C: Time-frequency spectrogram from 10 sec of the example recording. Sounds were isolated from the background and collected into words (a–k) with at least 250-msec spacings. Calls labeled a–c, f, and g are single-sound words; calls labeled d, e, and h–k are words with more than one sound. D: Expanded view of word "j" shows that word j comprises six unique sounds isolated in time-frequency space. Note that sounds 5 and 6 (at ~86 Hz) are the first harmonics of the loud fundamental sounds 3 and 4 (at ~43 kHz).

3.3.2 Statistical Analysis

Time–frequency spectrograms were developed for each 5-min trial via the following algorithm. Raw data at 200 kHz were convolved with a 10-msec-wide Hamming kernel. The Goertzel algorithm was used to calculate a frequency–space representation of the signal for 10-msec windows overlapping by 5 msec, in frequency bins 500 Hz wide. The resulting spectrograms were evaluated over their entire duration between 20 and 100 kHz. Spectrograms were transformed into z-score representations by dividing each time–frequency value by the standard deviation of the signal in that frequency bin (Fig. 3-1d).

3.3.2.1 Vocalization identification. Individual sounds were identified in time–frequency space (10 msec × 500 Hz pixels) by generating a binary mask and then removing small clusters and combining neighboring clusters iteratively through larger and larger cluster sizes. To begin, binary masks were made by thresholding; pixels with a z-score below 2.0 were set to zero. Mask clusters of fewer than four pixels were set to zero. The remaining clusters were inflated and then deflated by one time–frequency pixel in all eight directions. Mask clusters of fewer than eight pixels were set to zero. The remaining clusters were inflated and then deflated by 2.5 kHz toward higher and lower frequencies. Mask clusters of fewer than 12 pixels were set to zero. The remaining clusters were inflated and then deflated by two time–frequency pixels in all eight directions. Mask clusters of fewer than 16 pixels were set to zero. To smooth the boundaries, the remaining clusters were filtered so that adjacent pixels were added to the cluster if at least four of their eight neighboring pixels were in the cluster, and pixels were removed if at most two of their neighboring eight pixels were in the cluster. This

smoothing process was performed twice before mask clusters of fewer than 20 pixels were also set to zero. All clusters remaining after this process were taken as true sounds generated by the male rat. The analyses were performed with many variations on this isolation procedure, and all yielded similar results.

Sounds separated by less than 250 msec were grouped together into vocalization strings and identified as phonological words (Fig. 3-1c). Analyses repeated for vocalization strings with maximum sound separations of 100–500 msec yielded similar results. Sounds and words were also separated by frequency band into three call types, low, high, and complex. The division of low- and high-frequency bands was made to separate putatively aversive from putatively appetitive calls (Brudzynski, 2013; Willadsen et al., 2014; Wöhr and Schwarting, 2013). To protect against the possibility that our sound filtering and isolating processes generated spurious single-sound words, we included a category of complex sounds typical of rat vocalizations. Sound and call types are illustrated via examples in Figure 3-2A (sounds outlined in white). Low-frequency calls included sounds from 20 to 35 kHz. For example, in Figure 3-2A, the two-sound word (below the dashed line at left) and the one-sound word (below the dashed line in the middle) are both low-frequency calls. High-frequency calls included sounds from 35 to 100 kHz. For example, in Figure 3-2A, high-frequency calls include four-sound, three-sound, and two-sound words (above the dashed line at left, middle, and right, respectively). Complex calls could occur anywhere in the 20–100-kHz range but had to include more than one sound. Figure 3-2A, for example, depicts single complex words with six, four, and two sounds at left, middle, and right, respectively.

3.3.2.2 Statistical compilation. Sound and word duration (T_s and T_w) and

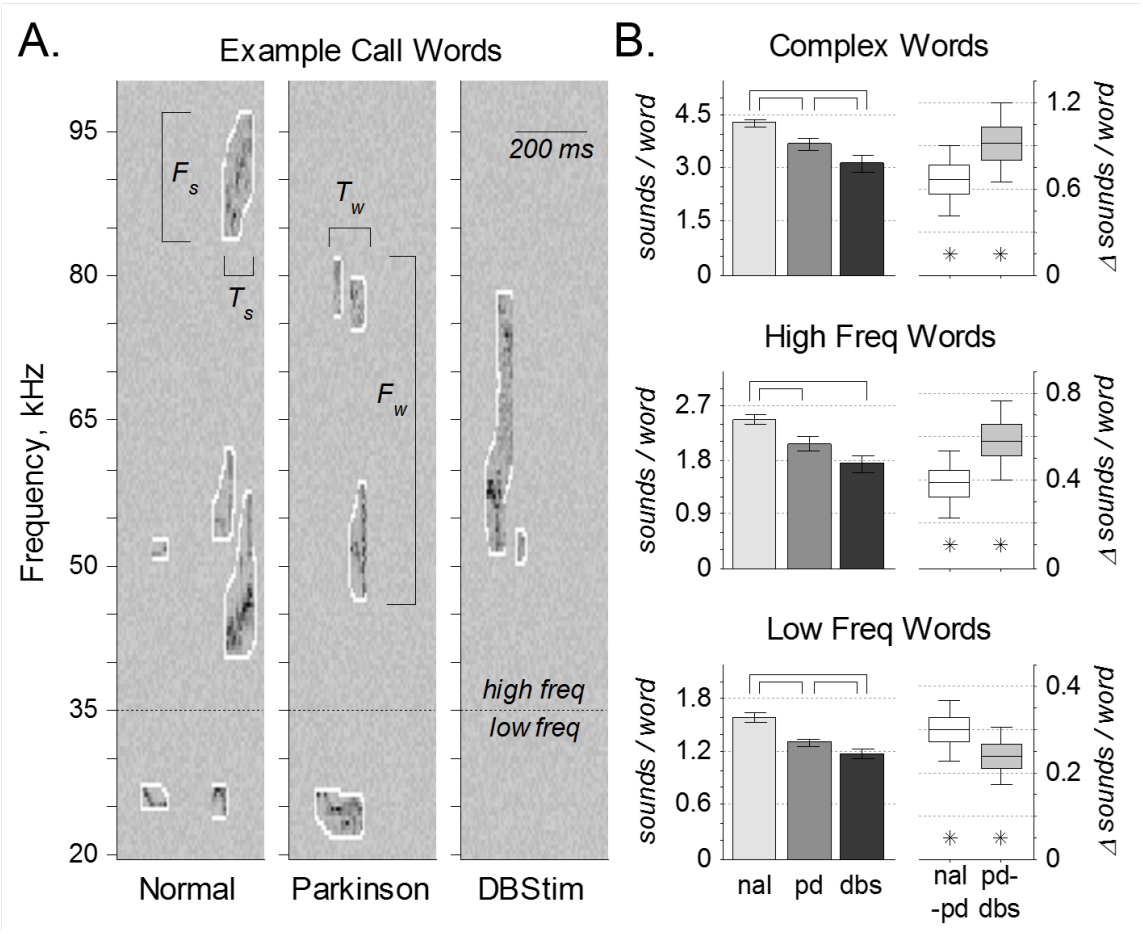

Figure 3-2. Vocalization complexity. A: Representative time-frequency spectrograms of three calls from the same rat under NAL, PD, and DBS conditions. Bandwidth (F_s) and duration (T_s) were calculated for each sound. Three call types were examined; low-frequency calls included words with sounds between 20 and 35 kHz, high-frequency calls included words with sounds between 35 and 100 kHz, and complex calls included all words with more than one sound in the 20–100-kHz range. Bandwidth (F_w) and duration (T_w) were also calculated for each word. B: Sounds per word for each call type. At left, complexity of words across the entire population (mean ± SE) quantified as the number of sounds per word. Word complexity was significantly reduced from normal to PD for all call types and from PD to DBS for complex calls (overbars, $P_{HSD} < 0.05$). At right, within-rat word complexity differences (median ± 50% ± 95% CI) from normal to PD (nal-pd) and from PD to DBS (pd-dbs). Word complexity was significantly greater in normal than in PD and in PD than in DBS (asterisks, $c_{95\%} > 0$).

bandwidth (F_s and F_w) were calculated for all calls. Averages of those values plus the mean number of calls per minute and the mean number of sounds per word were found for each trial of each animal under each condition. The average values of each of those measures in a given trial were taken as a population for statistical analysis. All animals included in the analysis were recorded during at least seven trials under each condition (mean 12.9 ± SD 4.6). Population analyses included recordings from 5 rats under NAL, 5 rats under PD, and 3 rats under DBS conditions. In figures, population changes are denoted with overbars when a one-way ANOVA confirmed significant changes between group means that were subsequently verified with Tukey's honest significant difference test at $\alpha = 0.05$ (i.e., $P_{HSD} < 0.05$); detailed statistics for Tukey's tests are listed in Table 3-1. Within-rat analyses include 5 rats in the NAL-to-PD transition and 3 rats in the PD-to-DBS transition. Within-rat differences are denoted with an asterisk in figures when the bootstrapped 95% confidence interval (CI) of the change between conditions did not include the zero value (i.e., $c_{95\%} > 0$ or $c_{95\%} < 0$).

3.4 Results

Eight male rats were implanted with a cannula to the right MFB and a four-channel stimulating electrode array to the right subthalamic nucleus. For 5-min trials, each rat was placed in the bottom of a pair of stacked behavioral chambers, with an estrous female in the top chamber (Fig. 3-1a). Mating calls were recorded from an ultrasonic microphone in the bottom chamber with the male rat (Fig. 3-1b). After sufficient healthy recordings, the neurotoxin 6-OHDA was injected through the cannula to the MFB to induce Parkinsonism. Five male rats survived surgical implantation and

Table 3.1. Tukey's honest significant difference statistics

	Low band		High band		Complex band	
	q	p	q	p	q	p
Fig. 2B		$p_{anova} = 3 \times 10^{-7}$		$p_{anova} = 3 \times 10^{-4}$		$p_{anova} = 1 \times 10^{-4}$
nal vs. pd	3.49	4×10^{-4}	2.26	0.013	2.33	0.011
pd vs. dbs	1.38	~~0.086~~	1.60	~~0.058~~	1.74	0.044
nal vs. dbs	4.12	7×10^{-5}	3.33	8×10^{-4}	3.53	5×10^{-4}
Fig. 3B, top		$p_{anova} = 1 \times 10^{-7}$		$p_{anova} = 6 \times 10^{-14}$		$p_{anova} = 1 \times 10^{-13}$
nal vs. pd	3.42	5×10^{-4}	4.43	2×10^{-5}	4.47	2×10^{-5}
pd vs. dbs	1.67	~~0.051~~	2.36	0.011	2.07	0.022
nal vs. dbs	4.34	4×10^{-5}	5.81	2×10^{-7}	5.56	6×10^{-7}
Fig. 3B, bot		$p_{anova} = 7 \times 10^{-8}$		$p_{anova} = 2 \times 10^{-11}$		$p_{anova} = 2 \times 10^{-10}$
nal vs. pd	3.52	4×10^{-4}	4.05	7×10^{-5}	3.96	9×10^{-5}
pd vs. dbs	1.60	~~0.058~~	2.14	0.018	1.96	0.028
nal vs. dbs	4.35	4×10^{-5}	5.29	1×10^{-6}	5.04	4×10^{-6}
Fig. 4A, top		$p_{anova} = 8 \times 10^{-6}$		$p_{anova} = 7 \times 10^{-5}$		$p_{anova} = 3 \times 10^{-5}$
nal vs. pd	2.99	0.002	2.52	0.007	2.19	0.016
pd vs. dbs	1.46	~~0.075~~	1.59	~~0.059~~	2.27	0.014
nal vs. dbs	3.79	2×10^{-4}	3.54	5×10^{-4}	3.91	1×10^{-4}
Fig. 4A, bot		$p_{anova} = 0.009$		$p_{anova} =$ ~~0.229~~		$p_{anova} =$ ~~0.118~~
nal vs. pd	1.67	0.050	1.15	~~0.128~~	0.53	~~0.298~~
pd vs. dbs	1.31	*0.098*	0.43	~~0.333~~	1.50	~~0.070~~
nal vs. dbs	2.59	0.006	1.34	~~0.094~~	1.85	0.035
Fig. 4B, top		$p_{anova} = 1 \times 10^{-4}$		$p_{anova} =$ ~~0.159~~		$p_{anova} =$ ~~0.751~~
nal vs. pd	1.77	0.041	1.49	~~0.071~~	0.43	~~0.333~~
pd vs. dbs	2.41	0.010	1.24	~~0.111~~	0.68	~~0.250~~
nal vs. dbs	3.70	3×10^{-4}	0.03	~~0.487~~	0.29	~~0.387~~
Fig. 4B, bot		$p_{anova} = 4 \times 10^{-7}$		$p_{anova} = 0.001$		$p_{anova} = 6 \times 10^{-4}$
nal vs. pd	2.76	0.004	0.67	~~0.252~~	1.42	~~0.080~~
pd vs. dbs	2.38	0.010	2.81	0.003	2.37	0.011
nal vs. dbs	4.48	2×10^{-5}	3.19	0.001	3.39	7×10^{-4}

Sample sizes for comparisons: N_{nal}=76, N_{pd}=65, N_{dbs}=27; crossed out values were not significant at the 0.05 level.

healthy recordings and had developed Parkinsonism by 2 weeks following 6-OHDA injection. Among those 5, 3 were placed in the experimental group and recorded with and without subthalamic DBS in separate trials. The other 2 were placed in the control group and never received DBS.

3.4.1 Vocalization Prevalence

Sounds recorded from an ultrasonic microphone between 20 and 100 kHz were filtered and isolated from background noise as described above (Fig. 3-1c). A *word* was defined as a vocalization string that comprised one or multiple sounds that were temporally isolated by at least 250 msec from other sounds (Fig. 3-1d) of the same call type: high frequency (35–100 kHz), low frequency (20–35 kHz), and complex for words with at least two sounds total in the 20–100 kHz range (Fig. 3-2a).

Word complexity, defined as the average number of sounds per word (Fig. 3-2b), varied as a function of condition for each call type: low, $F(2154) = 16.5$, $P = 3 \times 10^{-7}$; high, $F(2159) = 8.57$, $P = 3 \times 10^{-4}$; complex, $F(2155) = 9.58$, $P = 1 \times 10^{-7}$. Average word complexity was significantly reduced under the PD condition from the healthy condition for all call types. Similarly, within-rat differences between the healthy and the PD conditions were greater than zero for all call types, meaning that rat vocalizations were significantly more complex before 6-OHDA injection than after 6-OHDA injection. Across the population, word complexity was further reduced under the DBS condition for complex calls. Within-rat differences between the PD and DBS conditions were highly significant for all call types: parkinsonian rat vocalizations were significantly more complex without DBS than with it. In summary, the number of sounds per word was

reduced by parkinsonian onset and further reduced by DBS.

Call rates, in words per minute and sounds per minute, were computed for each condition and call type. Example data, all from the same animal, illustrate the statistically significant changes between conditions (Fig. 3-3a). Word rate varied as a function of condition for all call types (Fig. 3-3b, top): low, $F(2165) = 17.7$, $P = 1 \times 10^{-7}$; high, $F(2165) = 36.9$, $P = 5 \times 10^{-14}$; complex, $F(2165) = 34.3$, $P = 3 \times 10^{-13}$. Sound rate also varied as a function of condition for all call types (Fig. 3-3b, bottom): low, $F(2165) = 18.2$, $P = 7 \times 10^{-8}$; high, $F(2165) = 28.5$, $P = 2 \times 10^{-11}$; complex, $F(2165) = 25.7$, $P = 2 \times 10^{-10}$. Across the population, both word rate and sound rate were reduced from the normal to the PD condition. Similarly, within-rat differences between the normal and PD conditions were always greater than zero, meaning that rats had higher call rates before 6-OHDA injection than after 6-OHDA injection. Furthermore, DBS reduced both word and sound rates from the PD condition, although the population decrease trend for low-frequency calls did not reach statistical significance. However, within-rat differences between the PD and DBS conditions were all significantly greater than zero; parkinsonian rats had higher call rates without DBS for all call types. In summary, DBS exacerbated all the reductions of word rates and sound rates associated with parkinsonian onset.

3.4.2 Vocalization Dynamics

The time and frequency span of each word and sound were calculated for all call types (Fig. 3-2a). Note that these measures are independent of the call rate. Furthermore, the time and frequency spans of individual sounds (T_s and F_s, respectively) are

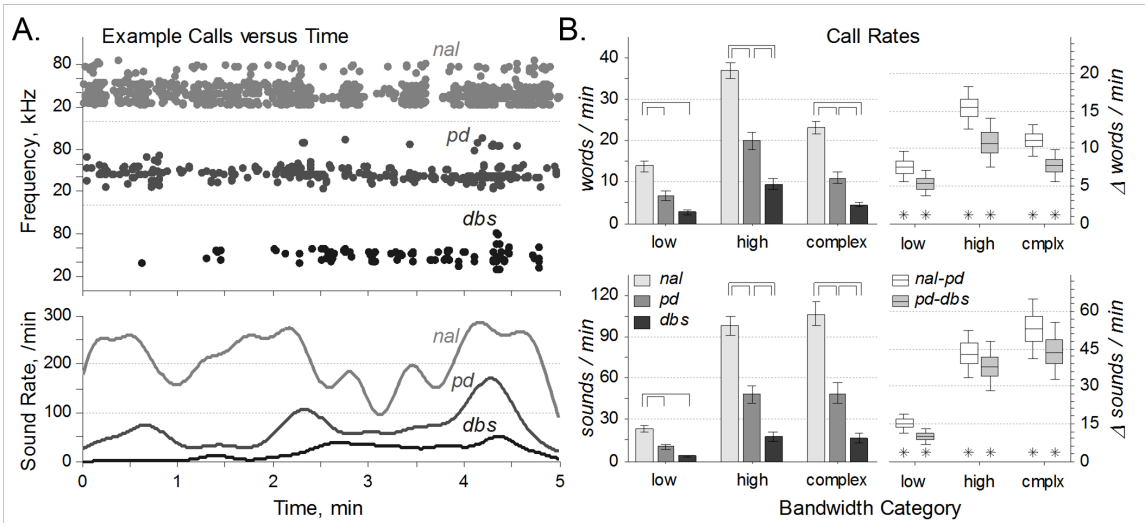

Figure 3-3. Vocalization rates. A: Representative call data of sounds vs. time from the same rat under each of the three conditions. At top, each sound is depicted as a single dot at its center frequency. At bottom, sound rates calculated by convolving the events from above with a gaussian kernel with a 10-sec SD. Note the substantial variability in sound rate over each 5-min interval. B: Call rates vary with condition. At left, call rates (mean ± SE) of words (top) and sounds (bottom) were reduced from normal to PD and typically reduced from PD to DBS conditions (overbars, $P_{HSD} < 0.05$). At right, within-rat word and sound rate differences (median ± 50% ± 95% CI) revealed higher call rates in normal relative to PD and in PD relative to DBS (asterisks, $c_{95\%} > 0$).

independent of call complexity as defined above. However, the time and frequency span of individual words (T_w and F_w, respectively) do depend on the call complexity; words with fewer sounds are more likely to have smaller time and frequency spans.

Across the population, word duration (T_w) varied with condition for all call types: low, $F(2154) = 12.7$, $P = 8 \times 10^{-6}$; high, $F(2159) = 10.1$, $P = 7 \times 10^{-5}$; complex, $F(2155) = 11.3$, $P = 3 \times 10^{-5}$. In particular, word duration was significantly reduced from the normal to the PD condition (Fig. 3-4a, top). Within-rat differences supported the idea that words were longer before 6-OHDA injection than after 6-OHDA injection. Between groups, word duration was further reduced from the PD to the DBS condition, although this universal trend was significant only for complex calls. However, within-rat differences between the PD and the DBS conditions were significantly greater than zero for all call types, meaning that the average rat vocalized shorter words in the presence of DBS for all call types. Thus, reductions in word durations brought on by Parkinsonism were exacerbated by DBS.

Relative to the large changes in word duration, changes in sound duration (T_s) were proportionally much smaller (Fig. 3-4a, bottom) and less significant: low, $F(2154) = 4.82$, $P = 0.009$; high, $F(2159) = 1.49$, $P = 0.229$; complex, $F(2155) = 2.17$, $P = 0.118$. Across the population, the only significant changes were that sounds in the low-frequency range were significantly shorter following 6-OHDA injection with and without DBS than under the control condition. Despite these small changes, within-rat differences from the control to the PD condition revealed that sounds were significantly longer (~3 msec) for high- and low-frequency calls. Furthermore, within-rat differences were longer still (3-6 msec) from the PD to the DBS conditions for

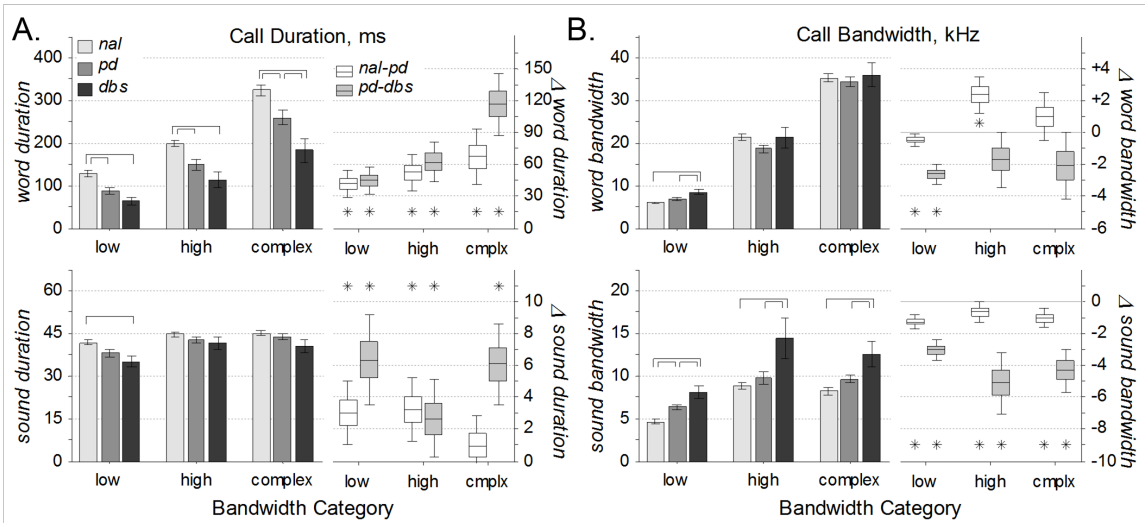

Figure 3-4. Vocalization statistics. A: Call durations of words (top) and sounds (bottom) for all call types. At left, population statistics (mean ± SE) reveal that word durations were decreased in the PD condition relative to control and for complex calls further decreased in DBS relative to PD (overbars, $P_{HSD} < 0.05$). Sound durations were not greatly affected by condition. At right, within-rat comparisons (median ± 50% ± 95% CI) reveal that words and sounds were shorter in the PD condition relative to normal and mostly shorter still under the DBS condition relative to PD (asterisks, $c_{95\%} > 0$). B: Frequency bandwidths of words (top) and sounds (bottom) for all call types. At left, population statistics (mean ± SE) reveal that sound durations were increased in the DBS condition relative to PD and normal (overbars, $P_{HSD} < 0.05$). Word bandwidths were not greatly affected by condition. At right, within-rat comparisons (median ± 50% ± 95% CI) reveal that frequency bandwidth was less in the normal condition relative to PD and less still in the PD condition relative to DBS (asterisks, $c_{95\%} < 0$). Changes in word bandwidth were less consistent.

all call types. Thus, sound duration was decreased by parkinsonian onset and decreased further by DBS, but the effects were too small and variable to manifest in the population measures.

Similarly, changes between conditions in word frequency span or bandwidth (F_w) were small and mostly insignificant (Fig. 3-4b, top): low, $F(2154) = 9.64$, $P = 1 \times 10^{-4}$; high, $F(2159) = 1.86$, $P = 0.159$; complex, $F(2155) = 0.29$, $P = 0.751$. The only population effects were slightly higher bandwidths of low-frequency calls under the DBS condition relative to the PD condition and under the PD condition relative to the healthy condition. Within-rat analysis supported this finding and added that the word bandwidth was slightly greater (~0.4 kHz) under the PD condition than under the healthy condition. In contrast to those low-frequency results, high-frequency word bandwidth was reduced under the PD condition relative to the healthy condition. These conflicting results are clarified by quantifying the sound bandwidth.

In contrast to small changes in sound duration and muddled changes in word bandwidth, the bandwidth of individual sounds (F_s) varied substantially with condition (Fig. 4-4b, bottom): low, $F(2154) = 16.2$, $P = 4 \times 10^{-7}$; high, $F(2159) = 7.04$, $P = 0.001$; complex, $F(2155) = 7.81$, $P = 6 \times 10^{-4}$. Across the population, the bandwidth of low-frequency calls was greater under the PD condition than under the healthy condition. This change was more evident from the within-rat differences, in which calls spanned greater bandwidth (~1 kHz) under the PD condition relative to control for all call types. The larger population effect was that the bandwidth of each call type was increased under the DBS condition relative to the PD condition. Furthermore, within-rat differences showed a significant bandwidth increase (3–5 kHz), indicating that increases in sound bandwidth

associated with PD were exacerbated by DBS.

3.5 Discussion

High-frequency stimulation of the subthalamic nucleus or globus pallidus internus can alleviate motor symptoms of PD, including tremor, rigidity, and bradykinesia (Limousin-Dowsey et al., 1999; Lyons and Pahwa, 2004). Effective DBS modifies neural firing activity within the basal ganglia (Benazzouz et al., 2000; Boraud et al., 1996; Da Cunha et al., 2015) and the motor thalamus (Hershey et al., 2003). With respect to this neural activity, however, DBS neither restores it to healthy-control levels (Anderson et al., 2003; Dorval and Grill, 2014; Hashimoto et al., 2003) nor modulates it in the same manner as dopamine-based drug therapies (Gilmour et al., 2011; Hilker et al., 2002; Hutchinson et al., 1997; Papa et al., 1999; Weick et al., 1990). Given their differential effects on neural activity, it is not surprising that electrical neuromodulation and medicaltherapy have disparate effects on various motor symptoms.

Despite decades of studies on hypokinetic dysarthria associated with PD, its origins are not fully understood (Kaplan et al., 1954; Logemann et al., 1978; Skodda, 2011). Further obscured are the mechanisms by which DBS may exacerbate dysarthria while simultaneously alleviating other parkinsonian motor symptoms (Burghaus et al., 2006; Romito et al., 2002; Umemura et al., 2011). The development of an animal model of these phenomena will facilitate the study of dysarthria in a high-throughput, patient-free manner, allowing new insights into both parkinsonian dysarthria and the maladaptive effects of DBS.

We built on a relatively recent rat model of parkinsonian dysarthria (Ciucci et al.,

2009), and differences between our studies are worth mentioning. First, Ciucci and colleagues identified vocalizations manually based on the quality of the acoustic signal, whereas we identified vocalizations algorithmically from z-score-transformed spectrograms. Second, they analyzed only 10% of the identified vocalizations, whereas we analyzed all vocalizations. Third, they categorized calls into simple, frequency-modulated, and harmonic types, whereas we separated them by frequency band (low, high, and complex) and looked at single vocalizations separately from vocalization strings.

These differences may account for minor contrasting results between the two studies. For the 6-OHDA condition relative to control, Ciucci and colleagues found that simple calls had smaller bandwidths, whereas we report that simple sounds had larger bandwidths, particularly in the 20–35-kHz range (Fig. 3-4b, bottom). That difference may be attributed to selection bias. More in line with the present findings, they reported that frequency-modulated calls had smaller bandwidths in the 6-OHDA condition, which is similar to our tentative finding that high-frequency words had smaller bandwidths under the 6-OHDA condition (Fig. 3-4b, top). However, DBS did not exacerbate that effect but rather significantly increased sound bandwidth in all frequency ranges, suggesting a potential DBS side effect that is not merely an exacerbation of existing dysarthric symptoms.

In general, however, the present findings confirm previous results associated with 6-OHDA-induced lesion (Ciucci et al., 2009). For example, Ciucci and colleagues reported no significant change in vocalization duration with PD onset yet with a trend toward shorter calls. Similarly, we report small decreases in mean sound duration that

were significant in within-animal paired tests but were merely trends across the population (Fig. 3-4a, bottom). Finally, they report a reduction in the fraction of frequency-modulated calls, and we report a reduction in the number of sounds per vocalization string in all frequency ranges (Fig. 3-2b).

Although precise parallels between human speech and rat vocalizations are difficult to draw, many aspects of parkinsonian hypokinetic dysarthria are qualitatively similar to 6-OHDA-induced changes in rats. Persons with PD can exhibit variable speech rates that slow with disease progression (Martínez-Sánchez et al., 2015; Skodda et al., 2009). Rats under the PD condition produced many fewer vocalizations per unit time for both individual sounds and more complex calls, and this symptom was exacerbated by DBS (Fig. 3-3). Persons with PD produce speech with less syntactic complexity by several measures (Illes et al., 1988; Walsh and Smith, 2011). Rats under the PD condition produced vocalization strings comprising fewer sounds, and this symptom was exacerbated by DBS (Fig. 3-2). Persons with PD produce words that are more variable in duration and shorter on average (Ackermann et al., 1997), although individual syllable duration may remain unchanged (Duez, 2006). Rats under the PD condition made shorter word calls on average, and this symptom was exacerbated by DBS (Fig. 3-4a, top), although the duration of individual sounds was largely unchanged (Fig. 3-4a, bottom). Together, these changes in vocalization constitute a reasonable quantification of parkinsonian hypokinetic dysarthria in a rat model.

One caveat with respect to this model involves the increased bandwidth of single sounds under the DBS relative to the PD conditions (Fig. 4-4b, bottom). Because human vocalizations are so much more intricate than those of rats, a reasonable human correlate

of this measure is difficult to identify. Persons with PD produce vowel sounds that are less dynamic than their healthy counterparts. For example, reductions in vowel-space area (Rusz et al., 2013) and articulatory–acoustic vowel-space (Whitfield and Goberman, 2014) metrics are both associated with PD. However, by measuring simultaneous changes in two formants, those metrics evaluate two simultaneous *sounds* as defined in the present study and are thus more analogous to word bandwidth. It may be that the increasing sound bandwidth is the rodent manifestation of speech slurring in human PD patients. Nevertheless, although sound bandwidths increase with PD and increase further with DBS, the decreased word complexity balances these effects to create only minimal (and generally insignificant) changes in word bandwidth (Fig. 3-4b, top).

Although we did not measure electroneurographic or electromyographic activity to study the mechanisms of hypokinetic dysarthria, our model provides a framework for such studies. An obvious candidate for examination is the differential responses of neural activity to pharmacological vs. neuromodulatory therapies, in particular, to ascertain how dopamine-based therapies alleviate dysarthria (De Letter et al., 2005, 2007a, 2007b), whereas DBS can worsen it (Burghaus et al., 2006; Romito et al., 2002; Umemura et al., 2011). Such studies might reveal changes in neural activity that would alleviate dysarthria and enable researchers to attempt appropriate neuromodulatory interventions in an ethical manner.

This study sought to develop a rodent model of DBS-exacerbated, parkinsonian hypokinetic dysarthria. However, dysarthria is not the only PD symptom poorly treated by DBS. For example, parkinsonian eyelid apraxia (Dewey and Maraganore, 1994; Yamada et al., 2004) has also been reported to worsen in response to DBS (Bologna et al.,

2012; Shields et al., 2006; Tommasi et al., 2012). One possible hypothesis is that increased hypokinetic dysarthria and eyelid apraxia result from stimulating the wrong target. The basal ganglia are somatotopically organized (Joint et al., 2013; Nambu, 2011), and the pathways responsible for orofacial and oculomotor control are likely specialized. Thus, stimulation of other basal nuclei or even other targets within the subthalamic nucleus may be more therapeutic, as has been demonstrated in a few patients (Dietz et al., 2013; Fuss et al., 2004; Mikos et al., 2011). Hence, a useful future direction would involve DBS during vocalization protocols with subsequent histology to map which subregions of neural tissue are most responsible for dysarthria and, potentially, other side effects of, or symptoms exacerbated by, DBS.

In conclusion, DBS of the subthalamic nucleus in the rodent 6-OHDA model of PD worsens parkinsonian symptoms related to hypokinetic dysarthria. Detrimental changes in vocalization complexity, vocalization rates, word durations, and individual sound bandwidths were all exacerbated by DBS. This study provides a framework for exploration into the electrophysiological mechanisms of parkinsonian hypokinetic dysarthria and its exacerbation by otherwise therapeutic DBS. Such explorations are essential to understand better and henceforth minimize this side effect of stimulation that greatly diminishes quality of life.

CHAPTER 4

DBS-INDUCED IMPULSIVITY DOES NOT OVERRIDE PARKINSONIAN APATHY

Patients implanted with deep brain stimulation (DBS) electrodes for the treatment of Parkinson's Disease (PD) frequently experience new impulse control disorders (Demetriades et al., 2011). Additionally, nearly three-quarters of patients with PD experience symptoms of apathy, frequently unrestored or even worsened by DBS of the subthalamic nucleus (STN) (Funkiewiez et al., 2004; Muhammed et al., 2015). We created a behavioral configuration and tested the behavioral effects of DBS on healthy and hemiparkinonian rodents. We found that DBS creates action suppression deficits and other impulse control disorders (ICDs) and, additionally, fails to alleviate parkinsonian apathetic behavior and action selection deficits. Our work provides a model for future studies into the electrophysiology of DBS-induced ICDs and PD-induced apathy and action selection deficits.

4.1 Abstract

DBS creates impulse control disorders and fails to restore parkinsonian apathetic behavior and action selection deficits. As many as 70% of PD patients experience symptoms of apathy, frequently unresolved or worsened by deep brain stimulation (DBS)

of the subthalamic nucleus (STN). Additionally, as many as 56% of patients receiving deep brain stimulation (DBS) for Parkinson's Disease (PD) may experience new-onset impulse control disorders of varying severity following therapy initiation. Some animal-based studies have been performed to examine these symptoms and side effects, but more work is needed. Thus, we created a behavioral configuration and tested the behavioral effects of DBS in the context of healthy-control and hemiparkinsonian rodents. We found that DBS of the STN in a healthy rodent leads to more impulsive behavior in the form of stop and no-go task failure, impulsive reward seeking, and non-instructed task attempts. Additionally, based on the timing of stop and no-go cue failures, we found evidence to support that STN-DBS interrupts signals responsible for action cancellation. Additionally, we have demonstrated that hemiparkinsonism leads to slowed go-cue response times and greatly reduced response rates, unrestored by DBS. Since DBS functions by overriding pathological electrophysiological activity, rather than restoring that seen under healthy conditions, it may be that certain neurological signals responsible for healthy action selection are interrupted by PD, not restored by DBS, leading to apathy and mis-weighting of various action in the context of reward-based action selection. This work will enable future electrophysiological studies into the mechanisms of DBS-induced action suppression deficits and PD-induced apathy and action selection deficits.

4.2 Introduction

Nearly three-quarters of Parkinson's Disease (PD) patients exhibit the non-motor symptom of apathy (Muhammed et al., 2015). While dopamine replacement therapies generally treat this symptom (Chong et al., 2015; Favier et al., 2014; Fleury et al., 2014),

deep brain stimulation (DBS) often fails to improve or worsens apathetic symptoms (Funkiewiez et al., 2004; Gesquière-Dando et al., 2015; Richard, 2007; Williams et al., 2015). Additionally, impulsive behaviors are commonly associated with dopamine agonist drug therapies and DBS. While both are frequently successful in reducing the severity of numerous motor symptoms — such as bradykinesia, rigidity, and tremor (Barcroft and Schwab, 1951; Limousin-Dowsey et al., 1999; Lyons and Pahwa, 2004; Treciokas et al., 1971) — they are associated with numerous side effects, including an increase in impulsive behavior. In fact, literature over the last decade has reported that as many as 39% of patients taking dopamine agonists and 56% of patients receiving DBS experience new-onset impulse control disorders (ICD) of varying severity (Bastiaens et al., 2013; Demetriades et al., 2011; Frank et al., 2007; Jahanshahi et al., 2015; Weintraub and Nirenberg, 2013; Witt et al., 2004).

It is difficult to study the mechanisms of ICDs and apathy in human PD patients; thus, a moderate amount of work has been performed examining ICDs induced by DBS in animal, mostly rodent, models. This work has shown that DBS leads to some impulsive behaviors, such as premature responding (Aleksandrova et al., 2013; Desbonnet et al., 2004; Sesia et al., 2010; Summerson et al., 2014), increased perseverative responses (Baunez et al., 2007), and changes in intertrial response (Sesia et al., 2010). Similarly, STN lesions in animals models have resulted in many related behaviors, such as premature response (Baunez et al., 1995; Phillips and Brown, 2000; Uslaner and Robinson, 2006), increased perseverative responses (Baunez and Robbins, 1997, 1999), increased stop response error (Eagle et al., 2008a), and impaired no-go responses (Eagle et al., 2008b). Additionally, animal work has shown that dopamine

agonists improve apathy (Favier et al., 2014) and that DBS may modulate striatal dopaminergic receptor levels in a way that induces apathy (Carcenac et al., 2015).

While mechanistic study of ICDs and apathy in humans is difficult, many reports have been made as to specific impulsivity side effects and their severity with DBS administration, with some studies demonstrating complex or conflicting results. Many measures of impulsivity are more often worsened than improved under DBS, such as Stroop interference tasks (Jahanshahi et al., 2000; Schroeder et al., 2002; Witt et al., 2004), high-conflict decision making (Cavanagh et al., 2011; Frank et al., 2007), response thresholds (Pote et al., 2016), and the influence of task difficulty on decision making (Green et al., 2013). However, some are reported both as worsening and unchanged, such as go/no-go response time (Campbell et al., 2008; Hershey et al., 2010). While PD patients with slow stop signal reaction times (SSRTs) usually see improvements with DBS, some patients with relatively normal SSRTs actually become slower with DBS (Ray et al., 2009). Additionally, work has been done to determine how to combat apathy post-DBS (Schrag et al., 2015), but researchers have specifically called for more work pursuing the mechanisms of PD-related apathy to be completed (Starkstein, 2012).

The aforementioned work has improved our understanding of impulsivity and apathy through a number of lenses, but we wanted to provide more evidence for the specific roles of action suppression and action selection within the basal ganglia in the context of impulsivity. Thus, we studied impulsive behavior and responses in a rodent STN-DBS model, specifically examining task response success and response timing, as well as other measures of impulsive behavior, such as impulsive reward seeking and non-instructed task attempts, in the context of both a go/stop task and a go/no-go task.

Our results demonstrate that DBS of a healthy rodent leads to more impulsive behavior in the form of stop and no-go task failure, impulsive reward seeking, and non-instructed task attempts. When analyzing the timing of stop and no-go failures, we discovered that DBS may induce more significant failures in a go/stop task than in a go/no-go task, lending support to the role of the basal ganglia in action suppression, with necessary information from the STN for action cancellation being interrupted by DBS (Schmidt et al., 2013).

Additionally, our results demonstrate that the depletion of dopaminergic neurons through Parkinsonism fundamentally alters reward circuitry in a way that is not restored by DBS, as seen by reduced responses to go cues, which quickly drop following reintroduction to the task after motor symptoms of 6-OHDA injection have been successfully identified. While DBS generally treats motor symptoms successfully, it does not restore go response times, which are slowed by PD. Thus, it may be that Parkinsonism induces apathy and changes the weighting of various actions in the context of reward-based action selection in ways that are not restored by DBS.

4.3 Materials and Methods

All surgical and experimental procedures were performed in the Department of Bioengineering at the University of Utah, were approved by the institutional animal care and use committee of the University of Utah, and complied with U.S. Public Health Service policy on the care and use of laboratory animals.

4.3.1 Experimental Protocols

Behavioral data were collected from rats of both genders. The timeline of the protocol for 8 Long-Evans rats weighing 200–250 g was as follows. Rats were trained on one of two behavioral tasks, with a group of four rats trained on a go/stop task and a group of four trained on a go/no-go task. After successful completion of training, rats underwent stereotactic surgery to receive three chronic brain implants (Chang et al., 2003; Dorval and Grill, 2014): a cannula accessing the medial forebrain bundle (MFB), and an electrode array to stimulate the subthalamic nucleus, and a recording electrode in the substantia nigra pars reticulata (SNr). Three rats in each group survived surgery; beginning 10 days after surgery, these rats were retrained on their respective behavioral tasks for a period of 10 days, alternating between days without a tether connected and days with a tether connected to ensure continued willingness and ability to complete the task. Following retraining, healthy-control and healthy-control + DBS behavioral and electrophysiological data were collected. For all recordings in both conditions, the DBS tether was connected to minimize potential bias created by the tether; additionally, healthy-control and healthy-control + DBS data were collected back to back in alternating 10 minute intervals for a total duration of 40 minutes to eliminate potential bias created by day-to-day variability.

After 1 week of healthy-control and healthy-control + DBS recordings, rats in the go/stop group were injected intracranially with 6-OHDA through the implanted cannula to the MFB to degenerate dopaminergic neurons in the substantia nigra pars compacta. After 14 days, hemiparkinsonism was diagnosed by two methods.

First, paw preference during exploration was tested using a plexiglass cylinder 30

cm tall and 10 cm in radius outfitted with a series of 24 white LEDs shone into the top surface. Rats were placed in chamber with the left and right front paws painted blue and red, respectively, with standard nail polish. When a rat touched the cylinder with either paw, frustrated total internal reflection resulted in either a blue or red illumination of the cylinder (Fig. 4-1a). A high-speed camera (Prosilica GE680C, Allied Vision, Exton, PA) captured video from the anterior side of the cylinder and 30 cm tall mirrors were placed at angles of 120° and 240° around the cylinder to enable visibility of the entire cylinder with one camera. Thirty-minute recordings were made for each rat under each of healthy-control, hPD and hPD+DBS conditions on two separate days and video was replayed at 50% speed while we manually counted left and right paw touches based on separate blue and red touches.

Second, rats were injected with 5 mg/kg intraperitoneal dextroamphetamine, and hemiparkinsonism was diagnosed by the manual counting of at least 10 more rotations ipsilateral than contralateral to 6-OHDA injection each minute; DBS was considered effective if it reduced the difference between ipsilateral and contralateral rotations per minute by a statistically significant margin (α=.05). One 30-min recording was made from each of the 6-OHDA-injected rats beginning 30 min after dextroamphetamine injection, with alternating 10-min sections on- and off-DBS. Under both metrics, we concluded that each of the three rats developed a severe, unilateral Parkinsonism contralateral to the 6-OHDA lesion; additionally, DBS was determined to be effective in all three. Similarly, this method was used to quantify the effects of DBS on animals under control conditions, quantifying the contralateral rotation induced by DBS in an otherwise healthy animal. After verification of hemiparkinsonism (hPD), data were collected under

hPD and hPD + DBS conditions. Following all data collection, rats were euthanized.

4.3.1.1 Surgical procedures. Rats were provided 20 mg of carprofen (Bio-Serv, Flemington, NJ) and were anesthetized with 2–3% isoflurane after consumption. The surgical site was shaved and disinfected, and the rats were placed on a body-temperature heating pad in a stereotactic frame (Kopf Instruments, Tujunga, CA). The scalp was opened and cleaned to the skull, and craniotomy sites were measured and marked with respect to bregma (Paxinos and Watson, 2008). Seven titanium bone screws were driven through burr holes into the skull to anchor the eventual acrylic cap. To allow the eventual injection of 6-OHDA into the MFB, a 23-gauge stainless-steel cannula was implanted through a burr hole 2.0 mm posterior and 2.0 mm lateral to bregma. For DBS of the subthalamic nucleus, a four-channel microstimulating array – 2×2 grid of 75-μm platinum–iridium electrodes (~100 kΩ at 1 kHz) with 400-μm spacing (Microprobes for Life Science, Gaithersburg, MD) – was implanted through a burr hole 3.6 mm posterior and 2.6 mm lateral to bregma at a ventral depth of 7.8 mm. Medial electrodes were 500 μm longer than their lateral counterparts to match the anatomy of the subthalamic nucleus. Sixteen-channel micro-recording arrays – 4×4 grid of 20 μm stainless steel electrodes (~1.0 MΩ @ 1 kHz) with 400 μm spacing (ibid) – were implanted into the SNr, reached their target (5.5 mm posterior, 2.3 mm lateral, and 7.7 mm ventral) by advancing 7.8 mm through a burr hole 6.5 mm posterior and 2.3 mm lateral, in the sagittal plane and angled 7.4° anteriorly from the coronal plane.

After each of the hardware elements was lowered to its target depth, a layer of dental acrylic was applied to attach it firmly to the anchor screws. After these implantations, the screws, cannula, and array were encased in a thick dental acrylic cap,

built smoothly over multiple layers. The incision was sutured around the acrylic cap and covered with topical antibiotics. Rats were returned to their home cages and given 7 days of recovery prior to experimental recordings.

After healthy-control and healthy-control + DBS recordings, rats in the go/stop group were injected with 6-OHDA to induce Parkinsonism (Dorval and Grill, 2014; Fibiger et al., 1972). Rats were anesthetized with 2–3% isoflurane and returned to the stereotactic frame. A needle was inserted to 0.5 mm beyond target depth, left for 5 min to create a pocket, and then retracted by 0.5 mm. A bolus of 8.0 μg 6-OHDA dissolved in 8.0 μl saline was injected at a rate of 1.0 μl/min. Ten minutes after the completion of the injection, the needle was withdrawn at a speed not exceeding 1.0 mm/min. Rats were returned to their home cages to develop Parkinsonism over the next 2 weeks, with efficacy confirmed as previously described.

4.3.1.2 DBS. Prior to all trials, rats were briefly anesthetized with 2–3% isoflurane, and a four-channel tether was attached to the connector of the microstimulating array on the head. Rats were quickly moved to the behavioral chamber before awaking, and the other end of the tether was connected to an analog current stimulator (Grass Technologies, Warwick, RI). Current amplitudes ranged from 100 to 500 μA, varying by animal; bipolar stimulation was delivered through the microstimulating array, with both medial contacts set as anodes and both lateral contacts set as cathodes. The stimulation waveform consisted of symmetric 100-μsec biphasic current pulses repeating at 100 Hz. It was qualitatively determined that rat behavior in the behavioral task may differ in the first 5 min that the rat was introduced to the box each time; in order to prevent biasing of results, rats were reintroduced to their respective behavioral tasks for 10 min with no stimulation

and data were not collected until after this introductory period.

Under both healthy-control and hPD conditions, starting 2 weeks after 6-OHDA injection in the latter, stimulation thresholds were determined by gradually increasing the current amplitude until the appearance of physical side effects, including atypical whisker twitching, other dystonic facial contractions, and dystonic movements contralateral to stimulation. DBS amplitude was then set to 90% of the minimum current that yielded side effects. Although stimulation was applied only during DBS trials, the tether was always connected during all behavioral recordings.

4.3.1.3 Behavioral configuration. A 30 cm-per-side plexiglass cube (Fig. 4-1d) was constructed, with the top mostly uncovered. The behavioral chamber was encased on 5 sides to keep light out – with a small hole on top to allow tethered cables to run into the configuration – and the sixth side was covered with red plexiglass— transparent to wavelengths outside the rats' visible range —to allow monitoring by experimenters without being seen by the rat. A 5 cm-by-20 cm plexiglass rectangle was overlaid on top of the top of the box, on which an orange LED and speaker were mounted. Two 2.5 cm holes were drilled in the front of the box. The right hole, from a vantage point within the box, was designated as the task hole, while the left was designated as the reward hole. Red LEDs – producing light invisible to rats – and photodiodes were fitted to either side of each hole to create a sensor for nose-poke detection, while a cup was fitted to the bottom of the right hole and a nozzle was secured above the hole. The nozzle was connected via standard tubing to a pump (NF5, KNF Neuberger, Trenton, NJ), which was, in turn, connected to a reservoir of 10% sucrose solution, pumping approximately 20 μL of sucrose solution for each reward. Each of the LEDs and photodiodes, the speaker, and

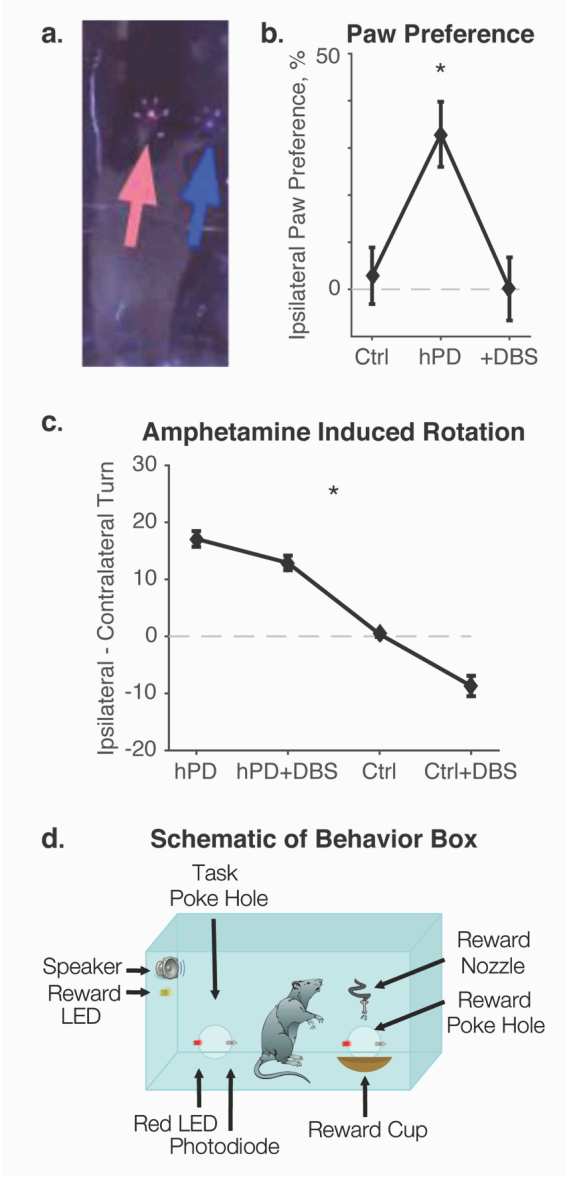

Figure 4-1. Behavioral verification and configuration. A. Frustrated total internal reflection test to measure paw preference. Right paw lit up cylinder in red, while left paw lit up cylinder in blue. B. Asterisk denotes significant ipsilateral paw usage preference. Rats under control and hPD+DBS conditions exhibited no paw preference, while rats under hPD conditions favored paw usage ipsilateral to 6-OHDA lesion. C. Rotations were induced using dextroamphetamine. Asterisk denotes significant difference between all six pairs using a Student's t-test with Holm-Bonferroni correction. Additionally, hPD, hPD+DBS, and Ctrl+DBS conditions were significantly different from zero. Rats had no preference for turn direction under control conditions, but had a preference for ipsilateral rotation under hPD conditions, which was significantly reduced by STN-DBS. DBS under control conditions induced a preference for contralateral rotations. D. Behavioral configuration. When given a go cue (tone), rats nose-poked in task hole to receive sucrose in reward hole. When given a stop or no-go cue, rats received reward for successful restraint.

the pump were connected to a standard desktop computer through a standard data acquisition (DAQ) board (National Instruments, Austin, TX) and interfaced with LabVIEW (National Instruments, Austin, TX).

Custom LabVIEW code was written to control the behavioral configuration. The program wrote a text file consisting of all important cues and behaviors, appending the text file with a timestamp and code for each cue and relevant behavior. Both red LEDs were kept on at all times and voltage was measured from photodiodes at all times. If the rat nose-poked in either hole at any point, this was detected by the photodiodes, and a numeric code corresponding to this behavior was written to the text file along with the time of the first time step that the behavior occurred for each behavioral occurrence. Specific cases were created for each of the following conditions: null (no instruction, no reward), go cue, instructing the rat to nose-poke in the task hole via a specific tone; stop and no-go cue, instructing the rat to refrain from nose-poking in the task hole via a different tone; and reward, consisting of a third tone and an orange light from the ceiling. Numeric codes and timestamps were written for each of the following: go cues, successful nose-poke during a go cue, failure to nose-poke during a go cue, stop or no-go cue, successful refrain from nose-poking during a stop or no-go cue, failure to refrain from nose-poking during a stop or no-go cue, nose-poke in the absence of a cue, and nose-poke into the sucrose reward hole at any time.

During all behavioral and electrophysiological recordings, go cues lasted 6 seconds, stop and no-go cues lasted 10 seconds, go cues that turned into stop cues lasted 3 seconds before turning into stop cues, the null condition time was sampled from a uniform distribution spanning from 10 to 20 seconds, and the reward state lasted up to 30

seconds if rats did not retrieve the reward. The last timing was mostly relevant in training, although it was kept long during recordings to prevent rewards from being triggered during a success, not retrieved prior to another cue being presented, and then later retrieved upon failure of a different cue.

4.3.1.4 Behavioral training. Rats were trained until they consistently met performance thresholds – task completion during at least 70% of go cues and refrain from task completion during at least 70% of stop and no-go cues – in sets of random tasks lasting 30 min. For the first day of training, rats were deprived of food, while, on the second and third days, they were given 5 grams of food. For 2 weeks starting on the fourth day, rats were given 10 grams per day. For 2 weeks following this period, rats were given 15 grams per day. For the next 2 weeks, rats were given 20 grams per day. Finally, after this, rats were given unlimited food access.

On the third day of training, in addition to the 5 grams of food, rats were given a bottle of 10% sucrose solution – temporarily replacing their standard water bottle – and allowed to drink freely until 20-30 mL had been consumed. Next, for 3 days, rats underwent 30-min training sessions consisting of being given repeated sucrose rewards in the reward hole. Next, for 4 days, rats underwent 30-min training sessions consisting of a sucrose reward given in the reward hole for successful nose poke in the sucrose hole. If, by day 3, the rat did not qualitatively appear to be frequently repeating the task, which was true for the majority of rats, the rim of the task hole was repeatedly lined with sucrose solution to encourage task completion. If necessary, a fifth day of successful nose poke and sucrose reward was utilized. However, this training was only necessary with one rat.

Following successful training on nose-pokes in the task hole leading to a reward, rats were on the go cue. For 12 +/- 2 days, rats underwent 30-min training sessions consisting of sucrose reward in response to successful completion of the task during a go cue. For the first sessions, the go cue was 20 seconds long to introduce the idea that the task would only be rewarded during a go cue. This time was gradually decreased throughout the training until it reached the final length of 6 seconds. Qualitatively, rats typically attempted responses considerably more quickly than 6 seconds after presentation of the cue, but the cue was not shortened further, as rats would often not nose-poke into the hole far enough to trip the sensor; the cue was kept long enough to allow the rat to attempt the cue, fail, and attempt again in order to reduce disinterest in task completion. Rats successfully completed go cue training once they had achieved 80% successful response to minimum time go cues for several sessions in a row.

Once rats successfully responded to at least 80% of go cues, the stop/no-go cue was introduced in the absence of any go cues, i.e., as a no-go cue. For 10 +/- 2 days, rats underwent 30-min training sessions consisting of sucrose reward in response to a successful refrain from a nose poke during the duration of the cue. The no-go cue started at 4 seconds in length and gradually increased throughout the training until it reached the final length of 10 seconds. Stop/no-go training continued until rats successfully refrained from nose-poking during 80% of no-go cues at maximum time no-go cues for several sessions in a row. Qualitatively, rats were additionally expected to demonstrate continued awareness and interest of the task through reward retrieval. If rats qualitatively demonstrated lack of interest at any time during this training block, a session of go cue training was reintroduced.

For rats being trained on a go/stop task, rats were next introduced to the stop/no-go cue specifically as a stop cue. For 7 +/- 1 days, rats underwent 30-min training sessions consisting of stop cues following 3 seconds of go cue. If the rat successfully nose-poked during the 3 seconds of go cue, it received a reward; however, once the task reverted to a stop cue, the rat was expected to refrain from poking. Stop training continued until rats successfully refrained from nose-poking during 75% of stop cues for several sessions in a row.

Following stop/no-go training, rats were re-presented with the go cue. For 3-4 days, rats underwent 30-min training sessions consisting of go cues. All of the rats successfully achieved at least 70% success on the go cue by the end of the 4^{th} training session.

Following reintroduction of the go cue, rats were trained to respond differentially to the two different tones. For 9 +/- 3 days, rats underwent 30-min training sessions consisting of alternating periods of go and go/stop or go and no-go cues. Given the eventual randomized average presentation of 70% go cue and 30% go/stop or no-go cues, rats were presented with repeatedly alternating bouts of go cues lasting 3.5 min and stop or no-go cues lasting 1.5 min. Alternating training continued until rats successfully achieved at least 70% success on both cues for multiple sessions.

Following alternating cue training, rats underwent 30-min training sessions consisting of randomized sets of go and go/stop or no-go cues, with 70% cues chosen as go cues and 30% of cues chosen as go/stop or no-go cues. Training was presented for 11 +/- 4 days until rats successfully responded to both cues with an average of more than 70% success over a period of 4 days.

Following this final block of training, rats were considered fully trained, and were surgically implanted with a cannula and electrodes, as previously described. Following surgical implantation, rats underwent 5 tether habituation sessions, in which rats were placed in home cages with a tether connected to the stimulation array connector, but stimulation turned off. Following this, rats underwent 30-min training sessions consisting of randomized sets of go and go/stop or no-go cues for a period of ten days, alternating between tethered and non-tethered training sessions. Within 10 days, all rats, once again, achieved 70% success on both cues both with and without a tether.

4.3.1.5 Behavioral recording. Behavioral recordings were recorded separate from electrophysiological recordings. Once rats were successfully trained on respective tasks, implanted, habituated to tether, and retrained, behavioral recordings commenced. Prior to all behavioral recordings, rats were deprived of water for 18 +/- 2 hours, and behavioral recordings were never made 2 days in a row for a given rat; thus, rats were never deprived of water for more than 20 hours of a 48-hour window. Rats were briefly anesthetized with 2-3% isoflurane and the connectors of their stimulating arrays were attached to tethers to the analog stimulator. Rats performed the task for a period of 10 min, and then recordings began, consisting of four alternating 10-min segments with DBS turned on and off, with a random selection as to which started first to eliminate bias. Behaviors and cues were recorded, as previously described. Following recordings, rats were, once again, anesthetized with 2-3% isoflurane and connectors were disconnected. Following five successful behavioral recording sessions, electrophysiological recordings were made.

4.3.1.6 Electrophysiological recording. Electrophysiological recordings were

performed in rats performing the go/no-go task; these recordings were made separately from full-length behavioral data recordings to prevent tangling of electrophysiology and DBS cables. Rats were briefly anesthetized with 2% isoflurane and the connectors of their micro-recording arrays were attached to sixteen-channel head stages and associated tethers to a multichannel stimulation and recording system (SnR, Alpha Omega, Alpharetta, GA). For STN-DBS trials, rats were additionally connected to an analog stimulator with a four-channel tether, as described above. While rats were always tethered to a DBS cable during behavioral recordings to prevent biasing of behavior, we did not have a reasonable expectation of electrophysiological recording biasing based on the presence of a second tether once an electrophysiological tether was already in place and, thus, we only connected the DBS tether during DBS trials. Signals pertaining to the timing of cues and behaviors were sent to the recording software from the behavioral computer via analog inputs in the recording system, discussed below. Five minutes after awaking from anesthesia in the behavioral configuration, electrophysiological recordings began; local field potentials (LFPs) were referenced to transcranial ground screws and recorded from SNr. Recordings lasted a maximum of 30 min, and were stopped shorter if either cable became disconnected due to tangling of cables. Following successful collection of data, rats were euthanized.

4.3.1.7 Statistical comparisons. Where statistical significances are associated with results – within subsections of each of the figures – the relevant statistical test is noted in the text. Summary values of approximately gaussian-distributed results are presented as mean plus or minus standard error, mean±s.e. Summary values of non-gaussian results were found from 100,000 bootstrapped populations resampled with replacement,

presented as means spanning the 25th to 75th percent confidence intervals, mean±c.i. Statistical test abbreviations: Ttest = student T test; bca = bootstrapped confidence assessment.

4.4 Results

Eight rats successfully completed training of their respective tasks, 4 in the go/stop task, and 4 in the go/no-go task. All 8 were implanted with a cannula to the right MFB and a four-channel stimulating electrode array to the right subthalamic nucleus. Rats in the go/no-go task additionally received a sixteen-channel recording array to the right substantia nigra pars reticulata; 3 rats from each task group survived the surgery. The results reported come from these 6 rats.

Behavioral recordings under healthy-control and healthy-control + DBS conditions were made in all 6 rats in both categories. After sufficient healthy recordings of rats in the go/stop task, the neurotoxin 6-OHDA was injected through their cannulas to the right MFB to induce left-side hemiparkinsonism. All 3 rats developed Parkinsonism by 2 weeks following 6-OHDA injection; hemiparkinsonian (hPD) and hPD + DBS recordings were made from each of these 3.

4.4.1 Model Validation

Motor symptoms of hPD and efficacy of DBS were assessed via two methods. First used was the method of comparing ipsilateral vs. contralateral paw touches while each rat explored a frustrated-total-internal-reflection-based light-emitting cylinder (Fig. 4-1a, blue/red paws) under each condition. Second, we injected rats with

dextroamphetamine intraperitonally to induce rapid movement and compared ipisilateral vs. contralateral rotations under each of hPD and hPD + DBS conditions.

Rats had a significant preference for ipsilateral paw usage under hPD conditions (P_{Ttest}=.0088) and exhibited no significant preference under healthy-control or hPD+DBS conditions (Fig. 4-1b). Additionally, rats turned more ipsilaterally than contralaterally in the hPD condition (P_{Ttest}<.00001) and hPD + DBS condition (P_{Ttest}<.00001). Finally, rats turned more contralaterally than ipsilaterally in the Ctrl + DBS condition (P_{Ttest}<.00001) and exhibited no directional preference in the Ctrl condition. (Fig. 4-1c). Paired tests (T_{test} with Holm-Bonferroni correction) revealed that each condition was significantly different from each other condition. Specifically, DBS reduced hemiparkinsonian ipsilateral rotations, but rats still rotated more ipsilaterally under hPD + DBS conditions than under control conditions. Finally, rats rotated more contralaterally under control + DBS conditions than under control conditions.

4.4.2 Behavioral Measures

Impulsivity measures grouped across task groups. Two measures of impulsivity were made under healthy-control and healthy-control + DBS conditions that were unaffected by rats' task grouping: un-cued task attempts and impulsive reward seeking. The go cue, poke task, and reward cues were identical in both groups and results were insignificantly different between the two task groups. Thus, we analyzed the two task groups together.

Rats attempted the task when un-cued significantly more often when DBS was turned on than when it was turned off (Fig. 4-2a, P_{bca} = .019). Taking into account day-to-

day variability and pairing back-to-back recordings on and off DBS, the difference between on-DBS and off-DBS recordings was significantly greater than zero (Fig 4-2c, $P_{bca} = .015$). Additionally, rats impulsively sought rewards significantly more often when DBS was turned on than when it was turned off (Fig. 4-2b, $P_{bca} = .0026$). Taking into account day-to-day variability and pairing back-to-back recordings on and off DBS, the difference between on-DBS and off-DBS recordings was significantly greater than zero (Fig 4-2c, $P_{bca} = .0002$).

4.4.2.1 Stop and no-go cue impulsivity. Two measures were made to examine DBS-induced impulsivity in the context of stop and no-go cue failure: fraction of stop/no-go cues that were failed and, given a failure, average time to failure following cue onset. Given the differences in tasks, but the overall similarity in failure during a cue instructing rats not to nose-poke, we analyzed fraction of failed cues both separately and together. While these results were similar in both tasks, differences between control and control + DBS average times to failure following cue onset were significantly different between the two task groupings.

In the context of a go/stop task, rats were significantly more likely to fail the stop task and nose-poke when specifically instructed not to when DBS was turned on than when it was turned off ($P_{bca} = .0090$). With a go/no-go task, rats were, similarly, significantly more likely to fail the no-go task and nose-poke when specifically instructed not to when DBS was turned on than when it was turned off ($P_{bca} = .032$). Combining the task groups to analyze total failure of stop/no-go tasks led to a lower p-value than either of the previous (Fig. 4-3a, $P_{bca} = .0042$).

While results were similar in terms of the fraction of failed no-go and stop cues,

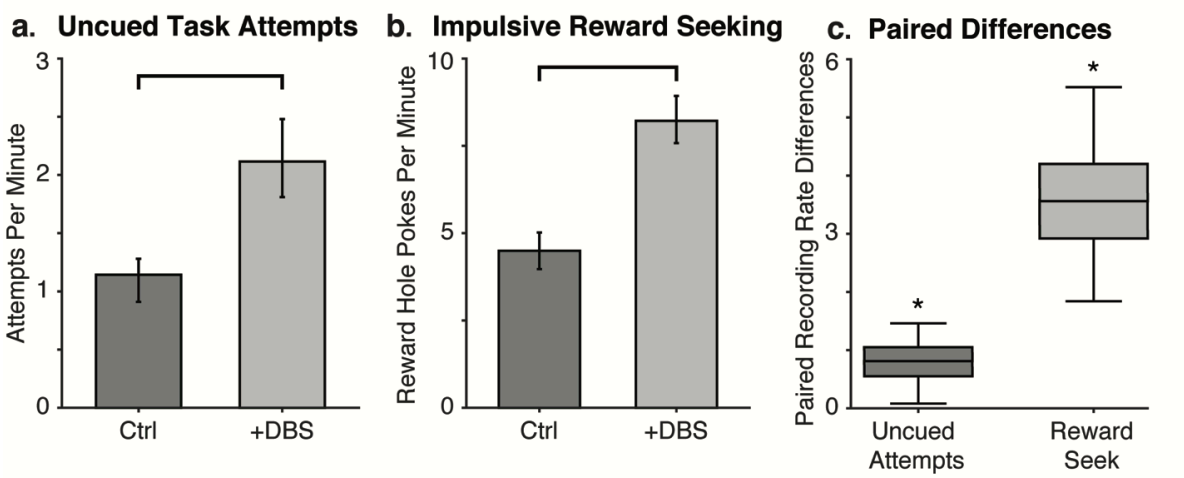

Figure 4-2. Impulsive behaviors shared across task groupings. Bars denote significant difference between conditions and asterisks denote significant difference from 0. A. Rats under control conditions nose-poked in the task hole significantly more often when not instructed to do so when DBS was turned on than when DBS was turned off. B. Rats under control conditions impulsively sought rewards in the absence of task completion significantly more often when DBS was turned on than when DBS was turned off. C. Back-to-back recordings on- and off-DBS were paired. Boxes represent median + interquartile range, while bars represent 95% confidence interval. In both cases, paired differences were significantly greater than zero.

the timing of failed cues revealed differences. When rats in the go/stop task group failed to obey a stop cue, the average time to failure following cue onset was significantly longer while DBS was on than while DBS was off (P_{bca} = .0049). However, this was not the case in the go/no-go task group. When rats in this group failed to obey a no-go cue, the average times to failure following cue onset were insignificantly different between DBS-on and DBS-off conditions. Additionally, the average time to failure following cue onset was longer in the context of stop cue failures than of no-go cue failures both in control (P_{bca} = .0015) and control + DBS (P_{bca} = .00036) conditions (Fig. 4-3b).

4.4.2.2 Effects of DBS on go-cue response. Response times to go cues were unaffected by rats' task grouping given the same go cue and task in both groups. Therefore, we analyzed the two task groups together and found that DBS had no significant effect on average response time to go cues (Fig. 4-4a). Similarly, DBS had no significant on go cue success fraction (Fig. 4-4b, Left).

4.4.2.3 Effects of Parkinsonism on go-cue response. After collection of control and control + DBS recordings was completed, rats in the go-stop task group were made hemiparkinsonian via 6-OHDA injection to the MFB. After symptoms were verified, 14 days after injection, behavioral recordings were made under hPD and hPD + DBS conditions.

Rats under hPD and hPD + DBS conditions successfully responded to the go cue at a significantly lower fraction than rats under control or control + DBS conditions (P_{Ttest}<.00001 for all four comparisons). Administration of DBS to rats under hPD conditions did not significantly increase the fraction at which rats successfully responded to the go cue. (Fig. 4-4b, Right). Additionally, response rates were significantly reduced

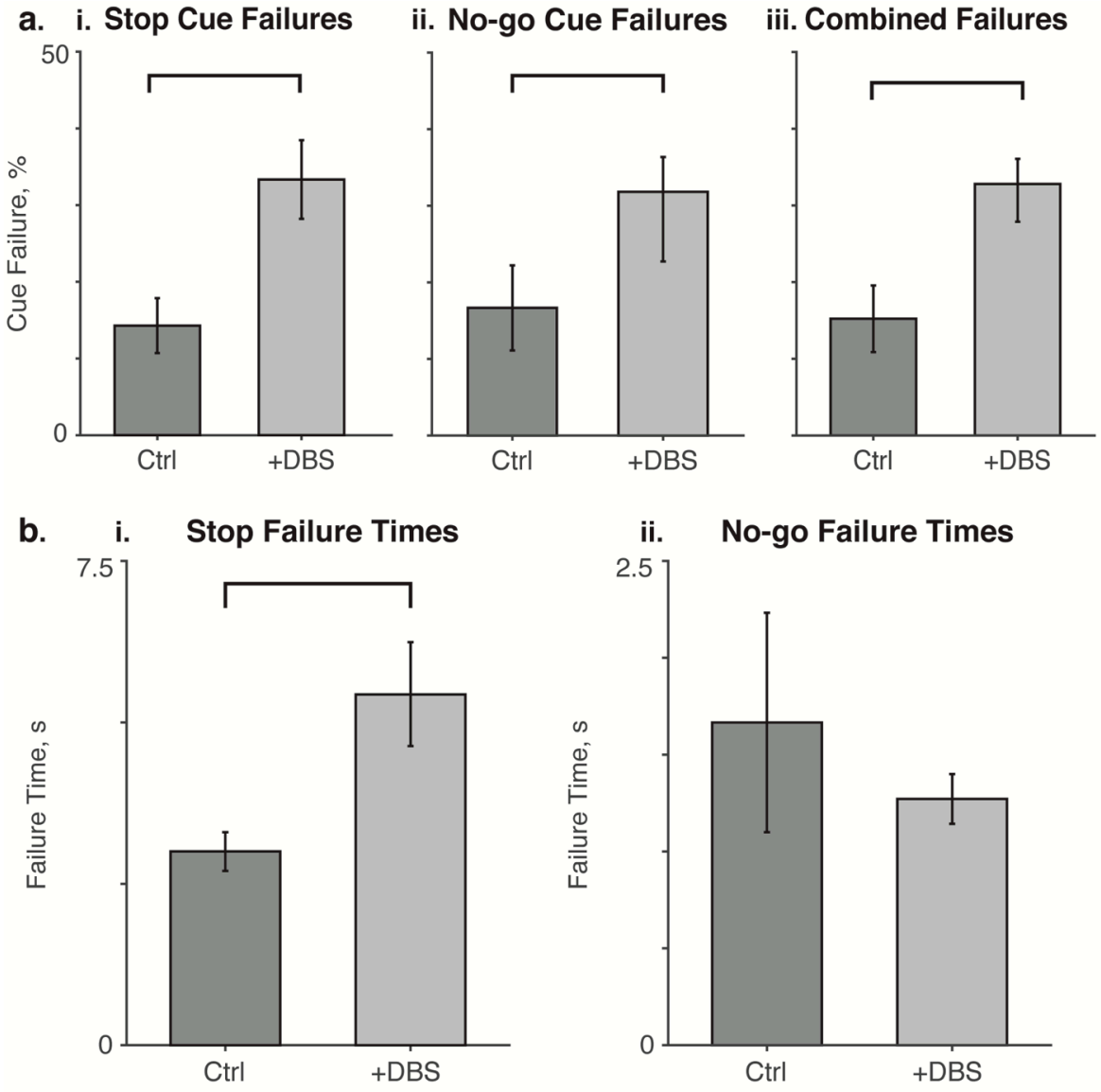

Figure 4-3. Stop and no-go impulsivity. Bars denote significant difference between conditions. A. DBS of control animals induced a greater percentage of failures in both the stop cue (i) and the no-go cue (ii). All stop and no-go cues are combined in (iii). B. In the context of a stop cue, the average time to failure was longer on DBS than off DBS. In the context of a no-go cue, the average failure times did not significantly differ. While most failures in each of the two conditions and each of the two task groupings were quick failures, rats under DBS conditions often nose-poked many seconds later, despite instruction not to.

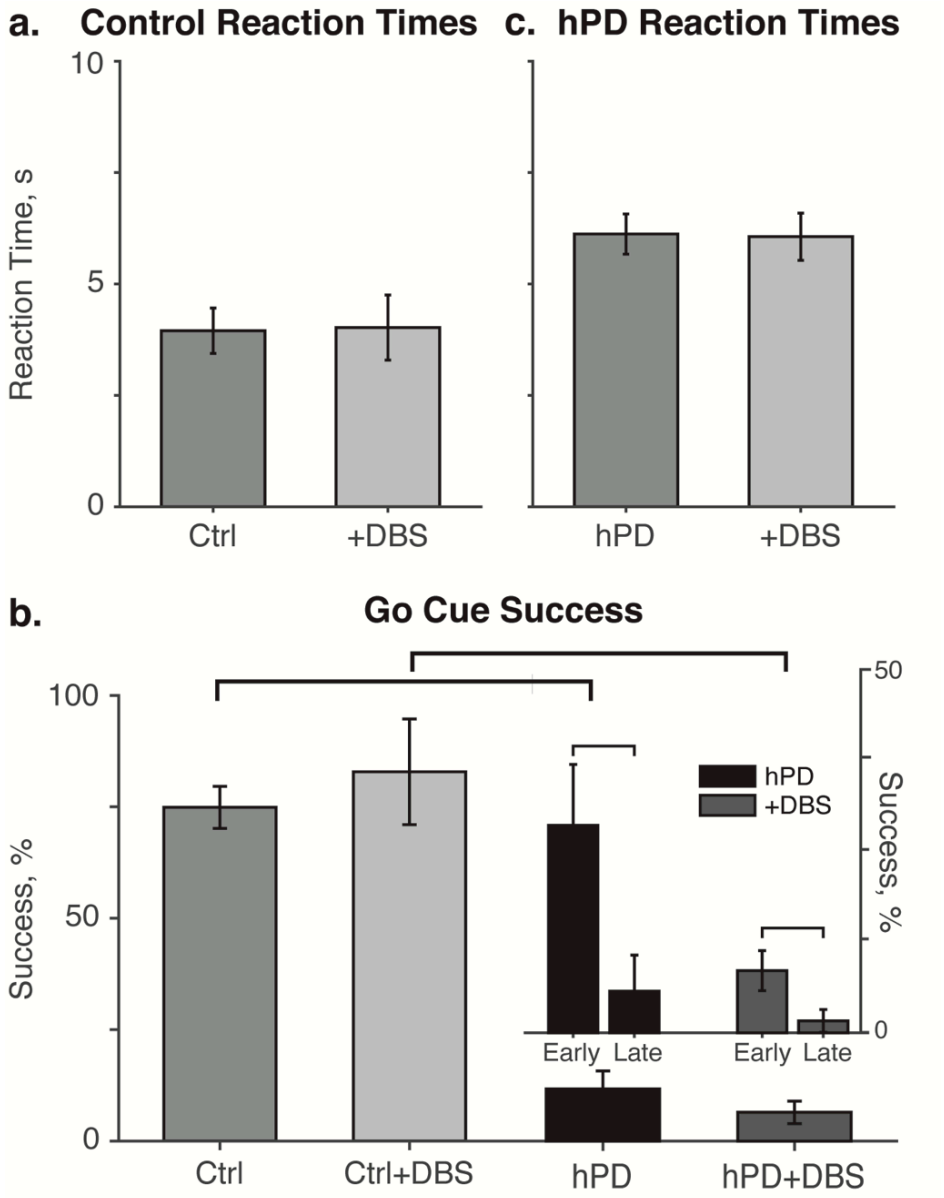

Figure 4-4. Go cue reaction times and success rates. Bars denote significant difference between conditions. A. DBS of control animals did not significantly change reaction times to the go cue. B. DBS did not significantly change the rate of successful response to the go cue in control animals. Hemiparkinsonian animals exhibited dramatically reduced success rates from control animals, unrestored by DBS, which failed to significantly change response rates. Note the reduced response rates from early (first 3 recordings) after symptom verification to later recordings, under both hPD and hPD+DBS conditions. C. DBS of hPD animals did not significantly change reaction times to the go cue.

from the first 3 days following symptom verification to later recordings, under both hPD (P_{Ttest}= .039) and hPD+DBS (P_{Ttest}= .047) conditions.

Due to the very small response rate to the go cue after hPD onset, we were unable to easily obtain enough data to have reliable response time results in either hPD or hPD + DBS conditions. Thus, we additionally made recordings with go cues lengthened to 8 seconds to enable the collection of enough data to allow the comparison of reaction times under hPD and hPD + DBS conditions. There was no significant difference between reaction times under hPD and hPD + DBS conditions (Fig. 4-4c).

4.4.2.4 Electrophysiological measures. While 3 rats in the go/no-go task group survived the implantation of a sixteen-channel recording microwire array to the SNr, we were unable to record useful data due to equipment failure for several months' time, unfortunately during the time when we would have had feasible recording ability from these rats. In the discussion section, we discuss expected results and future plans for such recordings.

4.5 Discussion

The typical motor symptoms of PD are driven by changes in basal ganglia neural activity, brought about by the death of dopaminergic neurons in the substantia nigra pars compacta. Thus, treatment for motor symptoms typically begins with levodopa and dopamine agonist medication and, oftentimes, once the therapeutic window of dopaminergic medications has closed, neuromodulatory efforts within the basal ganglia are made, either via stereotactic ablation or DBS. While these therapies are generally effective at reducing lateral motor symptoms of PD, they each result in side effects. DBS

has been tied to each of the following side effects: hallucinations, psychosis, depression, apathy, mania, hypomania, euphoria, mirth, hypersexuality, anxiety, cognitive deficits, and impulsive behavior (Burn and Tröster, 2004; Hälbig et al., 2009). While some side effects likely result from mis-stimulation, such as eyelid apraxia (Tommasi et al., 2012) and dysarthria (King, Anderson et al., 2016; Skodda, 2012), others, such as impulsive behaviors, which are also present with dopaminergic treatment (Weintraub and Nirenberg, 2013), may not be as simple as those dependent on exact location of stimulation.

Our results confirm that DBS leads to numerous impulsive behaviors independent from parkinsonian symptom severity, confirming the idea that impulsive behaviors associated with DBS are not, at least in all cases, simply an exacerbation of parkinsonian symptoms. Specifically, we found that DBS leads to more impulsive behaviors in the context of each of un-cued task attempts, reward seeking, and incorrect cue response when specifically instructed to refrain from a specific behavior, with distinct quantitative and qualitative differences between failures to obey stop cues, preceded by a go cue, and failures to obey no-go cues, not preceded by a go cue. This combination of behaviors, consistent across subjects, leads to the conclusion that DBS-related impulsivity is a complex set of side effects that is unlikely to caused by stimulating in one specific mis-targeted region or failing to stimulate properly in another region.

While our results indicating greater impulsivity in the context of un-cued task attempts and reward seeking were unsurprising, our findings in terms of the differences between stop cue failures and no-go cue failures were somewhat unexpected. While rats failed both cues more frequently while on DBS than off DBS, differences in the timing of

failures between the two were marked. When rats failed the no-go cue on DBS and off DBS, there was no significant difference in timing of failure between the two conditions. However, when presented with a go cue prior to a stop cue, rats frequently took a longer period of time in failing the stop cue on DBS than off DBS. Additionally, the difference between the fraction of failed no-go cues on and off DBS, while not significantly lower than the difference between the fraction of failed stop cues on an off DBS, trended smaller.

Qualitatively, we noticed behavioral differences as to how rats failed stop and no-go cues under different conditions. Generally speaking, when rats were presented with a stop or no-go cue, they preceded to the reward hole to wait for their sucrose reward at the completion of the tone. Off DBS, a large portion of the failures occurred when rats were already in the process of performing a go cue and were simply unable to stop their ongoing behavior when the cue changed to a stop cue. On DBS in the no-go cue group, this was largely true. Rats were often in the process of performing impulsive un-cued task attempts when the no-go cue came on and they were unable to stop in time to prevent failure. However, in the case of a stop cue preceded by a go cue, rats generally proceeded towards the reward hole, but would frequently leave the reward hole area and either glance at or partially walk towards the task hole, often multiple times during a stop cue. A majority of the time, rats would be able to restrain themselves from attempting the task, but frequently, they were unable. We believe that this qualitative behavior explains the long average fail time: with a 10-second stop cue, rats were forced to restrain themselves from the specific behavior of nose-poking in the task hole for a period of time that was frequently too long while on DBS. Like rats in other conditions, they had a

number of quick failures, many due to already being in the midst of performing a go cue that changed to a go cue; however, DBS appears to have induced an inability to cancel an action once an initial instruction had been given, often leading to failed restraint despite clear qualitative indications of understanding that the instruction was to not complete the task. This supports the idea that cancelling actions involves a competition between basal ganglia pathways, specifically that some stop signal must be transmitted from STN to SNr to cancel a behavior (Schmidt et al., 2013). We interpret our results as meaning that, since DBS overrides basal ganglia activity without restoring electrophysiological activity seen under healthy conditions (Agnesi et al., 2013; Dorval and Grill, 2014; Wichmann and Delong, 2011), presumably especially along the STN/SNr pathway when STN is the target of DBS, this stop signal is, at least in part, overridden. While the stop signal is likely still somewhat present, it must be, at least, reduced in scope or scale, leading to this specific action suppression deficit. We interpret that, once a go instruction has been given, setting into motion the intention to complete the task, this STN-SNr stop signal becomes increasingly important; the overriding of this signal by DBS is likely responsible for this behavioral deficit.

Our results under hemiparkinsonian conditions were not fully expected. While reports indicate that 70% of parkinsonian patients experience apathy (Muhammed et al., 2015), we did not expect to find that rats would, so consistently, have such a high failure rate of go cues under hPD conditions. As a result of this low obedience rate, we chose not to analyze stop, no-go, or other impulsivity measures: if the rats were not consistently performing the task, success in the no-go or stop task would not, in our view, be seen as proper restraint, but, rather, apathy. Coupled with this lack of task performance was a

slow average response time. While hemiparkinsonism certainly affected motor behavior – as seen in Fig. 4-1 – we interpret the slow response times and low success rates as more apathy related than reaction time related. Indeed, examining individual reaction times and qualitative descriptions of behavior indicates that rats were still capable of relatively fast reaction times after 6-OHDA injection; they simply did not perform the task most of the time when instructed to do so. Of particular note is the result in go-cue response rates after hPD symptom validation; as time went on following hemiparkinsonian symptom validation, rats generally demonstrated less success at the go task.

Human studies have shown that while DBS of other regions might help relieve apathy, STN-DBS generally does not relieve apathy and, in some cases, worsens it (Funkiewiez et al., 2004; Gesquière-Dando et al., 2015; Richard, 2007; Williams et al., 2015). Additionally, it has been demonstrated that PD leads to an increased dependence on recent motor history in action selection (Helmich et al., 2009). Coupled with the trend we observed above – following hemiparkinsonian onset, rats demonstrated less success at the go task with time – it may be that initial go-cue failure after symptom onset due to somewhat reduced reaction times increases growing task apathy and the recent motor history of failing to respond to go cues manifests with positive feedback. As the STN has a major role in action selection (Frank, 2006), it may be that PD negatively impacts STN's ability to properly weight reward-based actions through the loss of dopamine, heavily implicated in reward circuitry for more than four decades (Fibiger and Phillips, 1974; Lippa et al., 1973). While DBS restores information transmission from the basal ganglia from elevated rates under hPD conditions to that seen under healthy conditions (Anderson et al., 2015), it does so by overriding signals, rather than restoring them to

their healthy state and may thusly fail to restore action selection and apathy-related symptoms.

Additionally, our behavioral testing results under control + DBS conditions were not expected. Given that rats did not exhibit typical overstimulation side effects on stimulation without dosing of amphetamines, it was surprising that DBS induced contralateral rotations with amphetamine administration, even though insignificantly different parameters successfully treated PD symptoms without inducing side effects. In our view, this simply provides further evidence that DBS moves the basal ganglia from their current state, rather than restoring healthy activity to them. With this in mind, we stress the importance of research aimed at restorative neuromodulation in the future, rather than a focus on neuromodulation that simply overrides neural activity. We hypothesize that future work will demonstrate that STN-DBS inherently leads to more side effects without mis-stimulation than currently known, creating an impetus for researchers to develop alternate methods of neuromodulation for the treatment of PD and other neurological disorders.

One limitation to our studies is that we did not successfully record electrophysiological data to analyze alongside our behavioral data due to equipment failure. We therefore suggest the future study of unit and field measures in the rodent SNr in connection with the behaviors that were seen in our study. Possible outcomes we expected included decreases in beta-band oscillatory activity as well as increases in alpha-theta-band activity immediately prior to and during impulsive behavior, reported in human patients with impulsivity deficits (Rodriguez-Oroz et al., 2011). Additionally, as the STN sends the SNr a stop signal to enable action suppression, future

electrophysiological work may present changes in firing rate and/or pattern in control conditions that are not observed under DBS conditions.

In conclusion, we have demonstrated that DBS of a healthy rodent leads to more impulsive behavior in the form of stop and no-go task failure, impulsive reward seeking, and non-instructed task attempts. Further, analysis of stop signal failure timing lent support to specific action suppression roles of the basal ganglia. Additionally, we demonstrated that the depletion of dopaminergic neurons in the SNc fundamentally alters reward circuitry in a way that is unrestored by DBS, leading to apathy and action selection deficits. Our work enables future electrophysiological studies into systems- and neuron-level studies of these behavioral symptoms and side effects, something that is difficult to pursue in human patients and many other disease models. Future work will be essential to improve the understanding of these side effects, which affect many, perhaps even the majority, of PD patients taking advantage of STN-DBS therapy.

CHAPTER 5

SUMMARY, DISCUSSION, AND FUTURE DIRECTIONS

Our work, reported in the preceding chapters, supports the idea that deep brain stimulation (DBS) treats motor symptoms of Parkinson's Disease (PD) by overriding pathological neural activity and replacing it with activity different from that in healthy individuals. In this viewpoint, side effects resulting from both mis-stimulation and failure to restore neural activity present under healthy conditions. We have provided evidence to support the idea that symptoms of PD are driven by pathological information transmission, which reduces information channel independence and interferes with downstream information processing in the thalamus and motor cortex. DBS therapy succeeds, at least in part, by reducing pathological information transmission, restoring information channel independence and downstream information processing. Despite the successful treatment of lateral motor symptoms, DBS's overriding of pathological neural activity with patterns that do not reproduce healthy neural signaling creates side effects in the form of impulse control deficits. Other side effects, such as hypokinetic dysarthria and those related to central motor control, may arise from lead placement within the somatotopically organized basal ganglia.

5.1 Interpretations of Our Work

Our work in Chapter 2 is easily interpreted from the following set of ideas. When we were implanting recording arrays into each of SNr and VA, we were implanting into regions of the brain that are somatotopically organized, but, given the relatively small sizes of our targets and the capabilities of our stereotaxic system, we had no delusions of successfully targeting specific regions within the somatotopy. Even if we had been able to target very precisely, our arrays were large enough that most electrodes on the arrays could have been expected to fall within regions corresponding to different body parts and muscles. Additionally, prior to recording, it is impossible to determine which electrodes are likely to present single unit activity. Thus, when pairing neurons that were recorded on electrodes within SNr with neurons that were recorded on electrodes within VA, we can consider neurons to be pseudorandomly spaced within the somatotopic organization of targets. Consequently, with hundreds of distinct muscles within a rat, it is highly unlikely for any given pair of neurons to correspond to the same muscle or even muscle group. With this in mind, it is unsurprising that an insignificant portion of our neuron pairs demonstrated a significant amount of information passage in either direction under control conditions. Under the parkinsonian condition, a significant portion of pairs passed a significant amount of information in both directions and the average directed information transfer between neurons increased in both directions. DBS restored both of these measures, in both directions, to values insignificantly different from those in the control condition.

We interpret that the parkinsonian symptoms of rigidity, bradykinesia, akinesia, increased muscle tone, and difficulty in movement initiation arise from this increased

information transmission between pairs of neurons responsible for control of different muscles. We interpret this as representative of a lack of information channel independence, especially across nearby muscle groups, which matches the results of previous studies, which demonstrated that basal ganglia receptive fields widen under PD conditions (Leblois et al., 2006; Vitek et al., 1998). Perhaps, when a hemiparkinsonian rat attempts to move its left biceps brachii, the signal that should be contained within the neurons responsible for left biceps brachii control is not contained within these neurons and passes to neurons responsible for left triceps brachii control, resulting in rigidity of the left front limb. Under this framework, the rat would obviously experience rigidity and increased muscle tone. This lack of information channel independence could additionally lead to difficulty in movement initiation and bradykinesia; if the lack of information channel independence became severe enough with disease progression – and more recent work demonstrates that directed information transmission may increase further with increased symptom severity (Dorval et al., 2015) – it might become almost impossible to initiate movement in one muscle group without activating an opposing muscle group, leading to akinesia. Thus, we consider this increased information transfer to be pathological.

Important to note is that this interpretation does not depend on whether the increased information transmission is direct across neurons or indirect, based on common inputs – or, inputs that feed into the SNr cell, and through an intermediary, the VA cell. Obviously, given many millions of cells in each region, we do not expect that we had any number of pairs of directly connected cells and thus, we interpret our increases in directed information more as an increase in intercellular responsiveness and dependence

across information channels than as an increase in transmission between directly connected pairs. Biologically, it is still unknown why this information channel independence decreases. Perhaps, in the absence of dopamine inputs to the basal ganglia, inputs from other pathways, such as the cortico-subthalamo-nigral or cortico-striato-nigral, become increasingly common.

It is worth noting the fact that not all pairs of cells express a significant amount of information in the parkinsonian condition – in fact, while a significantly greater number of pairs pass a significant amount of information, the vast majority still do not. This can be interpreted simply as meaning that not all information channels are collapsed into one channel – there may simply be crosstalk across nearby channels. This would make sense from a somatotopic framework – cells from nearby muscle groups become pathologically interactive, but somatotopically far-removed groups remain independent. Indeed, when a parkinsonian patient attempts to move his or her arm, he or she may experience rigidity throughout the arm and a difficult time initiating movement, but an intended arm movement does not typically result in leg movement as well.

Given that PD often leads to increases in firing rates in the output from the basal ganglia, it can be thought that PD lowers the threshold for firing in these regions and we might consider extra spikes as containing the pathological information associated with PD. While DBS often further increases the firing rate within these regions, it replaces action potentials with ones generated by, and in phase with, STN stimulation. Thus, DBS's regularization of STN firing and downstream SNr firing can be considered to be beneficial by phase locking the SNr to stimulation, making it more difficult for cells to respond to pathological information inputs, thus reducing pathological information

transmission and restoring information channel independence. When strong signals specific to the intended information channel are presented, a cell can still respond, allowing it to faithfully relay signals responsible for healthy motor activity, while weak signals crossing from other information channels are not strong enough to create action potentials in SNr or VA and thus do not propagate.

The preceding all makes sense from the framework of previous work suggesting that application of randomized stimulation to the STN may result in parkinsonian pathology (Birdno et al., 2008; Dorval et al., 2010). If randomized low-frequency inputs are applied widely across a large portion of the STN, a large portion of the SNr will respond and, thus, information channel independence will be reduced. If, instead, high-frequency stimulation is applied, and cells only respond occasionally, in phase, when strong inputs responsible for healthy motor activity are presented, information channel independence will be increased and pathological symptoms will subside.

One last interpretation is that there could be multiple redundant pathways responsible for motor control and Parkinsonism does not affect all redundant pathways. In the case of Parkinsonism, the pathological information transmission causes the basal ganglia to dominate motor control, resulting in PD symptoms. When DBS is applied, it reduces information transmission through the basal ganglia to the thalamus, and thus functions as an informational lesion, restoring the ability of other redundant pathways to provide information. In this interpretation, DBS would not restore information transmission of signals responsible for healthy motor control through any basal ganglia – thalamic pairs, but instead removes the role of these pathways, allowing the system to depend on other redundant pathways that are unaffected by Parkinsonism. While this may

seem unlikely, this, perhaps, explains the functions of STN lesions, which largely cut communication through the basal ganglia, and allows for an explanation for the wash-on effects of DBS, which are present for up to hours in some symptoms: DBS functions as an informational lesion, but the brain requires time to adjust to the lack of informative, unpredictable signals traveling through this pathway, eventually adjusting to depend more on other pathways.

While our studies in Chapter 2 provide new insights as to how DBS functions, our studies in Chapters 3 and 4 lead to new ideas as to how and why DBS fails. Our dysarthria work provides an important and long-missing model from which to study the electrophysiological underpinnings of DBS's exacerbation of parkinsonian hypokinetic dysarthria, as well as novel methods for analyzing rodent vocalizations without selection bias.

An obvious candidate for examination of electrophysiology will be to study the changes in response of neural activity to pharmacological and neuromodulatory therapies. With wide electrode arrays capable of both stimulation and recording spanning the majority of the STN, recordings in STN under pharmacological treatment and DBS may help explain how dopamine-based therapies alleviate vocal symptoms while DBS worsens them.

Based on the somatotopy of the basal ganglia and modeling of STN-DBS, it seems that a good candidate to focus study, electrophysiologically, would be the dorsal-lateral tip of the STN. In the somatotopic organization within the STN, this region is responsible for medial motor and orofacial control (Fig. 5-1) (Nambu, 2011). Interestingly, given that this is directly short of the target along a typical STN-DBS

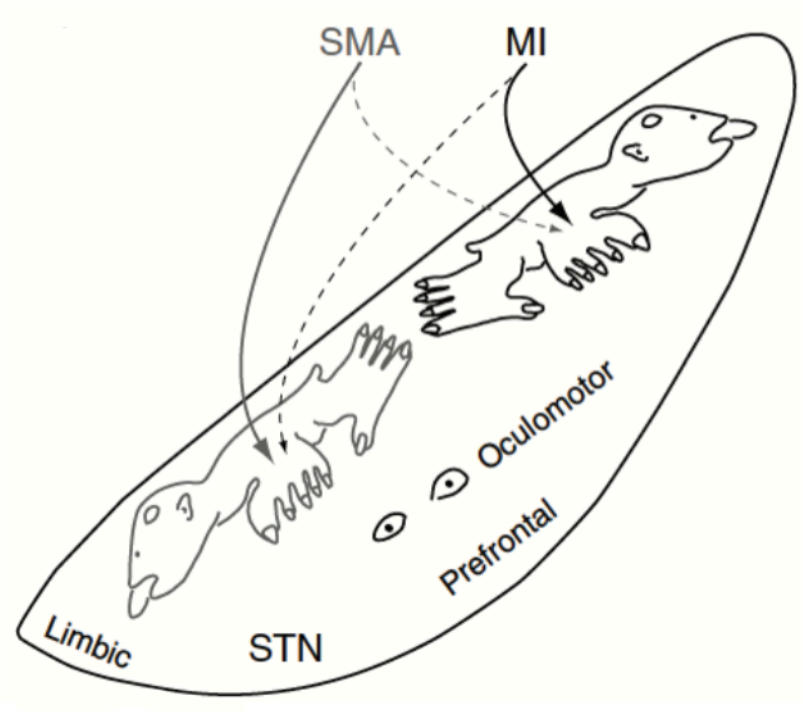

Figure 5-1. Somatotopy of the STN, adapted from Nambu, 2011.

trajectory, any fiber tracks parallel to the electrode would be hyperpolarized by stimulation, as demonstrated by an unpublished plot of an activating function approximation by Anderson (Fig. 5-2) (Anderson, 2015), in which the STN is made up from a combination of parallel and perpendicular fibers. Given that STN neurons are not particularly directionally organized (Fumi Sato, 2000), it stands to reason that many of the neurons responsible for medial motor and orofacial control may be hyperpolarized by STN-DBS that is roughly in line with its goal target, leading to a neuromodulation of the portion of the circuit responsible for motor control of vocal cords that is opposite in effect to the neuromodulation of the portions of the circuit responsible for lateral motor control. If depolarization of neurons leads to the information lesion described in Chapter 2, it is possible that hyperpolarization of neurons would further reduce information channel independence, worsening symptoms. Validating this hypothesis could allow for improvements, rather than exacerbations, of parkinsonian dysarthria. While new electrodes with current and/or voltage steering capability will allow for fine titration of target selection, allowing maximal target selection, even a standard four-contact DBS electrode inserted along the standard trajectory may be capable of reduction of parkinsonian vocal symptoms through the use of multiple contacts.

Our final set of studies provides a new model of PD's symptoms of apathy and action selection deficits, unrestored by DBS, as well as DBS's side effects of action suppression and impulsivity deficits, providing important insights into how DBS functions. Since PD motor symptoms arise from changes in neural activity in the basal ganglia and DBS does not restore neural activity to that seen pre-Parkinsonism, these DBS-related failures are unsurprising; however, they are still poorly understood,

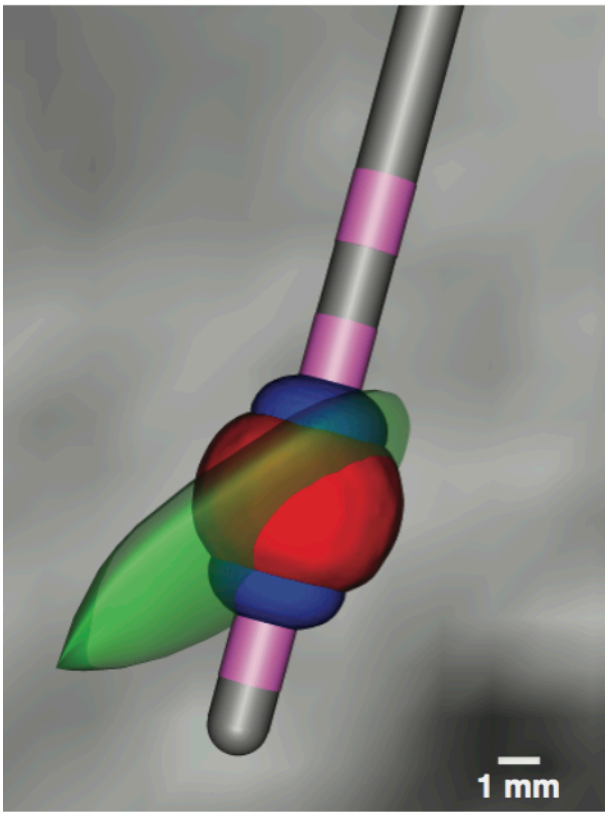

Figure 5-2. Adapted from Anderson (2015, unpublished). Activating function calculated from second difference of voltage between Nodes of Ranvier (.5 mm intermodal length) along axon fibers in both perpendicular and parallel directions from electrode. DBS electrode is inserted along a standard trajectory, with STN in green, threshold-crossing depolarization in red, and hyperpolarization in blue. The dorsal-lateral tip of the STN – the tip containing fibers relevant to motor control of vocal cords – is hyperpolarized, while the remaining somatotopic motor regions are depolarized.

necessitating models like ours to enable electrophysiological study.

Our results regarding the timing of failures of stop and no-go cues provide interesting insights into the basal ganglia's action suppression role. With reports of the importance of a stop signal from STN to SNr (Schmidt et al., 2013), we interpret that regularization of the STN and, to an extent, downstream targets, interrupts this important stop signal. The whole basal ganglia must work together to properly select action and improper activation of pathways can select or inhibit actions (Friend and Kravitz, 2014). Thus, it is unsurprising that the interruption of both the hyperdirect and indirect pathways through DBS's overriding of the STN can interrupt and prevent proper action suppression.

We interpret that, with current surgical limitation and DBS technology, action suppression side effects are largely unavoidable. It is possible, given the somatotopic organization of STN, that it may be possible to determine the precise location within the STN of fibers responsible for signaling to stop behaviors. However, given anisotropy of neural tissue and the fact that current surgeries often miss the optimal target by several mm (Butson et al., 2014), even if we were to know precisely where to not stimulate within the STN, it is not likely currently possible to avoid these specific fibers while successfully stimulating the optimal target.

In this interpretation, PD interrupts action selection and creates a greater dependence on recent motor history (Helmich et al., 2009). Initiating of movements and behaviors becomes more difficult in the parkinsonian state; thus, recent incompletion of tasks and movements – even those that were previously rewarding, but are less so now due to dopamine disruption – dominates action selection, leading to further task and

movement incompletion, possibly leading to the increasing apathy seen in our animals. The coupling of dopamine loss and a greater dependence on recent motor history seems as though it would lead to positive feedback: lack of movement, task completion, and intrinsic reward leads to further lack of movement, task completion, and intrinsic reward, leading to further difficulty in initiating movements as well as further apathy. DBS's failure to restore these symptoms validates the idea that replacement of pathological STN activity with activity that does not match that seen under healthy conditions is problematic. While we can relieve some motor symptoms with STN-DBS, not all symptoms can be reversed. At least with apathy and action selection deficits, unlike with DBS-induced action suppression deficits, it seems as though additional stimulation in other brain regions may help with symptom alleviation (Williams et al., 2015).

5.2 Proposed Future Work

Based on our work, we propose a number of future directions for both experiments and methodology. In regards to Chapter 2, we first propose advancing our analyses of percent of pairs of neurons that are significantly informative. Analysis with regard to percent of pairs passing a significant amount of information necessarily requires a somewhat arbitrary cutoff, and we chose a cutoff based on the estimated 95th percentile of directed information estimates of non-informative pairs. The specific cutoff value was not particularly important, as our results remained similar, qualitatively, through a large range of cutoffs. However, it is possible to improve upon our methodology, leading to an estimate of the 95th percentile that is both more accurate and more precise.

We determined that all pairs estimated as passing a negative amount of

information must be considered to be non-informative, as it is not possible to pass a negative amount of information; therefore, we created a distribution by mirroring the negative estimates around zero and used the standard deviation of this distribution to estimate the 95^{th} percentile of truly non-informative pairs, giving a threshold for estimating significant information transmission. However, since the estimates of both the truly informative and truly non-informative pairs are both considered to be coming from roughly normal distributions, it is, indeed, possible that an informative pair could be estimated as negative in certain circumstances, given our finite data bias correction. Because truly informative pairs necessarily pass a greater-than-zero amount of information and non-informative pairs necessarily pass zero information, the mean estimate value of directed information across truly informative pairs must be greater than the mean estimate value of directed information across truly non-informative pairs, which should be very close to zero, given enough data. Thus, given truly informative and truly non-informative estimated directed information standard deviations of similar magnitude, we should have a greater proportion of bias-corrected negative directed information estimates among truly non-informative pairs than among truly informative pairs. Additionally, the most negative estimates of directed information should come from truly non-informative pairs. Given that we may have had a small number of negative directed information estimates from truly informative pairs, our distribution of negative pairs may be biased closer to zero than a theoretical distribution comprising truly non-informative pairs. Thus, when we reflected the distribution around zero, the standard deviation estimated for truly non-informative pairs may have been a slight underestimate.

We propose that future work utilizing this analysis instead create a distribution of

bias-corrected directed neuronal information from truly non-informative pairs by instead pairing same-length recordings of neurons taken non-simultaneously. Given that all recordings of individual rats occurred on different days, neurons paired between different recordings are necessarily non-informative in both directions. Creating a distribution of directed information estimates of non-informative pairs this way, standard deviations will not trend towards underestimation and will, therefore, be more accurate. Additionally, given the greater number of pairs able to be created by pairing all recordings across separate days, the distributions will be more full, leading to greater precision in the standard deviation estimate. Despite the fact that the utilization of this slightly different method would not have qualitatively changed our results, it may have led to slight quantitative improvements in terms of both accuracy and precision.

Also relevant to Chapter 2, we propose future studies examining information transmission between more portions of the basal ganglia-thalamic-cortical circuit in a rat model of PD. While our results bring interesting interpretations, these interpretations could be further validated by determining whether the information changes we found between the SNr and VA are consistent throughout the circuitry. Additionally, given the recent surge in interest in the role of basal ganglia-cerebellar connectivity in the context of PD, studies examining informational changes between these two regions would be interesting and add to our work. It would be useful to use this rat model to determine whether SNr – VA informational changes hold true in the similar pathways between entopenduncular nucleus (EN) and ventrolateral thalamus (VL), although this may be difficult given the very small size of the rodent EN, and consequent difficulty in its targeting. It would also be useful to determine whether our information theoretic results

hold true in the rat model if symptoms are treated using dopaminergic medication, dopamine agonists, or target ablation rather than stimulation techniques. Finally, genetic models of PD are gaining in popularity, so it may be useful to retest our results in a genetic model of PD within a rat.

Using a mouse model, optogenetic stimulation, rather than electrical stimulation, could be used in conjunction with information theoretic metrics in several studies. First, excitatory stimulation could be applied to a greater portion of the STN with less stimulation outside the target, enabling a determination as to whether certain motor side effects come from poor stimulation. Additionally, these methods would enable inhibitory control of targets, which may be useful in restoring healthy signals, rather than just overriding pathological. Once more work has been performed to understand the nature of healthy and pathological basal ganglia signaling, it may be possible to optogenetically re-encode healthy signaling in a mouse STN; information analyses could be used in this context to determine, on an electrophysiological level, how well a given attempt at re-encoding is working.

Some very interesting studies relevant to chapter two could be performed using a non-human primate model. With larger targets, movable electrodes, a better understanding of the somatotopy of targets, and magnetic resonance / diffusion tensor imaging, it may be possible to determine very precise electrode location within target somatotopy. This would enable the comparison of information transfer between alternating muscle groups in different conditions, as well as other nearby somatotopic regions, enabling the determination of exactly how far, somatotopically speaking, information channel independence is lost in a parkinsonian animal. Additionally, it would

be particularly useful to study increases in directed information across more targets in a progressive model to ensure that these changes consistently increase with increased symptom severity across a number of target pairs.

In regards to our studies of dysarthria, we propose that similar work be done to analyze the effects of DBS on vocalization in a healthy rodent. It is known that improper stimulation parameters, even given stimulation within the correct target, can be detrimental (Dorval et al., 2009; So et al., 2012b), and the determination as to whether proper stimulation within the correct target induces vocal symptoms in a healthy rat would be enlightening. We do not know whether vocal side effects of DBS are simply representative of an exacerbation of pre-existing PD symptoms or, rather, independently develop, combining with PD symptoms to result in further vocal deficits. Therefore, ascertaining whether they do develop independently from PD would improve understand of PD vocal symptoms and help us treat them better.

Next, we propose that electrophysiological work should be performed using the framework that we have provided. A study of the differential responses to pharmacological and neuromodulatory therapies may help in the determination as to how dopamine-based therapies treat vocal symptoms, while DBS can worsen it. Despite minimal changes in entropy observed in Chapter 2, we propose STN entropy as an electrophysiological target to study in this context. We hypothesize that increased entropy is correlated with vocal symptoms, most readily understandable in the context of vocalization bandwidth. Given that entropy rises with wider, flatter ISI distributions, which are seen in PD – discussed in Chapter 2 – we hypothesize that these wider distributions correspond to wider vocalization ranges. Of course, given that we have

stressed the likely role that somatotopy plays in DBS's exacerbation of vocal symptoms of PD, precise localization of leads becomes important. Thus, large, sixteen-channel arrays spanning the STN with simultaneous stimulation and recording capacity would be necessary. We hypothesize that stimulation of the center of the STN would reduce entropy in nearby regions, while increasing entropy in the far dorsal-lateral corner, which is implicated in control of central, vocal muscles. We hypothesize that dopamine agonists would reduce entropy across the entire STN, including the dorsal-lateral region. This study would be difficult to complete in rodents, given the small STN and difficulty in determining extremely precise lead locations, but successful completion might enable improvements in the treatment of vocal symptoms for tens of thousands of future patients.

Due to the difficult nature of the previously proposed study, we additionally propose a similar study of electrophysiology in a non-human primate (NHP) model of PD. Given the ease of implantation of headcaps that allow repeated of insertion of electrodes to different targets in NHP models, researchers could implant DBS leads into the center of STN and repeatedly insert recording electrodes to neighboring regions in STN to test the hypothesis that DBS reduces PD-induced entropy in most regions of STN, while increasing it through the hyperpolarization of some cells within the dorsal-lateral region. Such a study could focus solely on electrophysiology, rather than using a model of vocalizations, given the difficult nature of recording as many vocalizations in an NHP model as we easily obtain in our rodent model.

Much of the above, in relation to Chapter 3, hinges on the idea that DBS's hyperpolarization of the dorsal-lateral corner of the STN, while depolarizing most of the rest of the STN, leads to an improvement in lateral motor symptoms while worsening

motor-related vocal symptoms. Thus, we propose the use of the Rubin/Terman 2004 model of the basal ganglia/thalamic connectivity (Rubin and Terman, 2004) to test how stimulatory hyperpolarization and depolarization of STN neurons differentially affect information transfer between STN-GPi and GPi-VL pairs. The demonstration that hyperpolarizing STN-DBS increases downstream entropy in the GPi and increases information transmission between STN and GPi and/or GPi and VL from measures taken in a healthy and parkinsonian state, while depolarizing STN-DBS decreases downstream entropy in the GPi while decreasing information transmission between STN and GPi and/or GPi and VL would provide strong evidence for our somatotopic explanation for DBS's exacerbation of parkinsonian dysarthria.

Finally, given the development of a novel electrode design with voltage steering capability in our lab (Willsie and Dorval, 2015a, 2015b), we propose to use said electrode in a non-human primate model of PD acutely to activate not only the standard portion of STN activated in an optimal surgical implantation, but also the dorsal-lateral region of STN. Unified Parkinsons's Disease Rating Scale motor scores could be used to demonstrate improvement of lateral motor symptoms, while a modified version of our vocalization analysis from Chapter 3 could be used to analyze the vocalizations that we are able to obtain. With these, we could test the idea that, by stimulating with contacts spanning a greater length of the electrode, it is possible to treat vocal deficits while still treating lateral motor deficits.

In regards to Chapter 4, we first propose that electrophysiological studies be performed within SNr and STN to tie local field potential activity to impulsive and apathetic behaviors. Given that the basal ganglia is responsible for signaling that

facilitates and inhibits various behaviors, one should be able to observe rapid changes in field potentials, likely either in beta or alpha-theta frequencies, responsible for movement inhibition and facilitation, immediately preceding and/or during incorrect behaviors. Perhaps, in the case of apathy, beta waves would be present prior to task performance in healthy conditions, reduced immediately following the cue, predicting future behavior. In the parkinsonian condition, this reduction may never occur, associated with failure to perform the task. In the case of action suppression deficits, one may see large changes in field signaling, particularly in movement-facilitating alpha-theta waves, between failure to demonstrate task restraint on-DBS and ability to do so off-DBS. The observance of the transmission of something resembling a stop signal from STN to SNr would require simultaneous unit recordings in STN and SNr with STN-stimulation, as well as time-dependent directed information analysis and precise electrode localization within STN and SNr somatotopy, which would be quite difficult to perform; however, the discovery of such a signal on a unit level would dramatically improve our understanding of DBS-induced impulsivity deficits.

Before any experiments examining stop signals on a unit-level could be performed, more work would need to be performed to help with the localization of recording and stimulation sites within the STN. With precise histological work, it may be possible to tie behavioral deficits to stimulation in very precise regions within the STN, enabling specific suggestions as to where to stimulate and record in the STN in such a study. However, such work may enable not only studies aimed at the understanding of the specific signaling between STN and SNr, but it may also enable new stimulation targets in human patients. While most surgical methods are not precise enough to avoid small

portions of the STN, future current steering electrodes, coupled with MRI, may eventually allow for the avoidance of action suppression deficits, given that the work has been performed to allow neurologists to know which specific regions of STN to avoid stimulating.

Finally, we find it important to determine whether our results in Chapter 4 pertaining to increasing apathy following 6-OHDA injection are brought about from a dependence on recent motor history – i.e., failed task performance due to slowed movement leading to more failed task performance – or simply from a longer time since injection. Therefore, we propose to train a moderate number of animals on just the go cue and inject with 6-OHDA immediately following training. Half of the rats will randomly be selected for a group that immediately begins task testing following symptom verification, 2 weeks after injection, while the other half will wait a month to begin testing. If results are similar between the two groups, we will conclude that the first interpretation will be correct. If, however, the second group demonstrates cue responses that are already fully reduced, we will interpret that some symptoms of PD simply take longer to present than motor symptoms.

5.3 Conclusions

In conclusion, our work supports the overarching idea that DBS can successfully treat motor symptoms of PD through the reduction of pathological information transmission between the basal ganglia and thalamus, though the fact that it does not restore the signals present under healthy conditions underlies some of the side effects generated by its use. Our work has provided clear evidence for an underlying cause of

parkinsonian symptom generation, as well as for the fact that some side effects are generated by not restoring neural activity in the basal ganglia to that seen under healthy conditions. Additionally, we have created a framework from which to study a common side effect likely related to somatotopy, therefore potentially preventable with improved treatment strategies. Future work based on our work can enable significant and direct improvements in the care of tens of thousands of patients. Additionally, the framework we have provided will enable a more long-term approach, allowing for many studies to be performed that will improve our knowledge of PD and DBS, ultimately leading to continuing improvements in disease treatments for years to come.

REFERENCES

Ackermann, H., Konczak, J., and Hertrich, I. (1997). The temporal control of repetitive articulatory movements in Parkinson's Disease. Brain Lang. *56*, 312–319.

Adrian, E.D.A.B. (1928). The Basis of Sensation: The Action of the Sense Organs (Christophers).

Agnesi, F., Connolly, A.T., Baker, K.B., Vitek, J.L., and Johnson, M.D. (2013). Deep brain stimulation imposes complex informational lesions. PloS One *8*, e74462.

Alam, M., Heissler, H.E., Schwabe, K., and Krauss, J.K. (2012). Deep brain stimulation of the pedunculopontine tegmental nucleus modulates neuronal hyperactivity and enhanced beta oscillatory activity of the subthalamic nucleus in the rat 6-hydroxydopamine model. Exp. Neurol. *233*, 233–242.

Alavi, M., Dostrovsky, J.O., Hodaie, M., Lozano, A.M., and Hutchison, W.D. (2013). Spatial extent of β oscillatory activity in and between the subthalamic nucleus and substantia nigra pars reticulata of Parkinson's disease patients. Exp. Neurol. *245*, 60–71.

Aleksandrova, L.R., Creed, M.C., Fletcher, P.J., Lobo, D.S.S., Hamani, C., and Nobrega, J.N. (2013). Deep brain stimulation of the subthalamic nucleus increases premature responding in a rat gambling task. Behav. Brain Res. *245*, 76–82.

Anderson, D.N. (2015). Activating function approximation for standard DBS electrode on typical STN-targeted trajectory.

Anderson, C.J., Sheppard, D.T., Huynh, R., Anderson, D.N., Polar, C.A., and Dorval, A.D. (2015). Subthalamic deep brain stimulation reduces pathological information transmission to the thalamus in a rat model of parkinsonism. Front. Neural Circuits *9*, 31.

Anderson, M.E., Postupna, N., and Ruffo, M. (2003). Effects of high-frequency stimulation in the internal globus pallidus on the activity of thalamic neurons in the awake monkey. J. Neurophysiol. *89*, 1150–1160.

Asanuma, K., Tang, C., Ma, Y., Dhawan, V., Mattis, P., Edwards, C., Kaplitt, M.G., Feigin, A., and Eidelberg, D. (2006). Network modulation in the treatment of Parkinson's disease. Brain J. Neurol. *129*, 2667–2678.

Barcroft, H., and Schwab, R.S. (1951). The effect of apomorphine and that of adrenalin,

on the tremor of Parkinson's disease. J. Nerv. Ment. Dis. *114*, 541–542.

Barfield, R.J., Auerbach, P., Geyer, L.A., and Mcintosh, T.K. (1979). Ultrasonic vocalizations in rat sexual behavior. Integr. Comp. Biol. *19*, 469–480.

Bar-Gad, I., Morris, G., and Bergman, H. (2003). Information processing, dimensionality reduction and reinforcement learning in the basal ganglia. Prog. Neurobiol. *71*, 439–473.

Bar-Gad, I., Elias, S., Vaadia, E., and Bergman, H. (2004). Complex locking rather than complete cessation of neuronal activity in the globus pallidus of a 1-methyl-4-phenyl-1,2,3,6-tetrahydropyridine-treated primate in response to pallidal microstimulation. J. Neurosci. Off. J. Soc. Neurosci. *24*, 7410–7419.

Bastiaens, J., Dorfman, B.J., Christos, P.J., and Nirenberg, M.J. (2013). Prospective cohort study of impulse control disorders in Parkinson's disease. Mov. Disord. Off. J. Mov. Disord. Soc. *28*, 327–333.

Bäumer, T., Hidding, U., Hamel, W., Buhmann, C., Moll, C.K.E., Gerloff, C., Orth, M., Siebner, H.R., and Münchau, A. (2009). Effects of DBS, premotor rTMS, and levodopa on motor function and silent period in advanced Parkinson's disease. Mov. Disord. Off. J. Mov. Disord. Soc. *24*, 672–676.

Baunez, C., and Robbins, T.W. (1997). Bilateral lesions of the subthalamic nucleus induce multiple deficits in an attentional task in rats. Eur. J. Neurosci. *9*, 2086–2099.

Baunez, C., and Robbins, T.W. (1999). Effects of transient inactivation of the subthalamic nucleus by local muscimol and APV infusions on performance on the five-choice serial reaction time task in rats. Psychopharmacology (Berl.) *141*, 57–65.

Baunez, C., Nieoullon, A., and Amalric, M. (1995). In a rat model of parkinsonism, lesions of the subthalamic nucleus reverse increases of reaction time but induce a dramatic premature responding deficit. J. Neurosci. Off. J. Soc. Neurosci. *15*, 6531–6541.

Baunez, C., Christakou, A., Chudasama, Y., Forni, C., and Robbins, T.W. (2007). Bilateral high-frequency stimulation of the subthalamic nucleus on attentional performance: transient deleterious effects and enhanced motivation in both intact and parkinsonian rats. Eur. J. Neurosci. *25*, 1187–1194.

Benabid, A.L., Benazzouz, A., Hoffmann, D., Limousin, P., Krack, P., and Pollak, P. (1998). Long-term electrical inhibition of deep brain targets in movement disorders. Mov. Disord. Off. J. Mov. Disord. Soc. *13 Suppl 3*, 119–125.

Benazzouz, A., Gao, D.M., Ni, Z.G., Piallat, B., Bouali-Benazzouz, R., and Benabid, A.L. (2000). Effect of high-frequency stimulation of the subthalamic nucleus on the neuronal activities of the substantia nigra pars reticulata and ventrolateral nucleus of the thalamus in the rat. Neuroscience *99*, 289–295.

Bergman, H., Wichmann, T., Karmon, B., and DeLong, M.R. (1994). The primate

subthalamic nucleus. II. Neuronal activity in the MPTP model of parkinsonism. J. Neurophysiol. *72*, 507–520.

Beurrier, C., Bioulac, B., Audin, J., and Hammond, C. (2001). High-frequency stimulation produces a transient blockade of voltage-gated currents in subthalamic neurons. J. Neurophysiol. *85*, 1351–1356.

de Bie, R.M.A., de Haan, R.J., Schuurman, P.R., Esselink, R. a. J., Bosch, D.A., and Speelman, J.D. (2002). Morbidity and mortality following pallidotomy in Parkinson's disease: a systematic review. Neurology *58*, 1008–1012.

Birdno, M.J., Kuncel, A.M., Dorval, A.D., Turner, D.A., and Grill, W.M. (2008). Tremor varies as a function of the temporal regularity of deep brain stimulation. Neuroreport *19*, 599–602.

Bologna, M., Fasano, A., Modugno, N., Fabbrini, G., and Berardelli, A. (2012). Effects of subthalamic nucleus deep brain stimulation and L-DOPA on blinking in Parkinson's disease. Exp. Neurol. *235*, 265–272.

Boraud, T., Bezard, E., Bioulac, B., and Gross, C. (1996). High frequency stimulation of the internal Globus Pallidus (GPi) simultaneously improves parkinsonian symptoms and reduces the firing frequency of GPi neurons in the MPTP-treated monkey. Neurosci. Lett. *215*, 17–20.

Bosch, C., Degos, B., Deniau, J.-M., and Venance, L. (2011). Subthalamic nucleus high-frequency stimulation generates a concomitant synaptic excitation-inhibition in substantia nigra pars reticulata. J. Physiol. *589*, 4189–4207.

Braak, H., Tredici, K.D., Rüb, U., de Vos, R.A.I., Jansen Steur, E.N.H., and Braak, E. (2003). Staging of brain pathology related to sporadic Parkinson's disease. Neurobiol. Aging *24*, 197–211.

Brittain, J.-S., Sharott, A., and Brown, P. (2014). The highs and lows of beta activity in cortico-basal ganglia loops. Eur. J. Neurosci. *39*, 1951–1959.

Brown, P., Mazzone, P., Oliviero, A., Altibrandi, M.G., Pilato, F., Tonali, P.A., and Di Lazzaro, V. (2004). Effects of stimulation of the subthalamic area on oscillatory pallidal activity in Parkinson's disease. Exp. Neurol. *188*, 480–490.

Brudzynski, S.M. (2005). Principles of rat communication: quantitative parameters of ultrasonic calls in rats. Behav. Genet. *35*, 85–92.

Brudzynski, S.M. (2013). Ethotransmission: communication of emotional states through ultrasonic vocalization in rats. Curr. Opin. Neurobiol. *23*, 310–317.

Burbaud, P., Gross, C., and Bioulac, B. (1994). Effect of subthalamic high frequency stimulation on substantia nigra pars reticulata and globus pallidus neurons in normal rats. J. Physiol. Paris *88*, 359–361.

Burghaus, L., Hilker, R., Thiel, A., Galldiks, N., Lehnhardt, F.G., Zaro-Weber, O., Sturm, V., and Heiss, W.-D. (2006). Deep brain stimulation of the subthalamic nucleus reversibly deteriorates stuttering in advanced Parkinson's disease. J. Neural Transm. Vienna Austria 1996 *113*, 625–631.

Burn, D.J., and Tröster, A.I. (2004). Neuropsychiatric complications of medical and surgical therapies for Parkinson's Disease. J. Geriatr. Psychiatry Neurol. *17*, 172–180.

Butson, C., Elias, W., Tse, W., Verhagen, L., Mandybur, G., Hung, S., Kopell, B., Gallo, B., Arle, J., Foote, K., et al. (2014). Effects of stimulation location on motor outcomes during current-controlled deep brain stimulation for Parkinson's Disease (Stockholm, Sweden).

Caballol, N., Martí, M.J., and Tolosa, E. (2007). Cognitive dysfunction and dementia in Parkinson disease. Mov. Disord. *22*, S358–S366.

Campbell, M.C., Karimi, M., Weaver, P.M., Wu, J., Perantie, D.C., Golchin, N.A., Tabbal, S.D., Perlmutter, J.S., and Hershey, T. (2008). Neural correlates of STN DBS-induced cognitive variability in Parkinson disease. Neuropsychologia *46*, 3162–3169.

Carcenac, C., Favier, M., Vachez, Y., Lacombe, E., Carnicella, S., Savasta, M., and Boulet, S. (2015). Subthalamic deep brain stimulation differently alters striatal dopaminergic receptor levels in rats. Mov. Disord. Off. J. Mov. Disord. Soc.

Castall, B., Marsden, C.D., Naylor, R.J., and Pycock, C.J. (1977). Stereotyped behaviour patterns and hyperactivity induced by amphetamine and apomorphine after discrete 6-hydroxydopamine lesions of extrapyramidal and mesolimbic nuclei. Brain Res. *123*, 89–111.

Cavanagh, J.F., Wiecki, T.V., Cohen, M.X., Figueroa, C.M., Samanta, J., Sherman, S.J., and Frank, M.J. (2011). Subthalamic nucleus stimulation reverses mediofrontal influence over decision threshold. Nat. Neurosci. *14*, 1462–1467.

Chang, J.-Y., Shi, L.-H., Luo, F., and Woodward, D.J. (2003). High frequency stimulation of the subthalamic nucleus improves treadmill locomotion in unilateral 6-hydroxydopamine lesioned rats. Brain Res. *983*, 174–184.

Chattha, P.K., Greene, P.E., and Ramdhani, R.A. (2015). Pseudobulbar laughter as a levodopa off phenomenon exacerbated by subthalamic deep brain stimulation. J. Clin. Mov. Disord. *2*.

Chesselet, M.F., and Delfs, J.M. (1996). Basal ganglia and movement disorders: an update. Trends Neurosci. *19*, 417–422.

Chong, T.T.-J., Bonnelle, V., Manohar, S., Veromann, K.-R., Muhammed, K., Tofaris, G.K., Hu, M., and Husain, M. (2015). Dopamine enhances willingness to exert effort for reward in Parkinson's disease. Cortex J. Devoted Study Nerv. Syst. Behav. *69*, 40–46.

Ciucci, M.R., Ma, S.T., Kane, J.R., Ahrens, A.M., and Schallert, T. (2008). Limb use and complex ultrasonic vocalization in a rat model of Parkinson's disease: deficit-targeted training. Parkinsonism Relat. Disord. *14 Suppl 2*, S172–S175.

Ciucci, M.R., Ahrens, A.M., Ma, S.T., Kane, J.R., Windham, E.B., Woodlee, M.T., and Schallert, T. (2009). Reduction of dopamine synaptic activity: degradation of 50-kHz ultrasonic vocalization in rats. Behav. Neurosci. *123*, 328–336.

Connolly, A.T., Jensen, A.L., Bello, E.M., Netoff, T.I., Baker, K.B., Johnson, M.D., and Vitek, J.L. (2015). Modulations in oscillatory frequency and coupling in globus pallidus with increasing parkinsonian severity. J. Neurosci. Off. J. Soc. Neurosci. *35*, 6231–6240.

Da Cunha, C., Boschen, S.L., Gómez-A, A., Ross, E.K., Gibson, W.S.J., Min, H.-K., Lee, K.H., and Blaha, C.D. (2015). Toward sophisticated basal ganglia neuromodulation: Review on basal ganglia deep brain stimulation. Neurosci. Biobehav. Rev.

Degos, B., Deniau, J.-M., Thierry, A.-M., Glowinski, J., Pezard, L., and Maurice, N. (2005). Neuroleptic-induced catalepsy: electrophysiological mechanisms of functional recovery induced by high-frequency stimulation of the subthalamic nucleus. J. Neurosci. Off. J. Soc. Neurosci. *25*, 7687–7696.

De Letter, M., Santens, P., and Van Borsel, J. (2005). The effects of levodopa on word intelligibility in Parkinson's disease. J. Commun. Disord. *38*, 187–196.

De Letter, M., Santens, P., De Bodt, M., Van Maele, G., Van Borsel, J., and Boon, P. (2007a). The effect of levodopa on respiration and word intelligibility in people with advanced Parkinson's disease. Clin. Neurol. Neurosurg. *109*, 495–500.

De Letter, M., Santens, P., Estercam, I., Van Maele, G., De Bodt, M., Boon, P., and Van Borsel, J. (2007b). Levodopa-induced modifications of prosody and comprehensibility in advanced Parkinson's disease as perceived by professional listeners. Clin. Linguist. Phon. *21*, 783–791.

Demetriades, P., Rickards, H., and Cavanna, A.E. (2011). Impulse control disorders following deep brain stimulation of the subthalamic nucleus in Parkinson's disease: clinical aspects. Park. Dis. *2011*, 658415.

Desbonnet, L., Temel, Y., Visser-Vandewalle, V., Blokland, A., Hornikx, V., and Steinbusch, H.W.M. (2004). Premature responding following bilateral stimulation of the rat subthalamic nucleus is amplitude and frequency dependent. Brain Res. *1008*, 198–204.

Dewey, R.B., and Maraganore, D.M. (1994). Isolated eyelid-opening apraxia: report of a new levodopa-responsive syndrome. Neurology *44*, 1752–1754.

Dietz, J., Noecker, A.M., McIntyre, C.C., Mikos, A., Bowers, D., Foote, K.D., and Okun, M.S. (2013). Stimulation region within the globus pallidus does not affect verbal fluency performance. Brain Stimulat. *6*, 248–253.

Dorval, A.D. (2008). Probability distributions of the logarithm of inter-spike intervals yield accurate entropy estimates from small datasets. J. Neurosci. Methods *173*, 129–139.

Dorval, A.D. (2011). Estimating neuronal information: logarithmic binning of neuronal inter-spike intervals. Entropy Basel Switz. *13*, 485–501.

Dorval, A.D., and Grill, W.M. (2014). Deep brain stimulation of the subthalamic nucleus reestablishes neuronal information transmission in the 6-OHDA rat model of parkinsonism. J. Neurophysiol. *111*, 1949–1959.

Dorval, A.D., Russo, G.S., Hashimoto, T., Xu, W., Grill, W.M., and Vitek, J.L. (2008). Deep brain stimulation reduces neuronal entropy in the MPTP-primate model of Parkinson's disease. J. Neurophysiol. *100*, 2807–2818.

Dorval, A.D., Panjwani, N., Qi, R.Y., and Grill, W.M. (2009). Deep brain stimulation that abolishes Parkinsonian activity in basal ganglia improves thalamic relay fidelity in a computational circuit. Conf. Proc. Annu. Int. Conf. IEEE Eng. Med. Biol. Soc. IEEE Eng. Med. Biol. Soc. Annu. Conf. *2009*, 4230–4233.

Dorval, A.D., Kuncel, A.M., Birdno, M.J., Turner, D.A., and Grill, W.M. (2010). Deep brain stimulation alleviates parkinsonian bradykinesia by regularizing pallidal activity. J. Neurophysiol. *104*, 911–921.

Dorval, A.D., Muralidharan, A., Jensen, A.L., Baker, K.B., and Vitek, J.L. (2015). Information in pallidal neurons increases with parkinsonian severity. Parkinsonism Relat. Disord. *21*, 1355–1361.

Duez, D. (2006). Syllable structure, syllable duration and final lengthening in Parkinsonian French speech. J. Multiling. Commun. Disord. *4*, 45–57.

Eagle, D.M., Baunez, C., Hutcheson, D.M., Lehmann, O., Shah, A.P., and Robbins, T.W. (2008a). Stop-signal reaction-time task performance: role of prefrontal cortex and subthalamic nucleus. Cereb. Cortex N. Y. N 1991 *18*, 178–188.

Eagle, D.M., Bari, A., and Robbins, T.W. (2008b). The neuropsychopharmacology of action inhibition: cross-species translation of the stop-signal and go/no-go tasks. Psychopharmacology (Berl.) *199*, 439–456.

Favier, M., Duran, T., Carcenac, C., Drui, G., Savasta, M., and Carnicella, S. (2014). Pramipexole reverses Parkinson's disease-related motivational deficits in rats. Mov. Disord. Off. J. Mov. Disord. Soc. *29*, 912–920.

Fibiger, H.C., and Phillips, A.G. (1974). Role of dopamine and norepinephrine in the chemistry of reward. J. Psychiatr. Res. *11*, 135–143.

Fibiger, H.C., Pudritz, R.E., McGeer, P.L., and McGeer, E.G. (1972). Axonal transport in nigro-striatal and nigro-thalamic neurons: effects of medial forebrain bundle lesions and 6-hydroxydopamine. J. Neurochem. *19*, 1697–1708.

Fleury, V., Cousin, E., Czernecki, V., Schmitt, E., Lhommée, E., Poncet, A., Fraix, V., Troprès, I., Pollak, P., Krainik, A., et al. (2014). Dopaminergic modulation of emotional conflict in Parkinson's disease. Front. Aging Neurosci. *6*, 164.

Fleury, V., Vingerhoets, F., Horvath, J., Pollak, P., and Burkhard, P. (2015). [Deep brain stimulation for movement disorders: indications, results and complications]. Rev. Médicale Suisse *11*, 962, 964–967.

Frank, M.J. (2006). Hold your horses: a dynamic computational role for the subthalamic nucleus in decision making. Neural Netw. Off. J. Int. Neural Netw. Soc. *19*, 1120–1136.

Frank, M.J., Samanta, J., Moustafa, A.A., and Sherman, S.J. (2007). Hold your horses: impulsivity, deep brain stimulation, and medication in parkinsonism. Science *318*, 1309–1312.

Friend, D.M., and Kravitz, A.V. (2014). Working together: basal ganglia pathways in action selection. Trends Neurosci. *37*, 301–303.

Fumi Sato, M.P. (2000). Axonal branching pattern of neurons of the subthalamic nucleus in primates. J Comp Neurol. J. Comp. Neurol. *424*, 142–152.

Funkiewiez, A., Ardouin, C., Caputo, E., Krack, P., Fraix, V., Klinger, H., Chabardes, S., Foote, K., Benabid, A.-L., and Pollak, P. (2004). Long term effects of bilateral subthalamic nucleus stimulation on cognitive function, mood, and behaviour in Parkinson's disease. J. Neurol. Neurosurg. Psychiatry *75*, 834–839.

Fuss, G., Spiegel, J., Magnus, T., Moringlane, J.R., Becker, G., and Dillmann, U. (2004). Improvement of apraxia of lid opening by STN-stimulation in a 70-year-old patient with Parkinson's disease. A case report. Minim. Invasive Neurosurg. MIN *47*, 58–60.

Galvan, A., Devergnas, A., and Wichmann, T. (2015). Alterations in neuronal activity in basal ganglia-thalamocortical circuits in the parkinsonian state. Front. Neuroanat. *9*, 5.

Gaudry, K.S., and Reinagel, P. (2008). Information measure for analyzing specific spiking patterns and applications to LGN bursts. Netw. Bristol Engl. *19*, 69–94.

Gesquière-Dando, A., Guedj, E., Loundou, A., Carron, R., Witjas, T., Fluchère, F., Delfini, M., Mundler, L., Regis, J., Azulay, J.-P., et al. (2015). A preoperative metabolic marker of parkinsonian apathy following subthalamic nucleus stimulation. Mov. Disord. Off. J. Mov. Disord. Soc.

Giannicola, G., Marceglia, S., Rossi, L., Mrakic-Sposta, S., Rampini, P., Tamma, F., Cogiamanian, F., Barbieri, S., and Priori, A. (2010). The effects of levodopa and ongoing deep brain stimulation on subthalamic beta oscillations in Parkinson's disease. Exp. Neurol. *226*, 120–127.

Giannicola, G., Rosa, M., Marceglia, S., Scelzo, E., Rossi, L., Servello, D., Menghetti, C., Pacchetti, C., Zangaglia, R., Locatelli, M., et al. (2013). The effects of levodopa and deep

brain stimulation on subthalamic local field low-frequency oscillations in Parkinson's disease. Neurosignals *21*, 89–98.

Gilmour, T.P., Lieu, C.A., Nolt, M.J., Piallat, B., Deogaonkar, M., and Subramanian, T. (2011). The effects of chronic levodopa treatments on the neuronal firing properties of the subthalamic nucleus and substantia nigra reticulata in hemiparkinsonian rhesus monkeys. Exp. Neurol. *228*, 53–58.

Green, N., Bogacz, R., Huebl, J., Beyer, A.-K., Kühn, A.A., and Heekeren, H.R. (2013). Reduction of influence of task difficulty on perceptual decision making by STN deep brain stimulation. Curr. Biol. CB *23*, 1681–1684.

Grill, W.M., Snyder, A.N., and Miocinovic, S. (2004). Deep brain stimulation creates an informational lesion of the stimulated nucleus. Neuroreport *15*, 1137–1140.

Groiss, S.J., Wojtecki, L., Südmeyer, M., and Schnitzler, A. (2009). Deep brain stimulation in Parkinson's disease. Ther. Adv. Neurol. Disord. *2*, 20–28.

Guo, Y., Rubin, J.E., McIntyre, C.C., Vitek, J.L., and Terman, D. (2008). Thalamocortical relay fidelity varies across subthalamic nucleus deep brain stimulation protocols in a data-driven computational model. J. Neurophysiol. *99*, 1477–1492.

Hälbig, T.D., Tse, W., Frisina, P.G., Baker, B.R., Hollander, E., Shapiro, H., Tagliati, M., Koller, W.C., and Olanow, C.W. (2009). Subthalamic deep brain stimulation and impulse control in Parkinson's disease. Eur. J. Neurol. Off. J. Eur. Fed. Neurol. Soc. *16*, 493–497.

Hariz, M., Blomstedt, P., and Zrinzo, L. (2013). Future of brain stimulation: new targets, new indications, new technology. Mov. Disord. Off. J. Mov. Disord. Soc. *28*, 1784–1792.

Hashimoto, T., Elder, C.M., Okun, M.S., Patrick, S.K., and Vitek, J.L. (2003). Stimulation of the subthalamic nucleus changes the firing pattern of pallidal neurons. J. Neurosci. Off. J. Soc. Neurosci. *23*, 1916–1923.

Hawkes, C.H. (2008). The prodromal phase of sporadic Parkinson's disease: Does it exist and if so how long is it? Mov. Disord. *23*, 1799–1807.

Helmich, R.C., Aarts, E., de Lange, F.P., Bloem, B.R., and Toni, I. (2009). Increased dependence of action selection on recent motor history in Parkinson's disease. J. Neurosci. Off. J. Soc. Neurosci. *29*, 6105–6113.

Hershey, T., Revilla, F.J., Wernle, A.R., McGee-Minnich, L., Antenor, J.V., Videen, T.O., Dowling, J.L., Mink, J.W., and Perlmutter, J.S. (2003). Cortical and subcortical blood flow effects of subthalamic nucleus stimulation in PD. Neurology *61*, 816–821.

Hershey, T., Campbell, M.C., Videen, T.O., Lugar, H.M., Weaver, P.M., Hartlein, J., Karimi, M., Tabbal, S.D., and Perlmutter, J.S. (2010). Mapping Go-No-Go performance within the subthalamic nucleus region. Brain J. Neurol. *133*, 3625–3634.

Herzog, J., Möller, B., Witt, K., Pinsker, M.O., Deuschl, G., and Volkmann, J. (2009). Influence of subthalamic deep brain stimulation versus levodopa on motor perseverations in Parkinson's disease. Mov. Disord. Off. J. Mov. Disord. Soc. *24*, 1206–1210.

Hilker, R., Voges, J., Thiel, A., Ghaemi, M., Herholz, K., Sturm, V., and Heiss, W.-D. (2002). Deep brain stimulation of the subthalamic nucleus versus levodopa challenge in Parkinson's disease: measuring the on- and off-conditions with FDG-PET. J. Neural Transm. Vienna Austria 1996 *109*, 1257–1264.

Hutchinson, W.D., Levy, R., Dostrovsky, J.O., Lozano, A.M., and Lang, A.E. (1997). Effects of apomorphine on globus pallidus neurons in parkinsonian patients. Ann. Neurol. *42*, 767–775.

Illes, J., Metter, E.J., Hanson, W.R., and Iritani, S. (1988). Language production in Parkinson's disease: acoustic and linguistic considerations. Brain Lang. *33*, 146–160.

Intemann, P.M., Masterman, D., Subramanian, I., DeSalles, A., Behnke, E., Frysinger, R., and Bronstein, J.M. (2001). Staged bilateral pallidotomy for treatment of Parkinson disease. J. Neurosurg. *94*, 437–444.

Jahanshahi, M., Ardouin, C.M., Brown, R.G., Rothwell, J.C., Obeso, J., Albanese, A., Rodriguez-Oroz, M.C., Moro, E., Benabid, A.L., Pollak, P., et al. (2000). The impact of deep brain stimulation on executive function in Parkinson's disease. Brain J. Neurol. *123 (Pt 6)*, 1142–1154.

Jahanshahi, M., Obeso, I., Baunez, C., Alegre, M., and Krack, P. (2015). Parkinson's disease, the subthalamic nucleus, inhibition, and impulsivity. Mov. Disord. Off. J. Mov. Disord. Soc. *30*, 128–140.

Jankovic, J. (2008). Parkinson's disease: clinical features and diagnosis. J. Neurol. Neurosurg. Psychiatry *79*, 368–376.

Johnson, A.M., Doll, E.J., Grant, L.M., Ringel, L., Shier, J.N., and Ciucci, M.R. (2011). Targeted training of ultrasonic vocalizations in aged and Parkinsonian rats. J. Vis. Exp. JoVE.

Joint, C., Thevathasan, W., Green, A.L., and Aziz, T. (2013). Pallidal somatotopy suggested by deep brain stimulation in a patient with dystonia. Neurology *80*, 685–686.

Kaplan, H.A., Machover, S., and Rabiner, A. (1954). A study of the effectiveness of drug therapy in parkinsonism. J. Nerv. Ment. Dis. *119*, 398–411.

Kim, R., Alterman, R., Kelly, P.J., Fazzini, E., Eidelberg, D., Beric, A., and Sterio, D. (1997). Efficacy of bilateral pallidotomy. Neurosurg. Focus *2*, e8.

King, N.O., Anderson, C.J., and Dorval, A.D. (2016). Deep brain stimulation exacerbates hypokinetic dysarthria in a rat model of Parkinson's disease. J. Neurosci. Res. *94*, 128–138.

Koller, W.C. (1992). When does Parkinson's disease begin? Neurology *42*, 27–31; discussion 41–48.

Krack, P., Fraix, V., Mendes, A., Benabid, A.-L., and Pollak, P. (2002). Postoperative management of subthalamic nucleus stimulation for Parkinson's disease. Mov. Disord. Off. J. Mov. Disord. Soc. *17 Suppl 3*, S188–S197.

Krack, P., Batir, A., Van Blercom, N., Chabardes, S., Fraix, V., Ardouin, C., Koudsie, A., Limousin, P.D., Benazzouz, A., LeBas, J.F., et al. (2003). Five-year follow-up of bilateral stimulation of the subthalamic nucleus in advanced Parkinson's disease. N. Engl. J. Med. *349*, 1925–1934.

Leblois, A., Meissner, W., Bezard, E., Bioulac, B., Gross, C.E., and Boraud, T. (2006). Temporal and spatial alterations in GPi neuronal encoding might contribute to slow down movement in Parkinsonian monkeys. Eur. J. Neurosci. *24*, 1201–1208.

Lehmkuhle, M.J., Bhangoo, S.S., and Kipke, D.R. (2009). The electrocorticogram signal can be modulated with deep brain stimulation of the subthalamic nucleus in the hemiparkinsonian rat. J. Neurophysiol. *102*, 1811–1820.

Limousin-Dowsey, P., Pollak, P., Van Blercom, N., Krack, P., Benazzouz, A., and Benabid, A. (1999). Thalamic, subthalamic nucleus and internal pallidum stimulation in Parkinson's disease. J. Neurol. *246 Suppl 2*, II42–II45.

Lindemann, C., Alam, M., Krauss, J.K., and Schwabe, K. (2013). Neuronal activity in the medial associative-limbic and lateral motor part of the rat subthalamic nucleus and the effect of 6-hydroxydopamine-induced lesions of the dorsolateral striatum. J. Comp. Neurol. *521*, 3226–3240.

Lippa, A.S., Antelman, S.M., Fisher, A.E., and Canfield, D.R. (1973). Neurochemical mediation of reward: a significant role for dopamine? Pharmacol. Biochem. Behav. *1*, 23–28.

Litvin, Y., Blanchard, D.C., and Blanchard, R.J. (2007). Rat 22kHz ultrasonic vocalizations as alarm cries. Behav. Brain Res. *182*, 166–172.

Logemann, J.A., Fisher, H.B., Boshes, B., and Blonsky, E.R. (1978). Frequency and cooccurrence of vocal tract dysfunctions in the speech of a large sample of Parkinson patients. J. Speech Hear. Disord. *43*, 47.

Lyons, K.E., and Pahwa, R. (2004). Deep brain stimulation in Parkinson's disease. Curr. Neurol. Neurosci. Rep. *4*, 290–295.

Maesawa, S., Kaneoke, Y., Kajita, Y., Usui, N., Misawa, N., Nakayama, A., and Yoshida, J. (2004). Long-term stimulation of the subthalamic nucleus in hemiparkinsonian rats: neuroprotection of dopaminergic neurons. J. Neurosurg. *100*, 679–687.

Magnin, M., Morel, A., and Jeanmonod, D. (2000). Single-unit analysis of the pallidum,

thalamus and subthalamic nucleus in parkinsonian patients. Neuroscience *96*, 549–564.

Martínez-Sánchez, F., Meilán, J.J.G., Carro, J., Gómez Íñiguez, C., Millian-Morell, L., Pujante Valverde, I.M., López-Alburquerque, T., and López, D.E. (2015). Speech rate in Parkinson's disease: A controlled study. Neurol. Barc. Spain.

McConnell, G.C., So, R.Q., Hilliard, J.D., Lopomo, P., and Grill, W.M. (2012). Effective deep brain stimulation suppresses low-frequency network oscillations in the basal ganglia by regularizing neural firing patterns. J. Neurosci. Off. J. Soc. Neurosci. *32*, 15657–15668.

McIntyre, C.C., Grill, W.M., Sherman, D.L., and Thakor, N.V. (2004). Cellular effects of deep brain stimulation: model-based analysis of activation and inhibition. J. Neurophysiol. *91*, 1457–1469.

Meissner, W., Leblois, A., Hansel, D., Bioulac, B., Gross, C.E., Benazzouz, A., and Boraud, T. (2005). Subthalamic high frequency stimulation resets subthalamic firing and reduces abnormal oscillations. Brain J. Neurol. *128*, 2372–2382.

Mikos, A., Bowers, D., Noecker, A.M., McIntyre, C.C., Won, M., Chaturvedi, A., Foote, K.D., and Okun, M.S. (2011). Patient-specific analysis of the relationship between the volume of tissue activated during DBS and verbal fluency. NeuroImage *54, Supplement 1*, S238–S246.

Mink, J.W. (1996). The basal ganglia: focused selection and inhibition of competing motor programs. Prog. Neurobiol. *50*, 381–425.

Molnar, G.F., Pilliar, A., Lozano, A.M., and Dostrovsky, J.O. (2005). Differences in neuronal firing rates in pallidal and cerebellar receiving areas of thalamus in patients with Parkinson's disease, essential tremor, and pain. J. Neurophysiol. *93*, 3094–3101.

Moran, A., Stein, E., Tischler, H., Belelovsky, K., and Bar-Gad, I. (2011). Dynamic stereotypic responses of Basal Ganglia neurons to subthalamic nucleus high-frequency stimulation in the parkinsonian primate. Front. Syst. Neurosci. *5*, 21.

Muhammed, K., Manohar, S., and Husain, M. (2015). Mechanisms underlying apathy in Parkinson's disease. Lancet Lond. Engl. *385 Suppl 1*, S71.

Nambu, A. (2011). Somatotopic organization of the primate Basal Ganglia. Front. Neuroanat. *5*, 26.

Okun MS, Tagliati M, Pourfar M, and et al (2005). Management of referred deep brain stimulation failures: A retrospective analysis from 2 movement disorders centers. Arch. Neurol. *62*, 1250–1255.

Papa, S.M., Desimone, R., Fiorani, M., and Oldfield, E.H. (1999). Internal globus pallidus discharge is nearly suppressed during levodopa-induced dyskinesias. Ann. Neurol. *46*, 732–738.

Paxinos, G., and Watson, C. (2008). The Rat Brain in Stereotaxic Coordinates: Compact, Sixth Edition (Academic Press).

Phillips, J.M., and Brown, V.J. (2000). Anticipatory errors after unilateral lesions of the subthalamic nucleus in the rat: evidence for a failure of response inhibition. Behav. Neurosci. *114*, 150–157.

Pieri, M., Pieri, L., Saner, A., Da Prada, M., and Haefely, W. (1975). A comparison of drug-induced rotation in rats lesioned in the medial forebrain bundle with 5,6-dihydroxytryptamine or 6-hydroxydopamine. Arch. Int. Pharmacodyn. Thérapie *217*, 118–130.

Pote, I., Torkamani, M. Kefalopoulou, Z., Zrinzo, L., Limousin-Dowsey, P., Foltynie, T., Speekenbrink, M., and Jahanshahi, M. (2016). Subthalamic nucleus deep brain stimulation induces impulsive action when patients with Parkinson's disease act under speed pressure. Exp. Brain Res.

Ray, N.J., Jenkinson, N., Brittain, J., Holland, P., Joint, C., Nandi, D., Bain, P.G., Yousif, N., Green, A., Stein, J.S., et al. (2009). The role of the subthalamic nucleus in response inhibition: evidence from deep brain stimulation for Parkinson's disease. Neuropsychologia *47*, 2828–2834.

Raz, A., Vaadia, E., and Bergman, H. (2000). Firing patterns and correlations of spontaneous discharge of pallidal neurons in the normal and the tremulous 1-methyl-4-phenyl-1,2,3,6-tetrahydropyridine vervet model of parkinsonism. J. Neurosci. Off. J. Soc. Neurosci. *20*, 8559–8571.

Richard, I.H. (2007). Depression and apathy in Parkinson's disease. Curr. Neurol. Neurosci. Rep. *7*, 295–301.

Rieke, F., Warland, D., and Bialek, W. (1993). Coding efficiency and information rates in sensory neurons. Europhys. Lett. EPL *22*, 151–156.

Ritz, B., Lee, P.-C., Lassen, C.F., and Arah, O.A. (2014). Parkinson disease and smoking revisited: ease of quitting is an early sign of the disease. Neurology *83*, 1396–1402.

Rocchi, L., Chiari, L., and Horak, F.B. (2002). Effects of deep brain stimulation and levodopa on postural sway in Parkinson's disease. J. Neurol. Neurosurg. Psychiatry *73*, 267–274.

Rodriguez-Oroz, M.C., López-Azcárate, J., Garcia-Garcia, D., Alegre, M., Toledo, J., Valencia, M., Guridi, J., Artieda, J., and Obeso, J.A. (2011). Involvement of the subthalamic nucleus in impulse control disorders associated with Parkinson's disease. Brain J. Neurol. *134*, 36–49.

Romito, L.M.A., Scerrati, M., Contarino, M.F., Bentivoglio, A.R., Tonali, P., and Albanese, A. (2002). Long-term follow up of subthalamic nucleus stimulation in Parkinson's disease. Neurology *58*, 1546–1550.

Rubin, J.E., and Terman, D. (2004). High frequency stimulation of the subthalamic nucleus eliminates pathological thalamic rhythmicity in a computational model. J. Comput. Neurosci. *16*, 211–235.

Rusz, J., Cmejla, R., Tykalova, T., Ruzickova, H., Klempir, J., Majerova, V., Picmausova, J., Roth, J., and Ruzicka, E. (2013). Imprecise vowel articulation as a potential early marker of Parkinson's disease: effect of speaking task. J. Acoust. Soc. Am. *134*, 2171–2181.

Sales, G.D. (1972). Ultrasound and mating behaviour in rodents with some observations on other behavioural situations. J Zool *168*, 149–164.

Santaniello, S., McCarthy, M.M., Montgomery, E.B., Gale, J.T., Kopell, N., and Sarma, S.V. (2015). Therapeutic mechanisms of high-frequency stimulation in Parkinson's disease and neural restoration via loop-based reinforcement. Proc. Natl. Acad. Sci. U. S. A. *112*, E586–E595.

Schmidt, R., Leventhal, D.K., Mallet, N., Chen, F., and Berke, J.D. (2013). Canceling actions involves a race between basal ganglia pathways. Nat. Neurosci. *16*, 1118–1124.

Schneidman, E., Bialek, W., and Berry, M.J. (2003). Synergy, redundancy, and independence in population codes. J. Neurosci. Off. J. Soc. Neurosci. *23*, 11539–11553.

Schneidman, E., Puchalla, J.L., Segev, R., Harris, R.A., Bialek, W., and Berry, M.J. (2011). Synergy from silence in a combinatorial neural code. J. Neurosci. Off. J. Soc. Neurosci. *31*, 15732–15741.

Schrag, A., Sauerbier, A., and Chaudhuri, K.R. (2015). New clinical trials for nonmotor manifestations of Parkinson's disease. Mov. Disord. Off. J. Mov. Disord. Soc. *30*, 1490–1504.

Schroeder, U., Kuehler, A., Haslinger, B., Erhard, P., Fogel, W., Tronnier, V.M., Lange, K.W., Boecker, H., and Ceballos-Baumann, A.O. (2002). Subthalamic nucleus stimulation affects striato-anterior cingulate cortex circuit in a response conflict task: a PET study. Brain J. Neurol. *125*, 1995–2004.

Seffer, D., Schwarting, R.K.W., and Wöhr, M. (2014). Pro-social ultrasonic communication in rats: Insights from playback studies. J. Neurosci. Methods *234*, 73–81.

Sesia, T., Bulthuis, V., Tan, S., Lim, L.W., Vlamings, R., Blokland, A., Steinbusch, H.W.M., Sharp, T., Visser-Vandewalle, V., and Temel, Y. (2010). Deep brain stimulation of the nucleus accumbens shell increases impulsive behavior and tissue levels of dopamine and serotonin. Exp. Neurol. *225*, 302–309.

Shi, L.-H., Luo, F., Woodward, D.J., and Chang, J.-Y. (2006). Basal ganglia neural responses during behaviorally effective deep brain stimulation of the subthalamic nucleus in rats performing a treadmill locomotion test. Synap. N. Y. N *59*, 445–457.

Shields, D.C., Lam, S., Gorgulho, A., Emerson, J., Krahl, S.E., Malkasian, D., and DeSalles, A. a. F. (2006). Eyelid apraxia associated with subthalamic nucleus deep brain stimulation. Neurology *66*, 1451–1452.

Skodda, S. (2011). Aspects of speech rate and regularity in Parkinson's disease. J. Neurol. Sci. *310*, 231–236.

Skodda, S. (2012). Effect of deep brain stimulation on speech performance in Parkinson's disease. Park. Dis. *2012*, 850596.

Skodda, S., Rinsche, H., and Schlegel, U. (2009). Progression of dysprosody in Parkinson's disease over time--a longitudinal study. Mov. Disord. Off. J. Mov. Disord. Soc. *24*, 716–722.

So, R.Q., Kent, A.R., and Grill, W.M. (2012a). Relative contributions of local cell and passing fiber activation and silencing to changes in thalamic fidelity during deep brain stimulation and lesioning: a computational modeling study. J. Comput. Neurosci. *32*, 499–519.

So, R.Q., McConnell, G.C., August, A.T., and Grill, W.M. (2012b). Characterizing effects of subthalamic nucleus deep brain stimulation on methamphetamine-induced circling behavior in hemi-Parkinsonian rats. IEEE Trans. Neural Syst. Rehabil. Eng. Publ. IEEE Eng. Med. Biol. Soc. *20*, 626–635.

Starkstein, S.E. (2012). Apathy in Parkinson's disease: diagnostic and etiological dilemmas. Mov. Disord. Off. J. Mov. Disord. Soc. *27*, 174–178.

Strong, S.P., Koberle, R., de Ruyter van Steveninck, R.R., and Bialek, W. (1998). Entropy and information in neural spike trains. Phys. Rev. Lett. *80*, 197–200.

Summerson, S.R., Aazhang, B., and Kemere, C.T. (2014). Characterizing motor and cognitive effects associated with deep brain stimulation in the GPi of hemi-parkinsonian rats. IEEE Trans. Neural Syst. Rehabil. Eng. *22*, 1218–1227.

Tai, C.-H., Pan, M.-K., Lin, J.J., Huang, C.-S., Yang, Y.-C., and Kuo, C.-C. (2012). Subthalamic discharges as a causal determinant of parkinsonian motor deficits. Ann. Neurol. *72*, 464–476.

Tang, J.K.H., Moro, E., Lozano, A.M., Lang, A.E., Hutchison, W.D., Mahant, N., and Dostrovsky, J.O. (2005). Firing rates of pallidal neurons are similar in Huntington's and Parkinson's disease patients. Exp. Brain Res. *166*, 230–236.

Thompson, J.A., Lanctin, D., Ince, N.F., and Abosch, A. (2014). Clinical implications of local field potentials for understanding and treating movement disorders. Stereotact. Funct. Neurosurg. *92*, 251–263.

Toleikis, J.R., Metman, L.V., Pilitsis, J.G., Barborica, A., Toleikis, S.C., and Bakay, R.A.E. (2012). Effect of intraoperative subthalamic nucleus DBS on human single-unit

activity in the ipsilateral and contralateral subthalamic nucleus. J. Neurosurg. *116*, 1134–1143.

Tommasi, G., Krack, P., Fraix, V., and Pollak, P. (2012). Effects of varying subthalamic nucleus stimulation on apraxia of lid opening in Parkinson's disease. J. Neurol. *259*, 1944–1950.

Treciokas, L.J., Ansel, R.D., and Markham, C.H. (1971). One to Two Year Treatment of Parkinson's Disease with Levodopa. Calif. Med. *114*, 7–14.

Trevelyan, A.J., Bruns, W., Mann, E.O., Crepel, V., and Scanziani, M. (2013). The information content of physiological and epileptic brain activity. J. Physiol. *591*, 799–805.

Tröster, A.I., Woods, S.P., and Fields, J.A. (2003). Verbal fluency declines after pallidotomy: an interaction between task and lesion laterality. Appl. Neuropsychol. *10*, 69–75.

Truong, D.D., and Wolters, E.C. (2009). Recognition and management of Parkinson's disease during the premotor (prodromal) phase. Expert Rev. Neurother. *9*, 847–857.

Umemura, A., Oka, Y., Yamamoto, K., Okita, K., Matsukawa, N., and Yamada, K. (2011). Complications of subthalamic nucleus stimulation in Parkinson's Disease. Neurol. Med. Chir. (Tokyo) *51*, 749–755.

Uslaner, J.M., and Robinson, T.E. (2006). Subthalamic nucleus lesions increase impulsive action and decrease impulsive choice - mediation by enhanced incentive motivation? Eur. J. Neurosci. *24*, 2345–2354.

Vaillancourt, D.E., Prodoehl, J., Verhagen Metman, L., Bakay, R.A., and Corcos, D.M. (2004). Effects of deep brain stimulation and medication on bradykinesia and muscle activation in Parkinson's disease. Brain J. Neurol. *127*, 491–504.

Vitek, J.L., Bakay, R.A., Hashimoto, T., Kaneoke, Y., Mewes, K., Zhang, J.Y., Rye, D., Starr, P., Baron, M., Turner, R., et al. (1998). Microelectrode-guided pallidotomy: technical approach and its application in medically intractable Parkinson's disease. J. Neurosurg. *88*, 1027–1043.

Walsh, B., and Smith, A. (2011). Linguistic complexity, speech production, and comprehension in Parkinson's disease: behavioral and physiological indices. J. Speech Lang. Hear. Res. JSLHR *54*, 787–802.

Wang, Y., Zhang, Q.J., Liu, J., Ali, U., Gui, Z.H., Hui, Y.P., Chen, L., and Wang, T. (2010). Changes in firing rate and pattern of GABAergic neurons in subregions of the substantia nigra pars reticulata in rat models of Parkinson's disease. Brain Res. *1324*, 54–63.

Weick, B.G., Engber, T.M., Susel, Z., Chase, T.N., and Walters, J.R. (1990). Responses of substantia nigra pars reticulata neurons to GABA and SKF 38393 in 6-

hydroxydopamine-lesioned rats are differentially affected by continuous and intermittent levodopa administration. Brain Res. *523*, 16–22.

Weintraub, D., and Nirenberg, M.J. (2013). Impulse control and related disorders in Parkinson's disease. Neurodegener. Dis. *11*, 63–71.

Wertheimer, J., Gottuso, A.Y., Nuno, M., Walton, C., Duboille, A., Tuchman, M., and Ramig, L. (2014). The impact of STN deep brain stimulation on speech in individuals with Parkinson's disease: the patient's perspective. Parkinsonism Relat. Disord. *20*, 1065–1070.

Whitfield, J.A., and Goberman, A.M. (2014). Articulatory-acoustic vowel space: application to clear speech in individuals with Parkinson's disease. J. Commun. Disord. *51*, 19–28.

Wichmann, T., and DeLong, M.R. (2003). Pathophysiology of Parkinson's disease: the MPTP primate model of the human disorder. Ann. N. Y. Acad. Sci. *991*, 199–213.

Wichmann, T., and Delong, M.R. (2011). Deep-brain stimulation for basal ganglia disorders. Basal Ganglia *1*, 65–77.

Willadsen, M., Seffer, D., Schwarting, R.K.W., and Wöhr, M. (2014). Rodent ultrasonic communication: Male prosocial 50-khz ultrasonic vocalizations elicit social approach behavior in female rats (rattus norvegicus). J. Comp. Psychol. *128*, 56–64.

Williams, N.R., Hopkins, T.R., Short, E.B., Sahlem, G.L., Snipes, J., Revuelta, G.J., George, M.S., and Takacs, I. (2015). Reward circuit DBS improves Parkinson's gait along with severe depression and OCD. Neurocase 1–4.

Willsie, A.C., and Dorval, A.D. (2015a). Computational field shaping for deep brain stimulation with thousands of contacts in a novel electrode geometry. Neuromodulation J. Int. Neuromodulation Soc. *18*, 542–551.

Willsie, A., and Dorval, A. (2015b). Fabrication and initial testing of the μDBS: a novel Deep Brain Stimulation electrode with thousands of individually controllable contacts. Biomed. Microdevices *17*, 9961.

Windels, F., Bruet, N., Poupard, A., Urbain, N., Chouvet, G., Feuerstein, C., and Savasta, M. (2000). Effects of high frequency stimulation of subthalamic nucleus on extracellular glutamate and GABA in substantia nigra and globus pallidus in the normal rat. Eur. J. Neurosci. *12*, 4141–4146.

Witt, K., Pulkowski, U., Herzog, J., Lorenz, D., Hamel, W., Deuschl, G., and Krack, P. (2004). Deep brain stimulation of the subthalamic nucleus improves cognitive flexibility but impairs response inhibition in Parkinson disease. Arch. Neurol. *61*, 697–700.

Wöhr, M., and Schwarting, R.K.W. (2013). Affective communication in rodents: ultrasonic vocalizations as a tool for research on emotion and motivation. Cell Tissue Res.

354, 81–97.

Yamada, S., Matsuo, K., Hirayama, M., and Sobue, G. (2004). The effects of levodopa on apraxia of lid opening A case report. Neurology *62*, 830–831.

Zsigmond, P., and Göransson, N. (2014). Deep brain stimulation and intracerebral infection: A case report and review of the literature. Neurol. Clin. Neurosci. *2*, 161–162.